

---

# CF6 Working Group Summary

## The Bright Side of the Cosmic Frontier: Cosmic Probes of Fundamental Physics

**Conveners: J.J. Beatty, A.E. Nelson, A. Olinto, G. Sinnis**

A. U. Abeysekara, L.A. Anchordoqui, T. Aramaki, J. Belz, J.H. Buckley, K. Byrum, R. Cameron, M-C. Chen, K. Clark, A. Connolly, D.F. Cowen, T. DeYoung, P. von Doetinchem J. Dumm, M. Errando, G. Farrar, F. Ferrer, L. Fortson, S. Funk, D. Grant, S. Griffiths, A. Groß, C. Hailey, C. Hogan, J. Holder, B. Humensky, P. Kaaret, S.R. Klein, H. Krawczynski, F. Krennrich, K. Krings, J. Krizmanic, A. Kusenko, J. T. Linnemann, J. H. MacGibbon, J. Matthews, A. McCann, J. Mitchell, R. Mukherjee, D. Nitz, R.A. Ong, M. Orr, N. Otte, T. Paul, E. Resconi, M. A. Sanchez-Conde, P. Sokolsky, F. Stecker, D. Stump, I. Taboada, G.B. Thomson, K. Tollefson, P. von Doetinchem, T. Ukwatta, J. Vandenbroucke, V. Vasileiou, V.V. Vassileiv, T.J. Weiler, D.A. Williams, A. Weinstein, M. Wood, B. Zitzer

### 1 Executive Summary

Over the past decade we have witnessed a revolution in our understanding of the high-energy universe. Some of the key discoveries have been:

- Supernovae have been shown to be a source of Galactic cosmic rays [1, 2, 3].
- Very high energy neutrinos that are likely to be astrophysical in origin have been observed [4].
- The GZK suppression [5, 6] in the cosmic-ray flux above  $10^{19.5}$  eV has been observed [7, 8, 9, 10].
- The positron fraction of the cosmic rays has been measured up to 300 GeV and provides solid evidence for a high-energy primary source of positrons in the Galaxy, either from dark matter annihilation or astrophysical processes [11, 3, 12, 13].
- Many sites of astrophysical particle acceleration have been directly observed, from supermassive black holes and merging neutron stars, to rapidly spinning neutron stars and supernova remnants in our Galaxy [14, 15, 16, 17].

These discoveries have been driven by the current generation of experiments: the IceCube neutrino detector at the South Pole [18, 19], the Fermi gamma-ray observatory [20] and the PAMELA [21] and AMS experiments [22] orbiting the earth, the High Resolution Flys Eye [23] and Pierre Auger [10] ultra-high-energy cosmic ray experiments, and the H.E.S.S. [24], VERITAS [25], MAGIC [26] and Milagro [27] experiments in very high energy gamma rays. Looking forward, a new generation of instruments with greater sensitivity and higher resolution hold the promise of making large advances in our understanding of astrophysical processes and the fundamental physics studied with astrophysical accelerators. The goals for the coming decade are:

- Determine the origin of the highest energy particles in the universe and understand the acceleration processes at work throughout the Universe.
- Measure particle cross sections at energies unattainable in Earth-bound accelerators.
- Measure the highest energy neutrinos that arise from interactions of the ultra-high-energy cosmic rays with the microwave background radiation.
- Measure the extragalactic background light between 1 and 100 microns to understand the star formation history of the Universe.
- Measure the mass hierarchy of the neutrinos.
- Search for physics beyond the standard model encoded in cosmic messengers as they cross the Universe.
- Understand the origins of the matter antimatter asymmetry of the Universe.
- Probe the fundamental nature of spacetime.

In many of these areas future progress will depend upon either the detailed understanding of particle acceleration in the universe or the development of methods for controlling systematic errors introduced by our lack of understanding of these processes. High-resolution gamma ray measurements (spectral, angular, and temporal) of many objects and classes of objects are needed to find the source invariant physics that is the signal for physics beyond the standard model. Such measurements in conjunction with measurements at other wavelengths and with measurements of cosmic rays, neutrinos, and gravity waves will enable us to understand Nature's particle accelerators.

### **Recommendations:**

- Significant U.S. participation in the CTA project [28]. U.S. scientists developed the imaging atmospheric Cherenkov technique. Continued leadership in this area is possible with the development of novel telescope designs. A U.S. proposal to more than double the number of mid-scale telescopes would result in a sensitivity gain of 2-3 significantly improving the prospects for the indirect detection of dark matter, understanding particle acceleration processes, and searching for other signatures of physics beyond the standard model.
- Simultaneous operation of Fermi, HAWC, and VERITAS. Understanding particle acceleration and separating astrophysical processes from physics beyond the standard model requires observations over a broad energy range. The above three instruments will provide simultaneous coverage from 30 MeV to 100 TeV. HAWC and VERITAS will simultaneously view the same sky enabling prompt follow up observations of transient phenomena.
- Construction of the PINGU neutrino detector [29] at the South Pole. U.S. scientists have been leaders in the field of high-energy neutrino observations. PINGU, by densely instrumenting a portion of the IceCube Deep Core array, will lower the energy threshold for neutrinos to a few GeV. This will allow for a measurement of the neutrino mass hierarchy using atmospheric neutrinos.
- Continued operation of the Auger and TA air shower arrays with upgrades to enhance the determination of the composition and interactions of cosmic rays near the energy of the GZK suppression, and flight of the JEM-EUSO mission [30, 31] to extend observations of the cosmic ray spectrum and anisotropy well beyond the GZK region.
- Construction of a next-generation ultra-high energy GZK neutrino detector either to detect GZK neutrinos [32] and constrain the neutrino-nucleon cross section at these energies [33, 34, 35, 36, 37], or rule out all but the most unfavorable parts of the allowed parameter space.

## 1.1 Ultra-High-Energy Cosmic Rays

HiRes [7], Auger [8, 10], and the Telescope Array (TA) [9] have established the existence of a suppression of the spectrum at the highest energies (above  $\sim 6 \times 10^{19}$  eV) as predicted by Greisen, Zatsepin, and Kuzmin (GZK) in 1966 [5, 6]. The GZK suppression is an example of the profound links between different regimes of physics, connecting the behavior of the highest-energy particles in the Universe to the cosmic microwave background radiation, and can be explained by the sub-GeV scale physics of photo-pion production occurring in the extremely boosted relativistic frame of the cosmic ray. A similar phenomenon occurs for primary nuclei due to excitation of the giant dipole resonance, resulting in photo-disintegration. For iron nuclei, this occurs at about the same energy per particle as the photo-pion process does for protons.

The composition of cosmic rays and their interactions with air nuclei may be probed by studies of the depth of shower maximum,  $X_{max}$  [38, 39, 40]. The mean value of  $X_{max}$  rises linearly as a function of the log of the energy, and depends on the nature of the primary particle, the depth of its first interaction, and the multiplicity and inelasticity of the interactions as the shower evolves. Lower energy observations of  $X_{max}$  indicate that the composition becomes lighter as the energy increases toward  $\sim 10^{18.3}$  eV [41, 42, 43], which suggests that extragalactic cosmic rays are mainly protons. However, at higher energies the Auger Observatory's high quality, high-statistics sample exhibits the opposite trend, along with a decreasing spread in  $X_{max}$  with increasing energy [10, 44]. Using current simulations and hadronic models tuned with LHC forward data, this implies the composition is becoming gradually heavier above  $10^{18.5}$  eV. A trend toward heavier composition could reflect the apparent GZK suppression being in fact the endpoint of cosmic acceleration in which there is a maximum magnetic rigidity for acceleration, resulting in heavy nuclei having the highest energy per particle.

Cosmic rays can be used to probe particle physics at energies far exceeding those available at the LHC. An alternative explanation for the observed behavior of  $X_{max}$  is a change in particle interactions not captured in event generators tuned to LHC data. Auger measurements using three independent methods find that these models do not describe observed showers well. For example, the observed muon content of showers measured in hybrid events at Auger is a factor 1.3 to 1.6 higher than predicted [45]. TA also observes a calorimetric energy that is about 1.3 times higher than that inferred from their surface detector using these models. An example of a novel phenomenon that may explain these observations is the restoration of chiral symmetry in QCD [46].

A critical step in fully understanding the  $X_{max}$  observations is to identify and correct the deficiencies in the beyond-LHC physics used in modeling showers. This requires continued operation of current hybrid detectors such as Auger and TA with upgrades to enable improved multiparameter studies of composition and interactions on a shower-by-shower basis. Enhancements of the surface detectors are particularly valuable because of the tenfold higher duty cycle than for fluorescence or hybrid operation.

Observations from space can extend studies of the spectrum and anisotropy beyond the GZK region with high statistics. Current ground-based observatories have observed hints of correlation of cosmic ray arrival directions with the local distribution of matter [47, 48, 49, 50, 51, 52], but higher statistics trans-GZK observations are required to identify sources. In addition, the question of whether the spectrum flattens again above the GZK suppression or continues to fall will distinguish between the GZK and acceleration limit scenarios. The JEM-EUSO mission has an instantaneous collecting area of  $\sim 40$  [30, 31] times that of existing ground-based detectors and, taking duty cycle into account, will increase the collecting area above the GZK suppression energy by nearly an order of magnitude.

## 1.2 Neutrinos

IceCube has recently reported the detection of two neutrinos with energies above 1 PeV and 26 events above 30 TeV with characteristics that point to an astrophysical origin [4]. These exciting results herald the beginning of the era of high-energy neutrino astronomy, and initiate the study of ultra-long baseline high-energy neutrino oscillations. Neutrino data complements observations of cosmic rays and gamma rays due to their origin in the decays following high-energy hadronic interactions and their weak couplings. Several acute issues in particle physics and astrophysics can be addressed by neutrino experiments.

*GZK Neutrinos* Neutrinos are produced by the weak decays of the mesons and neutrons produced in the interaction of UHE cosmic rays with the CMB [32]. The production of these neutrinos takes place via well-known physics at high Lorentz boost, so robust predictions of the neutrino flux can be made. This flux depends on the composition of the primary cosmic rays and the evolution of the cosmic ray source density with redshift. Unlike many searches, there is a lower limit on the expected flux. Current detectors such as IceCube [53, 54], Auger [55], RICE [56] and ANITA [57, 58] have begun to probe the highest predicted values of the neutrino flux. Next generation experiments such as ARA, ARIANNA, and EVA can increase our sensitivity by about two orders of magnitude, and will either detect GZK neutrinos or rule out much of the parameter space. If GZK neutrinos are detected, the event rate as a function of zenith angle can be used to measure the neutrino-nucleon cross section and constrain models with enhanced neutrino interactions at high energy.

*Atmospheric Neutrinos and the Neutrino Mass Hierarchy* PINGU [29] is a proposed high-density infill of the IceCube detector with a reduced energy threshold of a few GeV, employing the rest of IceCube as an active veto. PINGU has sensitivity to atmospheric  $\nu_\mu$  over a range of values of L/E spanned by the variation in the distance to the production region as a function of zenith angle and the energy spectrum of atmospheric neutrinos. Preliminary studies of PINGU indicate that over these values of L/E, atmospheric  $\nu_\mu$  oscillations can be used to determine the neutrino mass hierarchy with 3-5 $\sigma$  significance with two years of data with a 40 string detector [29].

*Supernova Neutrinos* The Long Baseline Neutrino Experiment [59] will consist of a large (10-35 kTon) liquid argon time projection chamber located at 4850 feet depth at the Homestake mine in South Dakota. Collective oscillations of neutrinos as they traverse the neutrinosphere lead to a spectral swap that leaves a signature in the energy spectrum of electron neutrinos that is dependent upon the neutrino mass hierarchy [60, 61, 62, 63]. In the event of a Galactic supernova, sufficient numbers of events would be detected to both measure the neutrino mass hierarchy and to elucidate the supernova mechanism.

## 1.3 Gamma Rays

High-energy gamma rays provide a unique view into the most extreme environments in the universe, allowing one to probe particle acceleration processes and the origin of the Galactic and extragalactic cosmic rays. Active galactic nuclei (AGN), supermassive black holes emitting jets of highly relativistic particles along their rotation axis, have been shown to be sites of particle acceleration [14, 15, 16, 17]. Outstanding issues in the acceleration processes include: the nature of the accelerated particles (hadronic or leptonic), the role of shock acceleration versus magnetic reconnection, and the formation and collimation of astrophysical jets [64, 65]. Answers to these questions will come from higher resolution measurements in the GeV-TeV regime, multi-wavelength campaigns with radio, x-ray, and gamma-ray instruments, multi-messenger observations with gamma rays, ultra-high energy cosmic rays, neutrinos, and potentially gravitational waves. Understanding these extreme environments and how they accelerate particles is of fundamental interest. In addition, these



high-energy particle beams, visible from cosmologically interesting distances, allow us to probe fundamental physics at scales and in ways that are not possible in earth-bound particle accelerators.

Recently, Fermi [1] and AGILE [2] measured the energy spectra of the supernova remnants W44 and IC44. The decrease in the gamma-ray flux below the pion mass in these sources is clear evidence for hadronic acceleration. This is the clearest evidence to date that some Galactic cosmic rays are accelerated in supernova remnants. The detection of high-energy neutrinos from a cosmic accelerator would be a smoking gun signature of hadronic acceleration. In the absence of multi-messenger signals multi-wavelength energy spectra (x-ray to TeV) can test both leptonic models, where the high-energy emission is derived from inverse Compton scattering of the x-ray synchrotron emission, and hadronic models, where gamma rays result from pion decays or proton synchrotron radiation.

*Backgrounds to dark matter searches.* Understanding the origin of the Galactic VHE gamma rays is critical in the interpretation of some signatures of dark matter annihilation. The recent results from PAMELA [11] and AMS [12] of the increasing positron fraction with energy is a clear signal that the current model of secondary production and transport through the Galaxy is not complete. There are three potential explanations for this signal: a new astrophysical source of positrons [66, 67], modified propagation of cosmic rays or secondary production in the source [68, 69], or dark matter annihilation [70]. An astrophysical source of positrons, pulsar wind nebula (PWN), is now known to also lead to an increasing positron fraction at high energies. Observations of the Geminga PWN in the TeV band by Milagro [71] have been used to normalize the flux of positrons in our local neighborhood from this source. The calculated positron fraction is an excellent match to the data [13]. Similarly, in searching for dark matter signatures from the Galactic center or galaxy clusters one must understand and measure the more standard astrophysical processes that may lead to signatures that are similar in nature to those expected from dark matter annihilation.

*Extragalactic background light.* In addition to advancing our understanding of particle acceleration and astrophysical backgrounds for dark matter searches, the intense gamma-ray beams generated by AGN and gamma-ray bursts can be used to probe the intervening space and search for physics beyond the standard model. Some areas that can be studied include: measuring the extragalactic background light (EBL), using the EBL to measure the intergalactic magnetic fields, and searching for axion-like particles (ALPs) (note, ALPs are not the QCD axion). The EBL pervades the universe and is the sum of all the light generated by stars and the re-radiation of this light in the infrared band by dust [72, 73, 74] and is therefore sensitive to the star formation history of the universe. The production of electron-positron pairs from photon-photon scattering of the EBL with high-energy gamma rays leads to an energy dependent attenuation length for high-energy gamma rays [75]. At the same time, cosmic rays (if they are accelerated by AGN) will interact with EBL and CMB along the line of sight and generate secondary gamma rays at relatively close distances of the observer [76]. This absorption, with the inclusion of secondary gamma rays, can be used to measure or constrain the EBL [73, 74]. Lower limits on the EBL can be established from galaxy counts [72]. A signature of new physics would be an inconsistency between these lower limits and the measurements of the TeV spectra from AGN. Such a discrepancy could be explained either by the secondary production of gamma rays from cosmic rays produced at AGN or by photon-alp mixing mediated by the intergalactic magnetic fields.

*Intergalactic magnetic fields.* The origin of the Galactic magnetic fields remains a mystery. While astrophysical dynamos can efficiently amplify pre-existing magnetic fields, the generation of a magnetic field is difficult [77]. The strength of the magnetic fields in the voids between galaxy clusters should be similar to the primordial magnetic field. Measurement of AGN spectra and time delays in the GeV-TeV region have been used to set both lower and upper bounds on the strength of the IGMF [78, 79]. Current bounds are model dependent and span a large range of values for the magnetic field [80]. Improved measurements of the EBL, the measurement of variability from distant AGN, and improved determinations of the energy spectra (and understanding of the intrinsic AGN spectra) are needed to significantly improve these limits.

*Tests of Lorentz invariance violation.* Experimentally probing Planck-scale physics, where quantum gravitational effects become large, is challenging. A unique signature of such effects would be the violation of Lorentz invariance (a natural though not necessary property of theories of quantum gravity) [81, 82, 83]. Short, intense pulses of gamma rays from distant objects such as gamma ray bursts and active galaxies, provide a laboratory to search for small, energy dependent, differences in the speed of light. Current limits have reached the Planck scale if the energy dependence of the violation is linear [84] and  $6.4 \times 10^{10}$  GeV if the violation is quadratic [85] with energy. Future instruments could improve upon these limits by at least a factor of 10 and 50 (respectively) and significantly increase the sample size used to search for these effects.

*TeV Gamma-Ray Instruments.* Ground-based TeV instruments fall into two classes: extensive air shower (EAS) arrays, capable of simultaneously viewing the entire overhead sky, and imaging atmospheric Cherenkov telescopes (IACTs), pointed instruments with high sensitivity and resolution. Current IACTs are VERITAS, MAGIC, and HESS, while the HAWC (under construction) and Tibet arrays are the only operating EAS arrays. The next generation of IACT, known as CTA, will consist of a large array of IACTs with roughly an order of magnitude greater sensitivity than current instruments. It is expected to discover over 1000 sources in the TeV band [28, 86]. The U.S. portion of the collaboration is proposing to more than double the number of mid-sized telescopes to over 50 using a novel optical design that will improve the sensitivity of CTA by a factor of 2-3 (a result of improved angular resolution of the new telescopes and an increase in the number of telescopes).

## 1.4 Baryogenesis

According to standard cosmology, the current preponderance of matter arises during the very early universe from an asymmetry of about one part per hundred million between the densities of quarks and antiquarks. This asymmetry must have been created after inflation due to some physical process known as baryogenesis. Baryogenesis requires extending the standard model of particle physics, via some new physics which must couple to standard model particles and which must be important during or after the end of inflation. Constraints on the inflation scale and on the reheat temperature at the end of inflation give an upper bound on the relevant energy scale for baryogenesis. The new physics must violate CP (symmetry between matter and antimatter) as the CP violation in the standard model is insufficient [87]. There are a very large number of theoretical baryogenesis proposals. Some well-motivated possibilities are:

*Leptogenesis* Theoretically, baryon number violation at high temperatures is rapid in the standard model via nonperturbative electroweak processes known as sphalerons. Sphalerons conserve the difference between baryon and lepton numbers, leading to the idea of leptogenesis [88]. The decay of very heavy neutrinos in the early universe could occur in a CP violating way, creating a lepton asymmetry that the sphalerons convert into a baryon asymmetry. Whether and how leptogenesis could occur can be clarified by intensity frontier experiments (CP violation and lepton number violation in neutrino physics) [89], cosmic frontier experiments (most leptogenesis proposals require a high inflation scale which can be constrained in cosmic microwave background measurements), and energy frontier experiments [90] (because whether or not other new physics exists has important implications for leptogenesis).

*Affleck-Dine baryogenesis* In supersymmetric theories condensates of the scalar partners of quarks and leptons have relatively low energy density and are likely to be present at the end of inflation [91]. The subsequent evolution and decay of the condensates can produce the baryon asymmetry, and in some models, the dark matter [92, 93]. The dark matter could be macroscopic lumps of scalar quarks or leptons known as Q-balls, which have unusual detection signatures in cosmic frontier experiments [94]. A critical test of this theory is the search for supersymmetry, primarily via collider experiments. Instruments such as HAWC and IceCube

will be sensitive to extremely low fluxes of Q-balls - over two orders of magnitude lower than current limits. While the non-observation of Q-balls can not rule out the Affleck-Dine mechanism, the observation of a Q-ball would have a profound impact on our understanding of the universe.

*Electroweak baryogenesis* New non-standard model particles that are coupled to the Higgs boson can provide a first order phase transition for electroweak symmetry breaking, which proceeds via nucleation and expansion of bubbles of broken phase. CP violating interactions of particles with the expanding bubble walls can lead to a CP violating particle density in the symmetric phase, which can be converted by sphalerons into the baryon asymmetry [95, 96]. The baryons then enter the bubbles of broken phase where the sphaleron rate is negligible. This scenario can be definitively tested via the search for new particles in high-energy colliders, and via nonvanishing electric dipole moments for the neutron and for atoms. Non-standard CP violation in  $D$  and  $B$  physics may appear in some models. A non standard Higgs self-coupling is a generic consequence. The first order phase transition in the early universe can show up via relic gravitational waves.

Other experiments that can shed light on baryogenesis include searches for baryon number violation. Neutron anti-neutron oscillations violate the difference between baryon and lepton numbers, and most leptogenesis scenarios will not work if such processes are too rapid. Proton decay would provide evidence for Grand Unification, which would imply the existence of heavy particles whose decay could be responsible for baryogenesis, and which is a feature of some leptogenesis and supersymmetric models.

## 1.5 Fundamental nature of spacetime

Quantum effects of space-time are predicted to originate at the Planck scale. In standard quantum field theory, their effects are strongly suppressed at experimentally accessible energies, so space-time is predicted to behave almost classically, for practical purposes, in particle experiments. However, new quantum effects of geometry originating at the Planck scale from geometrical degrees of freedom not included in standard field theory may have effects on macroscopic scales [97, 98] that could be measured by laser interferometers such as the holometer [99]. In addition, cosmic particles of high energies can probe departures from Lorentz invariance [100] and the existence of extra-dimensions on scales above the LHC.

## 1.6 Overview of the Report

The Cosmic Frontier number 6, named Cosmic Probes of Fundamental Physics, was charged with summarizing current knowledge and identifying future opportunities (both experimental and theoretical) in the use of astrophysical probes of fundamental physics. Because of the breadth of this area of research CF6 has been subdivided into 3 main topical areas:

- CF6-A Cosmic Rays, Gamma Rays and Neutrinos (conveners: Gus Sinnis, Tom Weiler)
- CF6-B The Matter of the Cosmological Asymmetry (convener: Ann Nelson)
- CF6-C Exploring the Basic Nature of Space and Time (conveners: Aaron Chou, Craig Hogan)

We received 14 whitepapers addressing the current challenges and future opportunities in each of these fields as they relate to the other frontiers of high energy physics.

### 1.6.1 CF6-A Cosmic Rays, Gamma Rays and Neutrinos

Cosmic rays, gamma rays, and neutrinos from astrophysical sources can be used to probe fundamental symmetries, particle interactions at energies not attainable on Earth, and understand the nature of particle acceleration in the cosmos. CF6-A encompasses the following topical areas: The Physics of Interactions Beyond Laboratory Energies (hadronic and weak interactions at high energies) Cosmic Particle Acceleration (origin of the cosmic radiation from GeV to ZeV, astrophysical backgrounds to fundamental physics) Cosmic Standard Model (SM) Particles as Probes of Fundamental Physics (violation of Lorentz invariance, extra dimensions, axions) New Particles (anti-nuclei, strangelets, Q-Balls, primordial black holes) Neutrino Physics from Astrophysics (in conjunction with the Intensity Frontier IF3: neutrino mass hierarchy, leptonic CP violation, neutrino interactions in supernovae, non-standard neutrino interactions with matter)

This field is ripe for new discoveries. Recent examples include the detection by the Fermi and AGILE space missions of a pion-zero decay produced gamma-ray signal in supernova remnants W44 and IC44 [101]; the first detection of 10 TeV to PeV neutrinos by Icecube [102]; and the precise positron fraction measurement of the Alpha Magnetic Spectrometer [103].

### 1.6.2 CF6-B The Matter of the Cosmological Asymmetry

The cosmological asymmetry between baryons and anti-baryons is one of the strongest pieces of evidence for physics beyond the standard model. There are diverse theoretical proposals for new physics at a range of energy scales, most of which include new sources of CP violation, and either additional baryon or lepton number violation. There are plausible theories with implications for experiments at all three frontiers. Leptogenesis theories predict new CP violation in the neutrino sector. Grand Unified theories predict proton decay. Electroweak baryogenesis models predict a cosmological phase transition which leaves traces in gravitational wave and CMB experiments, and new collider physics at or below a TeV.

We survey what we may expect to learn about the origin of matter from searches at ongoing, planned and proposed facilities such as the LHC, ILC, CLIC, muon collider, B-factories, neutrino experiments, gravitational wave experiments and CMB experiments.

### 1.6.3 CF6-C Exploring the Basic Nature of Space and Time

Space and time may be quantized at the Planck scale. Effects from this extremely high-energy realm may be studied through gravitational waves from the early universe and holographic noise.

We survey what we may expect to learn about the GUT and Planck energy scale with gravitational waves and holographic noise. Survey the theory and ongoing, planned, and proposed gravitational wave and holographic noise experiments. Examples of relevant experiments include the Holometer, LIGO, LISA, and CMB probes of early universe gravitational wave (covered in Dark Energy and CMB.)

## 2 CF6-A: Cosmic Rays, Gamma Rays, and Neutrinos

### 2.1 Cosmic rays and Particle Acceleration

#### 2.1.1 Ultra high energy cosmic ray origins

Ultra-high energy cosmic rays (UHECRs), now commonly taken to be CRs with energies  $> 6 \times 10^{19}$  eV, were first reported just over 50 years ago by John Linsley [104]. These are the only particles with energies exceeding those available at terrestrial accelerators. The Large Hadron Collider (LHC) will reach an equivalent fixed-target energy of  $10^{17}$  eV, whereas UHECRs have been observed with energies in excess of  $10^{20}$  eV. With UHECRs one can conduct particle physics measurements up to two orders of magnitude higher in the lab frame, or one order of magnitude higher in the center-of-mass frame, than the LHC energy reach. As discussed in more detail below, the properties of UHECR air showers appear to be inconsistent with models which are tuned to accelerator measurements; one possible explanation is that new physics intervenes at energies beyond the LHC reach. UHECR experiments are the only way to access this energy range and make detailed measurements of air showers in order to address this question. It is worth noting that cosmic ray experiments have already yielded particle physics results at energies far exceeding those accessible to the LHC, one of the latest being a measurement of the  $p$ -air cross-section at  $\sqrt{s} = 57$  TeV [40], a result which excludes some hadronic models' extrapolations beyond LHC energies.

The two largest currently operating UHECR observatories are the Pierre Auger Observatory in the Southern hemisphere, covering an area of 3000 km<sup>2</sup>, and the Telescope Array (TA) in the Northern hemisphere, covering about 700 km<sup>2</sup>. Both observatories employ hybrid detection techniques, sampling cosmic ray air shower particles as they arrive at the Earth's surface and also detecting the fluorescence light produced when UHECR air showers excite atmospheric nitrogen, for the  $\sim 10\%$  of events arriving on dark, moonless nights. Both Auger and TA feature "low energy" extensions, which will provide an overlap with the LHC energy regime, while also allowing measurements in the galactic-to-extragalactic transition region.

The most important result so far from the present generation of observatories is the conclusive evidence that the UHECR flux drops precipitously at high energy. The discovery of a suppression at the end of the cosmic ray spectrum was first reported by HiRes and Auger [7, 8] and later confirmed by TA [9]; by now the significance is well in excess of  $20\sigma$  compared to a continuous power law extrapolation beyond the ankle feature [10]. This suppression is consistent with the GZK prediction that interactions with cosmic background photons will rapidly degrade UHECR energies [5]. Intriguingly, however, there are also indications that the source of the suppression may be more complex than originally anticipated.

Lower energy observations of the elongation rate (the rate of change with energy of the mean depth-of-shower-maximum,  $X_{max}$ ) [41, 105, 106, 107], indicate that the composition becomes lighter as energy increases toward  $\sim 10^{18.3}$  eV, fueling a widespread supposition that extragalactic cosmic rays are primarily protons. At the highest energies however the situation remains ambiguous. HiRes and TA observe an elongation rate consistent with a light, unchanging composition, supporting the model in which the highest energy cosmic rays are protons and the energy spectrum is shaped by interactions with the CMBR [108, 45]. However the Auger Observatory's data exhibits a decreasing elongation rate as well as a decreasing spread in  $X_{max}$  with increasing energy. Interpreted with present shower simulations, this implies that the composition is becoming gradually heavier beginning around  $5 \times 10^{18}$  eV [109, 44]. If true, this would have important implications for the astrophysics of the sources. A trend toward heavier composition could reflect the endpoint of cosmic acceleration, with heavier nuclei dominating the composition near the end of the spectrum — which coincidentally falls off near the expected GZK cutoff region [110]. In this scenario, the suppression would

constitute an imprint of the accelerator characteristics rather than energy loss in transit. It is also possible that a mixed or heavy composition is emitted from the sources, and photodisintegration of nuclei and other GZK energy losses suppress the flux [108].

An alternative possibility for the origin of the break in the elongation rate could be even more interesting: this feature might arise from some change in the particle interactions at UHE not captured by event generators tuned to LHC and other accelerator data. Adding weight to this possibility are the Auger measurements, using three independent methods, showing that existing hadronic interaction models do not simultaneously fit all shower observables. For example, the actual hadronic muon content of UHE air showers measured in hybrid events is a factor 1.3–1.6 larger than predicted by models tuned to LHC data [45], even allowing for a mixed composition. Thus a critical step required to fully understand  $X_{\text{max}}$  observations is to identify and correct the deficiencies in current shower models. This is a strong motivation for upgrading present-generation detectors to enable full understanding of the hadronic interactions involved in air shower development. Fortunately, the information which will be accessible in shower observations – including the correlation between  $X_{\text{max}}$  and the ground signal in individual hybrid events [111], the comparison between  $X_{\text{max}}$  and  $X_{\text{max}}^{\mu}$  (the atmospheric depth where muon production is maximum), the dependence of ground signal on zenith angle, and other detailed shower observations – is so rich and multifaceted that it will enable composition and particle physics to be disentangled [111].

An additional intriguing twist in the present observational situation is that the HiRes and TA results are consistent with a proton dominated flux everywhere above the ankle [112, 113], although with present statistics the TA and Auger elongation rates are consistent within errors [114]. Since the sources seen by the HiRes and TA in the Northern hemisphere may not be the same sources as seen by the Auger Observatory in the South, the composition need not be the same. When TA statistics are sufficient to make a clear determination as to whether the elongation rate observed in the North is the same as recorded by the Auger observatory in the South, it will be of great consequence for astrophysics even without knowing exactly how to translate from elongation rate to composition. If the composition (elongation rate) in North and South are not the same, it will mean *i*) that there are at least two source types, one accelerating primarily protons and another accelerating a mixed composition, and *ii*) that in at least one hemisphere, the UHECRs are produced mainly by one or a small number of sources. This is a strong motivation for increasing the aperture of TA as described in Section 2.5.1.

Another major result of the present generation of observatories is the search for anisotropy in the distribution of arrival directions. Around  $10^{18}$  eV, Auger has provided a strong upper limit on the dipole anisotropy [115, 116] which is almost sufficient to rule out a Galactic origin assuming these cosmic rays are indeed predominantly protons and making reasonable assumptions about the Galactic magnetic field (GMF). When the TA and Auger data are combined, the limit will be even stronger or a signal will be found [117].

As the energy increases, evidence for anisotropy mounts. Auger has reported a notable correlation of cosmic ray arrival directions with nearby galaxies of the Veron-Cetty and Veron catalog of Active Galactic Nuclei (AGN) [47]. With more data accumulated, the central value of the correlation fraction has decreased but the significance has remained at the 3-sigma level [49, 50]. The HiRes experiment did not observe such a correlation [118], but the most recent results from TA [51, 52] show a degree of correlation compatible with that seen by Auger in its full data set, and with a similar pre-trial significance. Furthermore, TA finds a significant correlation between the highest energy events' pointing directions and the local large-scale structure of the universe [119].

While indications of anisotropy are becoming stronger, a completely clear picture is thus far elusive, especially regarding the identity of the sources themselves. Perhaps a clear picture should not be expected, given the possibility of multiple types of sources and that fact that the composition in the South could be mixed or become heavy at the highest energies, while at the same time the flux could be more proton-dominated in

the North. Adding to the difficulty of comparing correlation results of Northern and Southern hemisphere observatories is the fact that the magnitude and directions of magnetic deflections and the degree of multiple-imaging are expected to vary quite strongly across the sky [120]. Fortunately astrophysical observations and theoretical effort are rapidly improving GMF models [121], so that the back-tracking to correct for deflections should become feasible, to some extent, on the time-scale of the next generation of experiments.

### 2.1.2 Astrophysical Particle Acceleration and Gamma Ray Observations

In the very-high-energy (VHE) band (defined here as gamma rays between approximately 50 GeV and 100 TeV) one sees only non-thermal radiation, mostly from the acceleration of charged particles by the most extreme objects in the universe (some non-thermal radiation may be due to the decay or annihilation of fundamental particles). Within our Galaxy these objects include supernova remnants, rapidly spinning neutron stars, stellar mass black holes, and x-ray binary systems (composed of a black hole or neutron star orbited by another star). Extragalactic objects that accelerate particles include supermassive black holes, gamma-ray bursts, starburst galaxies, and galaxy clusters. Many of these objects have extreme gravitational and magnetic fields, which may play a central role in the acceleration of particles in relativistic jets. By studying these sources we can discover the sources of the Galactic and extragalactic cosmic rays, study physics in extreme environments, and search for signatures of physics beyond the Standard Model.

In the past decade we have discovered that particle acceleration is ubiquitous in the universe. As VHE telescopes have improved in sensitivity we have found more objects and more classes of objects where particle acceleration occurs. From both gamma-ray and cosmic-ray observations we know that somewhere in the universe there are objects capable of accelerating fundamental particles to over  $10^{20}$  eV. Understanding these extreme environments and how they accelerate particles is of fundamental interest. In addition, these high-energy particle beams, visible from cosmologically interesting distances, allow us to probe fundamental physics at scales and in ways that are not possible in earth-bound particle accelerators. In most cases the astrophysical signatures of the particle acceleration processes are encoded and multiplexed with signatures from physics beyond the Standard Model. Thus, to extract information related to Beyond the Standard Model Physics it is necessary to understand the particle acceleration mechanisms and any imprints on the gamma-ray energy spectrum that may arise from the local environment.

**Galactic Sources of VHE Gamma Rays** Cosmic rays were discovered over one hundred years ago [122]. Cosmic rays with energies below about  $10^{17}$  eV are likely accelerated within the Galaxy. Because protons and other cosmic-ray nuclei are charged they bend in the Galactic magnetic field and do not point to their origin. Any site of cosmic rays should also produce gamma rays. Recent gamma-ray measurements by Fermi and VERITAS have conclusively shown that supernovae are sites of cosmic-ray acceleration [1, 3], solving a century old problem.

The recent observations of an increasing positron:electron ratio above 100 MeV [11, 123] may be attributed to the annihilation of dark matter particles with mass  $\sim 100$  GeV. However, before attributing this signature to the dark matter it is important to understand any potential astrophysical backgrounds that may contribute to (or even dominate) the positron fraction at high energies. Pulsar wind nebulae (PWN) are a potential source of high-energy positrons that could mimic the signature from dark matter decay. Thus it is important to understand the energy spectrum of PWN and the propagation of cosmic-ray electrons and positrons to understand the origin of the PAMELA signal. At VHE energies PWN dominate the Galactic sources with over 30 discovered to date [17]. PWN accelerate electrons and positrons in equal numbers at the termination shock of the pulsar wind. These electrons and positrons are then trapped by the magnetic field of the nebula and produce gamma rays via inverse Compton interactions with the CMB and low energy photons in the

nebula. As the nebula expands, the magnetic field weakens and eventually the electrons and positrons are released to propagate through the Galaxy. Vela X-1 and Geminga are two nearby pulsars that may contribute significantly to the local positron/electron ratio. Recent measurements of TeV gamma rays from Geminga by the Milagro telescope [84] have been used to show that the local positron to electron ratio, based solely on Geminga as a source, is consistent with the observations of PAMELA [13]. Data at higher energies will be needed to distinguish a dark matter source (where one expects the ratio to fall above the dark matter mass) from PWN.

**Extragalactic Sources of VHE Gamma Rays** The predominate class of extragalactic object detected in the VHE energy band are active galactic nuclei (AGN), accretion powered super-massive black holes with relativistic jets emitted along their rotation axes. VHE gamma rays have also been detected from starburst galaxies [124], presumably from cosmic-ray generation and interactions in those galaxies. Galaxy clusters and gamma-ray bursts are other important potential sources of VHE gamma rays that so far have eluded detection in this energy band. Here we discuss these sources and their implications for particle acceleration and fundamental physics (details on the fundamental physics can be found in other sections of this chapter).

VHE observations of galaxy clusters may provide the best sensitivity to the annihilation or decay of dark matter. However, there are several astrophysical mechanisms by which galaxy clusters can produce VHE gamma rays. Galaxy clusters may contain active galaxies, known sources of VHE gamma rays, structure formation shocks can accelerate injected electrons and protons, and cosmic rays accelerated within the cluster will produce gamma rays through the decay of neutral pions when they interact with the intracluster medium. While the non-observation of VHE emission from a galaxy cluster can be used to set stringent limits on the presence of WIMP-like dark matter, the detection of a dark matter signal will rely on our understanding of astrophysical production of gamma rays within galaxy clusters.

AGN have proved to be prolific sources of VHE gamma rays. The observed high-energy emission is strongly dependent on the viewing angle with respect to the jet, as the bulk of the VHE gamma rays are produced by processes within the jets. AGN provide an excellent beam of photons with which to perform fundamental physics studies. If one can understand the inherent spectrum of these objects the observed spectrum at earth can be used to search for the existence of axion-like particles. Since active galaxies exhibit strong flaring behavior on short timescales they can be used to time the relative arrival time of photons of different energies to search for violations of Lorentz invariance. Since there are many active galaxies detected over a large range of redshifts when can use the redshift dependence of an observed signature to help disentangle the astrophysical phenomena from the fundamental physics. However, before extracting such fundamental physics one must understand the acceleration mechanism, the inherent spectrum of gamma rays, and the observed source-to-source variations.

Currently there is much that is not understood about particle acceleration in AGN. The standard model of acceleration in jets is based on the first-order Fermi mechanism, where particles are accelerated via reflections from fast moving shocks. However, the importance of magnetic reconnection as an acceleration mechanism in AGN is not understood and depends on the relative energy carried by particles or an electromagnetic field. The nature of the particles accelerated by jets is also not known. Most observations are consistent with the acceleration of electrons and the subsequent production of gamma rays via inverse Compton scattering from lower energy photons. However, hadronic models can not be ruled out and are required if the ultra-high-energy cosmic rays are produced in AGN.

Gamma-ray bursts (GRBs) are the most violent objects in the universe, emitting over  $10^{52}$  ergs in gamma rays. There are believed to be two classes of GRBs: the first whose progenitors are massive stars undergoing core collapse supernovae and the other merger events of neutrons stars or neutron star black hole systems. In both cases it is believed that accretion onto a black hole powers highly relativistic jets where particles



are accelerated to high energies. In some GRBs a solar mass of material may be accelerated to bulk velocities approaching the speed of light ( $\Gamma \sim 1000$ ). The time duration of GRBs spans the range from a few milliseconds to 1000 seconds and in many cases fine substructure is present in the gamma-ray arrival times. Energy dependent time lags in the GRB onset and the structure within a burst can be used to search for small effects due to violation of Lorentz invariance. As with AGN it is necessary to understand the inherent time evolution of the GRB energy spectrum to extract the fundamental physics. To date the highest energy gamma ray detected from a GRB had an energy at earth of 94 GeV [125], which corresponds to an energy of 125 GeV at the GRB's redshift of 0.34. No convincing detection of a GRB has been made by a ground-based VHE instrument, though the next generation of wide-field instrument, HAWC, should have sufficient sensitivity to detect the more energetic GRBs [126].

Detecting an axion signature in the energy spectrum of AGN requires knowledge of the inherent AGN spectrum and the density of the extragalactic background light (as a function of redshift). To attribute any observed energy dependent time delay of photons from distant sources such as AGN or GRBs requires knowledge of the time evolution of the gamma-ray spectra from these objects. While the current generation of VHE instruments has made enormous progress in detecting new sources and classes of sources, the next generation of instruments must have the precision and sensitivity to disentangle the astrophysical processes from the fundamental physics processes. This will require excellent energy and angler resolution, multiple source detections with a large span of redshifts, and multi-wavelength and multi-messenger campaigns to truly understand the astrophysical process of particle acceleration in these extreme objects.

## 2.2 Neutrino Physics from Astrophysics

### 2.2.1 GZK Neutrinos

Neutrinos result from the cascade of decays following cosmic ray interactions with the microwave background. The processes involved in the production of these neutrinos are well-known low-energy particle physics boosted by the large Lorentz factor of the cosmic ray-CMB frame, and thus predictions of their fluxes are on a firm footing. The flux of these neutrinos depends on the composition of the highest energy cosmic rays and on the evolution of the cosmic ray sources with redshift. Measurement of the GZK neutrino flux would help disentangle the effect of cosmic ray interactions, composition, and source evolution, and provides a unique beam of high energy neutrinos to probe neutrino cross sections at EeV energies.

### 2.2.2 Supernova Burst Neutrinos

The measurement of the time evolution of the neutrino energy and flavor spectrum from supernovae can revolutionize our understanding of neutrino properties, supernova physics, and discover or tightly constrain non-standard interactions. Collective oscillations of neutrinos leaving the neutron star surface imprint distinct signatures on the time evolution of the neutrino spectrum that depend, in a dramatic fashion, on the neutrino mass hierarchy and the mixing angle  $\theta_{13}$  [60, 61, 62]. With  $\theta_{13}$  now measured to be non-zero [127] the measurement of the electron neutrino energy spectrum from a supernova burst can be used to determine the neutrino mass hierarchy. Figure 1 shows the resulting neutrino and antineutrino energy spectra for the normal and inverted hierarchies, before and after the spectral swapping from collective oscillations. Note that the change in the anti-neutrino energy spectrum (between the normal and inverted hierarchies) is much less dramatic than for the neutrino spectrum. A liquid argon detector such as LBNE is most sensitive to the electron neutrinos from a supernova burst measure the neutrino through the reaction  $\nu_e + {}^{40}\text{Ar} \rightarrow e^- + {}^{40}\text{K}^*$

and therefore best suited to measure the mass hierarchy of the neutrinos with supernova neutrinos. However, since the cosmic-ray backgrounds at the surface are quite large, the detector must be located underground to perform this physics. In addition, with the detection of 1000 or more neutrinos from a supernova one could temporally resolve the energy and flavor spectrum of the neutrinos and glean information about the supernova process and the formation of the remnant neutron star. For nearby Galactic supernovae, large detectors such as IceCube complement low-background detectors by providing data with high temporal resolution[128].

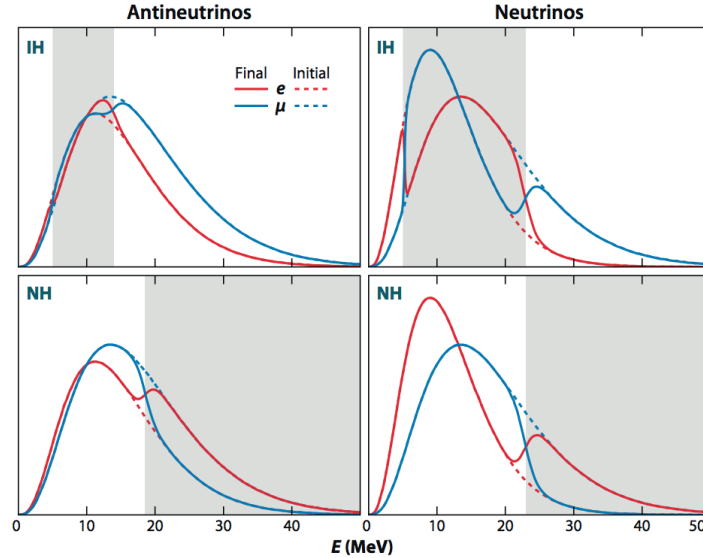


**Figure 1.** The antineutrino (left panels) and neutrino energy spectra (right panels) for the normal hierarchy (bottom panels) and the inverted hierarchy (top panels). In all 4 figures the dashed lines show the observed spectra in the absence of collective oscillations and the solid lines the spectra after the effect of collective oscillations. The figure is from [63]

### 2.2.3 Atmospheric Neutrinos

In addition to neutrinos from supernova bursts, nature provides a steady source of neutrinos that can be used to determine the neutrino mass hierarchy. The atmospheric neutrinos generated by extensive air showers travel through the earth. A detector sensitive to these neutrinos can measure neutrinos of with different energies that have traversed a range of baselines, thus probing a large space of  $L/E$ . The baselines available are approximately the diameter of the earth ( $\sim 12700$  km), in principle enabling sensitive searches for matter effects and sensitivity to the neutrino mass hierarchy. The Precision IceCube Next Generation Upgrade (PINGU) experiment [29], would provide an additional 20-40 strings (each with 60-100 photomultiplier tubes) to further “infill” the DeepCore array [18] within IceCube. With a string spacing of 20-25 meters (compared to 73 m spacing within DeepCore and 125 m spacing for IceCube), the energy threshold for neutrinos of would be  $\sim 5$  GeV.

Figure 2 shows the expected statistical significance on the determination of the neutrino mass hierarchy as a function of time for PINGU. The vertical band encompasses different configurations (20-40 strings) as well as varying detector efficiencies. A 5 standard deviation measurement could be made in 2-5 years of data taking. Since this is essentially a muon neutrino disappearance experiment, comparing the surviving fraction of muon neutrinos as a function of  $L$  and  $E$ , proper knowledge of the angular and energy resolutions

of PINGU are key to understanding the sensitivity to the neutrino mass hierarchy. The studies presented in [29] use algorithms developed for DeepCore to estimate these resolutions and the curves in Figure 2 are based on those algorithms.

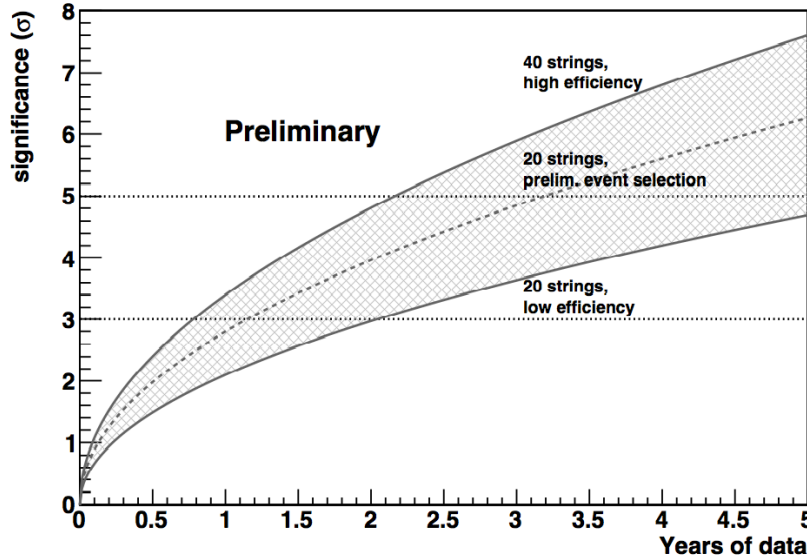


**Figure 2.** Estimated significant for determination of the neutrino mass hierarchy with PINGU. The top range is based on a 40 string detector with a high assumed signal efficiency in the final analysis. The bottom curve uses a 20 string detector and a lower assumed signal efficiency. The figure is from [29]

## 2.3 Cosmic Particles as Probes of Particle Physics Beyond Laboratory Energies

### 2.3.1 Hadronic Interactions

Ultra high energy cosmic ray measurements can be used to constrain hadronic interaction cross sections and multiplicities at energies far beyond those accessible using terrestrial accelerators. While the composition of the primary cosmic ray beam remains an open question, even a small admixture of protons allows extraction of the proton-air cross section from the tail of the distribution of the depth of shower maximum  $X_{max}$  toward large atmospheric depths. For example, Auger data has been used to perform a measurement of the  $p$ -air cross-section at  $\sqrt{s} = 57$  TeV [40], a result which excludes some hadronic models' extrapolations beyond LHC energies.

In addition, detailed analysis of the spectrum and anisotropy of cosmic rays together with  $X_{max}$  and other observables that are diagnostics of composition and hadron interactions may ultimately allow the composition and interactions of cosmic rays to be disentangled. Recent developments in this area are discussed below in [cross reference to cosmic ray origins section].

### 2.3.2 Neutrino Cross Sections at Extremely High Energies

Large neutrino telescopes can measure the neutrino-nucleon cross-section by studying neutrino absorption in the Earth [33, 34, 35]. At high energies, this cross-section is sensitive to new physics. In particular, if there

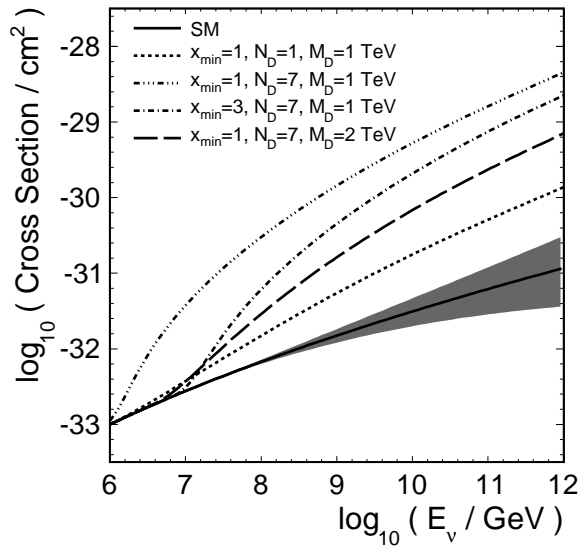


**Figure 3.** The neutrino interaction cross-section for the standard model, plus several models that incorporate additional dimensions.[36]

are additional rolled-up dimensions, then the cross-section will increase sharply at an energy corresponding to the inverse size of the extra dimension(s). Figure 3 shows the neutrino-nucleon cross-sections calculated for the Standard Model, plus several models with additional dimensions[36]. Other types of new physics can produce similar effects. For example, the presence of leptoquarks could produce a similar increase in the cross-section[37].

Neutrino absorption becomes an effective technique for measuring the cross section at neutrino energies above about 50 TeV, the energy at which absorption (assuming the Standard Model cross-sections) begins to reduce the flux of vertically upward-going neutrinos, altering the zenith angle distribution. Figure 4 shows the expected zenith angle distribution for neutrinos with energies between  $10^{13}$  and  $10^{21}$  eV. Lower energy neutrinos can be used as a normalization, to check the angular acceptance of the detector, and to calibrate for the small zenith angle dependence in the atmospheric neutrino flux.

At neutrino energies much above  $10^{17}$  eV, the cross sections depend significantly on parton distributions at Bjorken  $x$  and  $Q^2$  values beyond the reach of HERA data, so extrapolations are required to predict the cross sections. LHC data can be used to constrain the parton distributions, but, even at current experiments like IceCube, the neutrino energies are 100 times higher than are accessible at accelerators. So, surprises are certainly possible, especially for new physics with large couplings to the neutrino sector.

### 2.3.3 Violation of Lorentz Invariance

The development of theories that merge general relativity and quantum mechanics - quantum gravity, typically lead to the violation of invariance principles that have been sacrosanct in physics. The simple fact that quantum mechanics requires a minimum length scale (typically taken to be the Planck length ( $1.6 \times 10^{-35}$  m or  $1.2 \times 10^{19}$  GeV)) that is independent of reference frame, is in itself a violation of Lorentz invariance which is scale independent [81]. Probing physics at the Planck scale is difficult or impossible in earth-bound experiments, however nature has provided a mechanism by which we may probe certain aspects

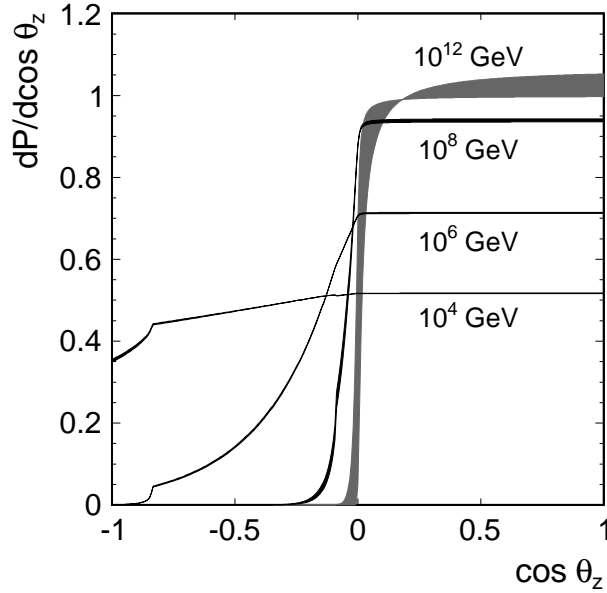


**Figure 4.** The zenith angle distribution for high-energy neutrinos of different energies, for Standard Model cross sections. At energies above  $10^{17}$  eV, absorption in the Earth limits the flux of upward-going neutrinos, except near the horizon. [36]

of Lorentz invariance violation to extraordinary precision. In addition to quantum gravity, other motivations for considering violations of Lorentz invariance include the need for a high-energy cutoff to control divergences in quantum field theory [82], and to develop a consistent theory of black holes [83]. One possible manifestation of the breaking of Lorentz invariance is a vacuum dispersion relation, an energy dependence to the velocity of light. The energy dependence of the speed of light can be probed to high accuracy by measuring the time of high-energy, short pulses of light that have travelled cosmological distances. Gamma-ray bursts and flares from active galaxies provide an excellent laboratory for such an investigation. (For a review of other manifestations of a violation of Lorentz invariance see [129].)

When considering a vacuum dispersion relation for electromagnetic radiation one typically performs a simple expansion with linear and quadratic terms:

$$\frac{v(p)}{c} = 1 + \zeta_1 \left( \frac{p}{E_{QG}} \right) + \zeta_2 \left( \frac{p}{E_{QG}} \right)^2 \quad (1)$$

where  $\zeta_n^s$  is either zero or one. The linear and quadratic terms are often treated independently (i.e. one of the  $\zeta_n^s$  is zero). The linear term violates CPT invariance [130, 131], while the quadratic term preserves CPT invariance. The above dispersion relation then leads to an energy dependent delay [100]:

$$\Delta t \approx \left( \frac{\Delta E}{\zeta_n E_{QG}} \right)^n \frac{L}{c} \quad (2)$$

The dispersion relation may have a directional dependence [132], which argues for a sample of bursts and flares large enough to probe the dispersion relation in several directions.

The best limits on the linear term come from Fermi LAT observations of distant gamma-ray bursts and have probed to energies above the Planck scale [84]. The best limits on the quadratic term (where energy

reach is more important than distance) are derived from observations of flaring active galaxies by imaging atmospheric Cherenkov telescopes ( $E_{QG} > 6 \times 10^{11}$  GeV [133]. Current limits on both the linear and quadratic terms are given in Table 0-1.

**Table 0-1.** Current lower bounds on the energy scale where Lorentz invariance is violated. Limits for the linear(quadratic) term are given assuming that the quadratic(linear) term is zero. Adapted from [134]. A superscript  $l, q$  indicates that the limit applies to either the linear or quadratic term.

Source	Experiment	Limit	Reference
Mrk 421	Whipple	$E_{QG}^l > 4 \times 10^{16}$ GeV	[135]
PKS 2155-304	H.E.S.S.	$E_{QG}^l > 2.1 \times 10^{18}$ GeV	[85]
PKS 2155-304	H.E.S.S.	$E_{QG}^q > 6.4 \times 10^{10}$ GeV	[85]
GRB 090510	Fermi GBM+LAT	$E_{QG}^l > 1.5 \times 10^{19}$ GeV	[84]
GRB 090510	Fermi GBM+LAT	$E_{QG}^q > 3 \times 10^{10}$ GeV	[84]

Future experiments such as CTA and HAWC are expected to improve upon these limits and increase the sample size of bursts and flares to probe any directional dependence to the vacuum dispersion relation. For example if HAWC observed a single gamma-ray burst at a redshift of 1 and could time the arrival of the high energy photons ( $> 100$  GeV) to one second, the limit on  $E_{QG}$  from that single observation would be  $4.9 \times 10^{19}$  GeV for the linear term and  $1.5 \times 10^{11}$  GeV for the quadratic term, roughly a factor of 2 higher than the best current limits [136]. The improvement from CTA is more dramatic. CTA will have roughly an order of magnitude greater sensitivity than VERITAS or H.E.S.S. Therefore CTA should improve the current limits on the quadratic term by a factor of 50 and be capable of probing to orders of magnitude above the Planck energy in the linear term [137]. If AGN flares exhibit greater variability than current instruments can resolve, the limits from CTA will be even more sensitive.

## 2.4 Rare and New Particles

### 2.4.1 Antiparticles and antinuclei

Modern cosmological models strongly favor a universe in which an early baryon asymmetry develops followed by annihilation, leading to a negligible abundance of antiparticles in the present-day universe. Antiparticles and anti-nuclei can nevertheless be produced in energetic astrophysical processes and through decays.

**Electrons and Positrons** Cosmic ray electrons are produced and accelerated in various astrophysical contexts and are considered primary cosmic rays, making up about 1% of the total cosmic ray flux. No primary sources of cosmic ray positrons are known. However, positrons may also be injected by  $\beta^+$  decays, from the magnetospheres of compact objects due to pair production, and as the result of primary cosmic ray interactions with the interstellar medium during the propagation. As a result, the number of cosmic ray positrons compared to the number of electrons is expected to decrease with energy. Observations by PAMELA [138], Fermi [139], and AMS-02 [140] have shown that the positron fraction instead rises with energies above 10 GeV. The high statistics positron fraction measurement by AMS-02 shows a steady increase up to 350 GeV, with a decreasing slope above 250 GeV. AMS-02 will expand the measurements to the TeV energy scale with 2% energy resolution and unprecedented high statistics. These measurement could be a

hint for a possible primary positron component as the kinematic characteristics of such a new primary process are most likely different from the production mechanisms of secondary positrons and could materialize in the form of an excess on top of the conventional diffuse positron spectrum. The interpretation will be tightly constrained by how the positron fraction continues at higher energies. Possible explanations span a wide range where dark matter particle self-annihilations or decay [141, 142, 143, 144, 145] and so far unknown astrophysical sources like nearby pulsars [146, 147] are the most popular ones. Studying the anisotropy level of the positron flux helps to distinguish between diffuse and more concentrated sources. The AMS-02 limit on the dipole anisotropy of the positron fraction is currently 3.6% at the 95% confidence level [140]. However, a  $\sim 10$  times lower level of anisotropy is expected from nearby pulsars [146].

**Antiprotons** The conventional astrophysical source of antiprotons is the production of antiproton-proton pairs in high energy collisions of cosmic rays with the interstellar medium. Low energy antiprotons can only be produced in high energy collisions, since sufficient energy must be available in the CM frame to allow antiprotons produced in the backward (anti-beam) direction to appear to be nearly at rest in the lab frame. These high energy collisions are rare due to the falling cosmic ray spectrum, so the flux of antiprotons below a GeV is kinematically suppressed.

The best measurements of the cosmic ray antiproton flux are from BESS [148, 149] and PAMELA [150]. Antiprotons are a powerful tool to constrain dark matter annihilation and decay models as the astrophysical production has only small uncertainties and the antiproton propagation is better under control than for positrons. However, dark matter annihilation (decay) fluxes from different channels (modes) are very similar in shape and, in addition, also very similar in shape to the models for astrophysical production. This makes the interpretation challenging, but upcoming AMS-02 antiproton results have the potential to further constrain dark matter properties [151]. The existing measurements do not require to introduce an additional primary antiproton component, which has to be taken into account for the interpretation of the positron fraction.

**Antideuterons** Secondary antideuterons, like antiprotons, are produced when cosmic ray protons or antiprotons interact with the interstellar medium, but the production threshold for this reaction is higher for antideuterons than antiprotons. Collision kinematics also disfavor the formation of low energy antideuterons in these interactions. Moreover the steep energy spectrum of cosmic rays means there are fewer particles with sufficient energy to produce secondary antideuterons, and those that are produced will have relatively large kinetic energy. As a consequence, a low energy search for primary antideuterons has very low background. Figure 5 shows the expected antideuteron flux from secondary and tertiary interactions as well as several dark matter models. The different boxes demonstrate the antideuteron flux limits of BESS [155] and the sensitivity reaches of AMS and GAPS [156, 157, 158], which reach for the first time the sensitivity to probe predictions of well-motivated models. GAPS is a dedicated low energy antideuteron balloon experiment and had a successful prototype flight in 2012 [159, 160]. AMS and GAPS have mostly complementary kinetic energy ranges but also some overlap in the most interesting low energy region. Another very important virtue comes from the different detection techniques. AMS identifies particles by analyzing the event signatures of different subsequent subdetectors and a strong magnetic field and GAPS by slowing down antideuterons with kinetic energies below 300 MeV, creating exotic atoms inside the target material, and analyzing the decay structure. The combination of AMS and GAPS allows the study of both a large energy range and independent experimental confirmation, which is crucial for a rare event search like the hunt for cosmic-ray antideuterons.

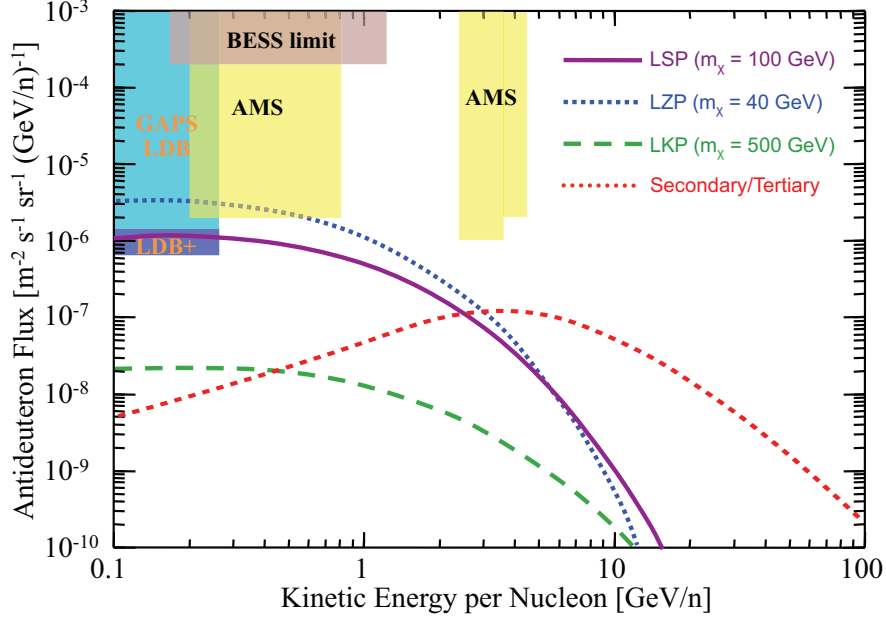


**Figure 5.** Predicted antideuteron fluxes from different dark matter models updated by more recent coalescence momentum value (purple, red, green lines) [152, 153] and secondary/tertiary background flux from cosmic ray interactions with the interstellar medium (blue line) [154]. Antideuteron limits from BESS [155] and sensitivities for the running AMS [156, 157] and the planned GAPS experiments [158] are also shown.

#### 2.4.2 Primordial Black Holes

Primordial density fluctuations can lead to the formation of black holes, the typical black hole mass will be of order the horizon mass (or smaller) at the time of formation ( $M \approx 10^{15}(t/10^{-23}s)g$ ) [161]. Therefore the mass spectrum of PBHs can span the range from supermassive black holes to Planck mass black holes. Hawking demonstrated that black holes radiate energy and have a temperature that is proportional to the inverse of their mass ( $T \approx 1/M_{13}$  GeV, where  $M_{13}$  is the black hole mass in units of  $10^{13}g$  [162]. Primordial black holes with an initial mass of less than  $10^{15}g$  would have evaporated completely. Such black holes would have been formed in the first  $10^{-23}$  seconds after the Big Bang. The cosmological consequences of primordial black holes are many, their existence (or absence) and mass spectrum probe the density perturbations at early times and very small scales [163, 164]. They can seed dark matter clumping, forming ultra compact minihalos and primordial stellar mass size black holes (formed during the QCD phase transition about 10 microseconds after the Big Bang [165]) may make up the dark matter [166, 167].

The luminosity of a black hole is inversely proportional to the square of the black hole mass and the proportionality constant is related to the number of available degrees of freedom. The emission mechanism can be thought of as the creation of particle anti-particle pair creation at the event horizon, with one of the particles being absorbed and the other emitted. All fundamental particles will be produced at the event horizon if their mass is less than the black hole temperature. Therefore the time evolution of the emission spectrum of a PBH is sensitive to physics at energy scales not attainable on earth. The observed emission spectrum can be found by convolving the emitted particle spectrum with particle fragmentation functions to derive the gamma-ray and neutrino luminosity functions [168]. Black holes with an initial mass of roughly  $5 \times 10^{14}g$  would now be in their final stages of evaporation, emitting GeV-TeV particles.



The discovery of a primordial black hole would have an enormous impact on science - informing us of the existence of particle states at extremely high energies (well above those available at the LHC) and the spectrum of the primordial density fluctuations at extremely small scales (roughly 30 orders of magnitude smaller than the scales probed by the CMB measurements).

Experimentally there are several ways to search for the existence of PBHs. Indirect techniques rely on detecting the cumulative emission of particles (typically anti-protons or 100 MeV gamma rays) by black holes that have or are in the process of evaporating. Direct detection techniques rely on the detection of a black hole in the final stages of evaporation. Understanding the relationship between the two techniques is complex as it depends upon the mass spectrum of primordial black holes and their clustering (direct techniques are sensitive to relatively local black hole evaporation). While the indirect methods have essentially reached the limits of their sensitivity (the actual measured anti-proton and diffuse 100 MeV gamma-ray flux is used to set limits on the number of primordial black holes that could have evaporated in the past), direct techniques hold the promise of significantly improving upon the current limits.

The diffuse gamma-ray flux measured by EGRET has been used to set an upper limit of  $\Omega_{pbh} < (5.1 \pm 1.3) \times 10^{-9} h_0^{-2}$  [169] on the contribution to the mass density of the universe from primordial black holes of mass less than  $10^{15}$  g. If PBHs cluster in our Galaxy as ordinary matter the offset of the Sun from the Galactic Center would lead to an anisotropy in the fraction of the diffuse gamma-ray background that is due to emission from PBHs. Wright [170] found such an anisotropy in the gamma-ray background measured by EGRET, however at a level much smaller than expected if PBHs clump as luminous matter. From the measured anisotropy one can set an upper limit on the rate density of evaporating PBHs in the Galactic halo of  $< 0.42 \text{ pc}^{-3} \text{ yr}^{-1}$  [170].

The evaporation of PBHs would produce equal numbers of protons and antiprotons (and similarly for anti-deuterons and deuterons). A PBH signature would manifest itself as an increase in the antiproton to proton fraction at low energies (below  $\sim 1$  GeV, where the effects of solar modulation are important). The absence of such an increase and the measured value of the antiproton flux by the BESS-Polar II instrument sets an upper limit to the local (within a  $\sim \text{few kpc}$  [171]) rate density of evaporating PBHs of  $1.2 \times 10^{-3} \text{ pc}^{-3} \text{ yr}^{-1}$  [172]. Anti-deuteron data from AMS and or GAPS could improve upon this limit [173].

Experiments sensitive to the final stages of the PBH evaporation process, IACTS and EAS arrays, probe the very local distribution of PBHs with mass near  $5 \times 10^{14}$  g. Figure 6 shows the current limits and the expected sensitivity of future instruments (HAWC and CTA). Note that the CTA limit is an estimate based upon the current limit established by the H.E.S.S. collaboration, the increased sensitivity of CTA compared to H.E.S.S. ( $10\times$  sensitivity allows one to probe a volume  $10^{3/2}$  greater), and the larger field-of-view of CTA relative to H.E.S.S. CTA could improve upon current limits by 2 orders of magnitude.

### 2.4.3 The Extragalactic Background Light and the Search for Axion-like Particles

The extragalactic background light (EBL) is the sum over the history of the universe of the ultraviolet (UV) through far infrared (IR) photon fields and their evolution. The light sources are predominantly stars and starlight reradiated in the infrared (IR) band by dust. The EBL thus contains an imprint of the past history of the universe including galaxy and star formation and any other sources of radiation. In principle it is possible to calculate the EBL spectrum from first principles - initial mass functions of stars, stellar evolution theory, and the effect of dust. Alternatively one can sum the radiation fields from observed galaxy counts. A direct measurement of the EBL could then be compared to these estimates. If the measured EBL is higher than expectations this would be a signature of the injection of a new radiation source, for example the decay of weakly interacting particles or an early population of massive stars. If the measured EBL (as measured by the resultant opacity of the universe at VHE energies, see below) is lower than expected, this

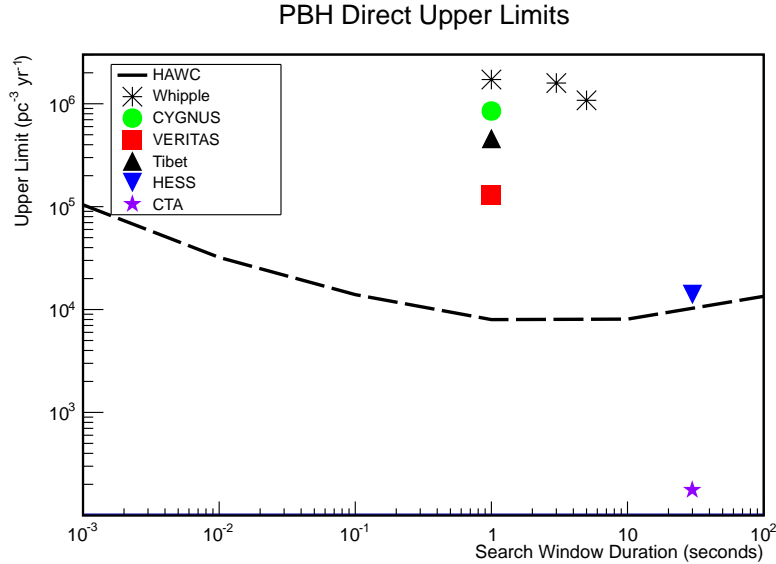


**Figure 6.** Current and potential limits on the local rate-density of evaporating primordial black holes. The sensitivity of CTA has been estimated see text for details. References for figure: HAWC [174], Whipple [175], VERITAS [176], CYGNUS [177], Tibet [178], and H.E.S.S. [179].

would be a strong indication that the VHE photons are mixing with an axion-like particle via interactions with intergalactic magnetic fields or that distant high-energy gamma rays are a by-product of the production of the ultra-high-energy cosmic rays. This uncertainty is borne out by calculations based on observational uncertainties in determinations of galaxy luminosity densities[72]. Just as the CMB is responsible for the absorption of ultra-high-energy protons [5, 6] and photons above 100 TeV, the EBL interacts with gamma rays with energies between  $\sim 100$  GeV and  $\sim 100$  TeV through the resonant production of electron-positron pairs, resulting in an energy and distance dependent attenuation of VHE gamma rays from distant sources. Direct measurements of the EBL are difficult due to sources of foreground light. If one understands the inherent energy spectra of AGN then the observed spectra at earth in the VHE regime can be used to measure the spectrum of the EBL. To date the best upper bounds on the EBL spectral energy distribution (SED) are derived from observations of AGN spectra. These limits are near the lower bounds established by the contribution to the EBL from galaxies. Figure 7 shows the current limits and measurements of the spectral energy distribution of the EBL [180].

As can be seen from the figure there is a large uncertainty in our knowledge of the SED of the EBL. The sensitivity of CTA to distant AGN should dramatically improve our knowledge of the EBL and therefore our understanding of the history of star and galaxy formation in the universe.

**Axion-like Particles** Axions were first postulated in [181] to solve the strong CP problem (the fact that CP symmetry is apparently conserved in QCD). Such axions couple to the electromagnetic field through a term in the Lagrangian of the form  $g_{a\gamma} \mathbf{E} \cdot \mathbf{B} a$ , where  $a$  is the axion field and  $g_{a\gamma}$  is the axion photon coupling, which for traditional axions is inversely proportional to the axion mass. Axion-like particles (ALPs) have a similar coupling to the electromagnetic field, however they do not have the same relationship between coupling strength and mass. Axions and axion-like particles are a leading dark matter candidate and searches for them are discussed in CF-3 of this document. A common feature of axion/ALP searches is exploitation of the axion/ALP photon coupling in the presence of a large magnetic field. In the cosmic arena

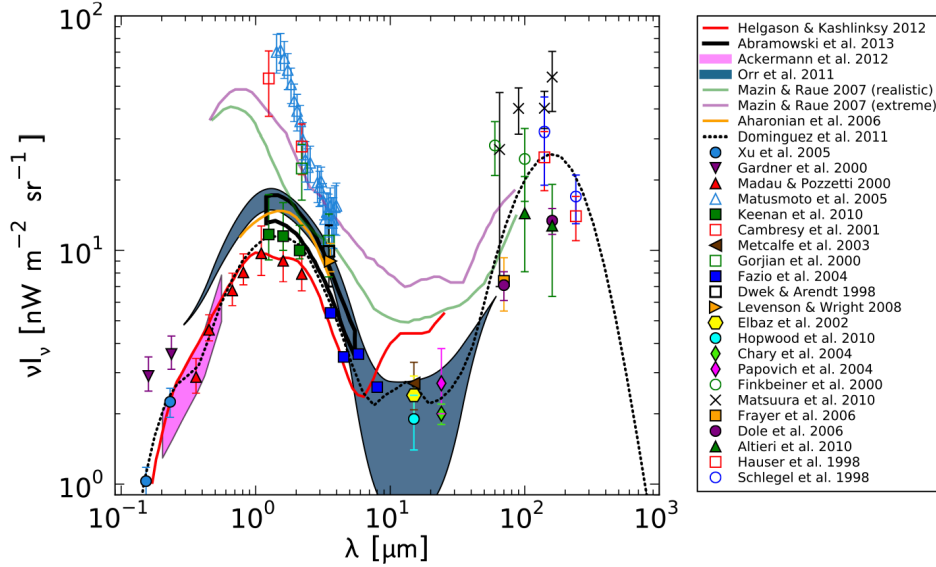


**Figure 7.** A summary of our current knowledge of the extragalactic background light intensity as a function of wavelength. Direct measurements are shown with open symbol, limits from IACT blazar observations are given by the legend listings 2-7, legend 1 is a model based on galaxy luminosity functions and the dashed black line is the model of Dominguez et al. [73]. Other legend references can be found in [74]. This figure was taken from [180].

gamma rays emitted by distant sources such as AGN can mix with ALPs via the intergalactic magnetic fields (or stronger local fields near the acceleration region). A fraction of these ALPs then reconvert to gamma rays before reaching the earth. While this would lead to a decrease in the gamma-ray flux reaching the earth in the absence of the EBL there can be an increased gamma ray flux at earth compared to the EBL absorbed expectations. The spectrum measured at earth will depend upon the intrinsic AGN spectrum, the EBL spectral energy distribution, and the intergalactic magnetic fields. These measurements can provide the most sensitive searches for axion-like particles with extremely low masses.

We are now entering an era where there significant number of AGN have been observed over a broad energy range from 100 MeV - few TeV. A detailed analysis of 50 AGN spectra (out to a redshift of 0.5) measured in the TeV region has found evidence for a suppression of EBL absorption at the 4.2 standard deviation level [182]. The measured spectra are consistent with expectations based on photon-ALP mixing, with an IGMF of 1 nG and a photon-ALP coupling strength of  $g_{a\gamma} = 10^{-11} \text{ GeV}^{-1}$  (below the upper bound from CAST [183]). Though given the large range of IGMF/ $g_{a\gamma}$  parameter space available it is difficult to draw strong conclusions based upon this analysis.

Another approach is to search for irregularities in AGN spectra, expected if there is a photon-ALP coupling due to magnetic field irregularities in the IGMF. The H.E.S.S. collaboration, finding no such irregularities has set limits on the photon-ALP coupling of  $2 \times 10^{-11} \text{ GeV}^{-1}$  in the mass range of near 20 neV [184]. This limit is the most restrictive in this mass range.

At present the situation is undecided and it should be noted that if AGN produce ultra-high-energy protons, interactions of these protons with the CMB will produce secondary gamma rays that can also lead to an enhanced flux of VHE gamma rays (over that expected with EBL absorption) [185, 186, 187, 188, 80, 189, 190, 191, 192, 193, 194, 195]. The observation of a single flare at energies above  $\sim 1 \text{ TeV}$  from a distant AGN ( $z > 0.15$ ) could negate the UHECR interpretation. What is needed are more measurements spanning

a larger redshift range, with greater sensitivity and energy resolution from 100 GeV to 10 TeV. CTA should detect at least an order of magnitude more AGN and HAWC can monitor every AGN in its field of view for flaring activity - for detailed followup observations by CTA. Figure 8 shows the current limits on  $g_{a\gamma}$  as a function of axion mass along with an estimate of the expected improvement in sensitivity from CTA [196]. The line marked "WD cooling hint" comes from the observation that the cooling rate white dwarf stars is faster than expected, possibly indicating another energy loss mechanism (such as ALPs) [197]. Not shown in the figure is a limit on the coupling for axion masses less than  $\sim 16$  meV around  $1.3 \times 10^{-12}$  to  $2.2 \times 10^{-12}$  from the duration of the neutrino burst from SN1987a (an additional energy loss mechanism would have shortened the duration of the neutrino burst) [197]. The expected sensitivity of CTA could probe the region of the white dwarf cooling hint, which is below the bound from SN1987a.

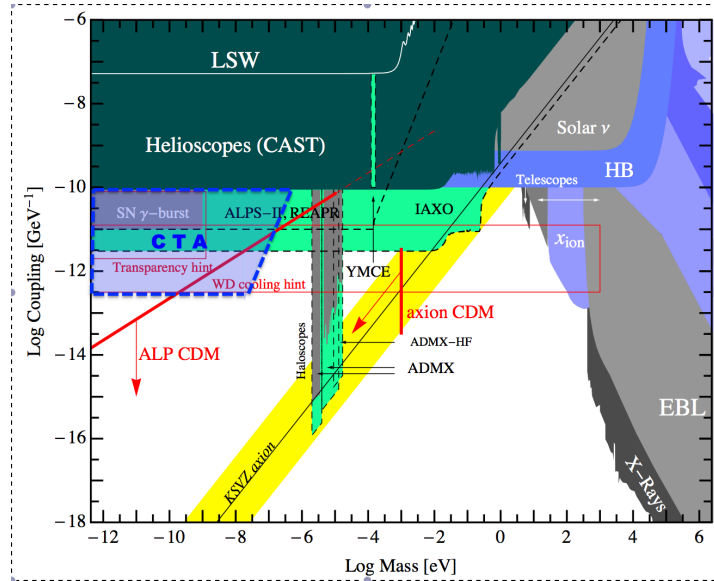


**Figure 8.** Current limits and expected sensitivity of axion searches. The potential sensitivity of CTA to axion-like particles is delimited by the dashed blue line. Note a limit on the coupling strength of  $1.3\text{--}2.3 \times 10^{-12} \text{ GeV}^{-1}$  (for axions with mass less than  $\sim 16 \text{ meV}$ ) from the duration of the neutrino burst from SN1987A is not shown in the figure. See text for an explanation.

#### 2.4.4 Intergalactic Magnetic Fields

Intergalactic magnetic fields (IGMFs) offer a new window on the early-universe cosmology and new physics. The magnetic fields deep in the voids between galaxies, where no significant star formation or gas convection could take place, are the closest approximation to primordial seed magnetic fields left over from the Big Bang. These fields are vestiges of some non-thermal events in the early cosmological history. They could have been produced at the end of inflation from inflaton dynamics, or in the course of a cosmological phase transition, or due to some other processes in the early universe that involve new physics [77]. The strength of IGMFs is still poorly understood [198, 199]. Until recently, only the upper limits of  $10^{-9} \text{ G}$  were inferred from the observational data [200]. Theoretical models assuming the dynamo origin of galactic magnetic fields require primordial seed fields of  $B > 10^{-30} \text{ G}$  [201], which can be considered a theoretical lower limit.

With the advent of a new generation of gamma-ray instruments, one can measure the values of IGMFs deep in the voids, along the line of sight to distant gamma-ray sources, such as blazars. One can measure IGMFs using time delays [78], or by searching extended halos around the point objects [76, 79]. Recent analyses of spectra

of distant blazars produced both lower and upper bounds:  $0.01 \text{ fG} < B < 30 \text{ fG}$  on Mpc scales [188]. The narrowing of the range of primordial fields to a vicinity of a femtogauss [188, 187, 202, 185, 186] has already stimulated a number of studies in primordial magnetogenesis [77, 203, 204, 205, 206, 207, 208, 209, 210].

Future observations of distant blazars with CTA will allow mapping out of IGMFs, as well as a determination of both the average strengths and the correlation length distributions of these fields. These observations can also measure the presence of helical magnetic fields [211], predicted in scenarios in which cosmic baryogenesis and magneto-genesis occur concurrently during a cosmological phase transition [212, 213, 214, 215, 216]. In addition to providing a clear signal for a primordial origin of the IGMF, helicity is also an important factor in the evolution of magnetic fields enabling their growth to astrophysically relevant scales at the present epoch.

This will offer a new exciting possibility to test models of inflation and new physics via a new and unique window on the early universe.

### 2.4.5 Magnetic Monopoles

The possibility of magnetic monopoles goes back at least to 1931 [217]. It is theoretically attractive, as it could explain the observed quantization of electrical charge. This argument also gives the 'natural' size of the magnetic charge. Monopoles appear naturally in many grand unified theories (GUTs). In most of these theories, monopoles have masses comparable to the unification scale, and so are far beyond the reach of current or planned accelerators. However, they might have been produced in the early universe [218]; since they do not decay, they may still be present.

Direct and indirect techniques have been used to search for monopoles. The indirect searches rely on how monopoles effect on various astrophysical phenomena. For example, the Parker bound [219] is based on the fact that a sufficient density of magnetic monopoles would short circuit the galaxy's magnetic fields. From the existence of these fields, a flux limit is set at roughly one monopole per football field per year; this is roughly the upper limit for direct searches to be useful.

The required technique for direct searches depends on the monopole velocity. Heavy (GUTs scale) monopoles are expected to be slow, with velocities of order  $10^{-4} - 10^{-3} c$ . The most sensitive search for monopoles with this velocity was by the MACRO experiment, which set limits a factor of several below the Parker bound [220]. Newer experiments have set lower limits on non-relativistic monopoles, but only if they catalyze proton decay [221]. The catalysis of proton decay is not unexpected in GUTs theories, but the details are heavily theory-dependent. These experiments set two-dimensional limits, in terms of monopole flux catalysis cross-section. Assumptions are also required about the final state(s) of the decaying proton.

If monopoles have masses below the GUTs scale, then they could be accelerated to relativistic velocities. Then, they would emit Cherenkov radiation, and could be detected by neutrino telescopes. This signature has some similarities to that for nuclearites. Several neutrino detectors have searched for relativistic monopoles, with negative results [222, 223, 224, 225]. These experiments mostly observe monopoles underground, so one must account for the energy loss before the monopole reaches the detector. They set limits ranging from of order 1/10 of the Parker limit (for slightly relativistic monopoles, observed in optical detectors, to limits several orders of magnitude tighter, for ultra-relativistic monopoles observed with radio detectors.

A future dedicated experiment for non-relativistic, non-catalyzing significantly larger than MACRO would be quite expensive, and, absent new findings, is probably not worthwhile. However, optical and radio Cherenkov detectors will continue to set tighter limits. Although the searches are quite speculative, a positive detection would drastically change our view of particle physics.

### 2.4.6 Q Balls

Understanding the origin of the matter anti-matter asymmetry in the universe is one of the most fundamental problems facing modern physics. Though there are several viable explanations, experimental evidence has been lacking. Leptogenesis is being probed by experiments such as the Long Baseline Neutrino Experiment (LBNE), which is searching for CP violation in the neutrino sector, and neutrinoless double beta decay experiments, sensitive to the Majorana nature of the neutrino. Other sources of baryonic CP violation are being probed with  $\mu \rightarrow e\gamma$  experiments and searches for neutron and electron dipole moments. An alternate scenario for baryogenesis, the Affleck-Dine mechanism [226], active at the end of the inflationary epoch, can naturally generate a large baryon asymmetry - if supersymmetry is the correct theory of unification. A prediction of this theory is the formation of Bose condensates of the scalar field. The condensates of squarks would form Q-balls, potentially stable states (Q-balls with masses larger than about  $10^{15}$  GeV are stable) with large baryon number. Stable Q-balls are candidates for the dark matter in the universe. Reasonable values of Q-ball charge and the SUSY breaking scale put the detection of Q-balls within the reach of planned high-energy gamma-ray, cosmic-ray, and neutrino telescopes.

S. Coleman [227] first realized that supersymmetric theories have non-topological stable solutions which he called "Q-balls". A review of Q-balls and baryogenesis may be found in [228]. Here we give some of the important parameters for Q-balls:

$$M_Q = \frac{4\pi\sqrt{(2)}}{3} M_S Q^{3/4} \text{ GeV} \quad (3)$$

$$\sigma = \pi R_Q^2 = \frac{\pi}{2} \frac{Q^{1/2}}{M_S^2} \approx \frac{10}{M_S^2} \sqrt{Q/10^{14}} \text{ mbarns} \quad (4)$$

$$(5)$$

where  $M_S$  is the SUSY breaking scale in TeV and  $Q$  is the baryon number (charge) of the Q-ball. Note that the cross section is purely geometrical and quite large. Since the mass grows slower than the charge Q-balls will be stable, when it is energetically impossible for them to decay into an equivalent number of protons, which occurs at  $Q > 5.0 \times 10^{14} (M_S/\text{TeV})^4$  [229]. Because of their high mass, the expected flux of Q-balls at earth would be low (if they comprise the dark matter in the universe):

$$F \approx \frac{\rho_{DM} v}{4\pi M_Q} \approx 7.2 \times 10^5 \left( \frac{\text{GeV}}{M_Q} \right) \text{ cm}^{-2} \text{ sec}^{-1} \text{ sr}^{-1} \text{ [229]}. \quad (6)$$

where we have assumed that  $\rho_{DM} = 0.3 \text{ GeV/cm}^3$  and  $v = 300 \text{ km sec}^{-1}$ , the virial velocity. For stable Q-balls and interesting values of the SUSY breaking scale Q-ball fluxes of  $\sim 10^{-16}$  or less may be expected. Such a low flux requires the large effective areas that are now common in cosmic-ray, gamma-ray, and neutrino experiments.

The interaction of a Q-ball with ordinary matter proceeds would leave a spectacular signal in the appropriate detector. As a Q-ball interacts with a proton, the proton is absorbed (increasing the baryon number of the Q-ball) and an anti-proton is emitted. Therefore at each interaction with a nucleus the energy released into the detector will be approximately 1 GeV/nucleon, most of which will be in the form of pions.

Currently the best limits on Q-balls have been set by the Super Kamiokande [230] experiment and MACRO [231]. The limits from Super Kamiokande are only valid for relatively small values of the cross set ion (and

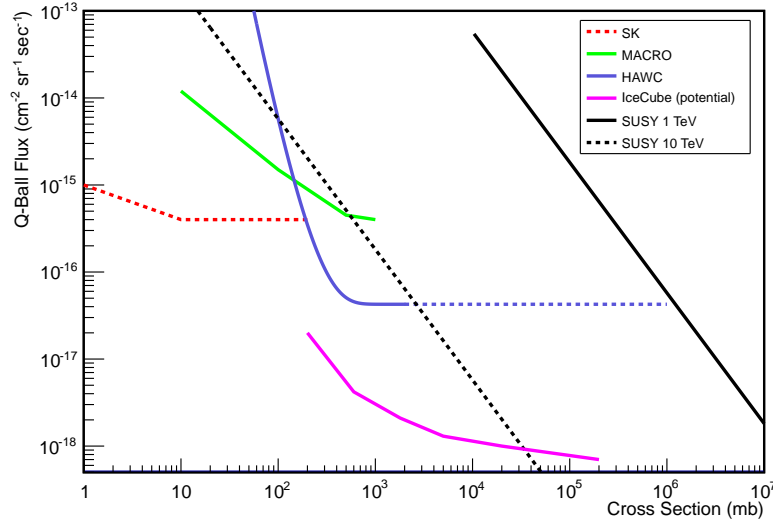


**Figure 9.** Current and potential limits on the flux of Q-balls as a function cross section from current and future neutrino, gamma-ray, and cosmic-ray instruments. The diagonal lines are possible values of flux as a function of cross section for different values of the SUSY breaking scale assuming that the dark matter is entirely composed of Q-balls. The IceCube potential limit is taken from an unpublished limit on monopoles with a velocity of  $0.001c$ , a typical expected velocity for Q-balls. References for the figure: SuperKamiokande [230], MACRO [231], HAWC [232], IceCube [233].

therefor mass and charge) due to the requirement that a Q-ball not interact in the veto region of the detector. Current neutrino detectors such as IceCube and future gamma-ray and cosmic-ray detectors such as HAWC and JEM-EUSO (note that JEM-EUSO has not published a sensitivity to Q-balls at the time of this report) should be able to significantly improve upon the current limits and extend the search to more theoretically interesting parameter space of large cross sections. Figure 9 shows the current limits with the expected sensitivity of HAWC, IceCube. The diagonal lines are theoretical expectations of for SUSY breaking scales of 1 and 10 TeV. In any of these detectors one should be able to determine the direction of a Q-ball. In this scenario, these instruments serve as directional direct dark matter detectors.

#### 2.4.7 Strangelets

Quark nuggets, nuclearites, and strangelets are different names for lumps of a hypothetical phase of absolutely stable quark matter, named *strange quark matter* because it is made of about one-third up, down, and strange quarks [234, 235]. Whether strange quark matter (SQM) is absolutely stable is a question yet to be decided by experiment or astrophysical observation (see [236, 237, 238, 239] for reviews). If stable, strange quark matter objects may exist with baryon numbers ranging from ordinary nuclei to about  $2 \times 10^{57}$  corresponding to gravitational instability of strange stars [240, 241].

Small SQM lumps with baryon number  $A < 10^7$  are called strangelets [242]. Strangelets have an electron cloud neutralizing the slightly positive quark charge. They are unlikely to survive the early Universe, but may form at collisions of strange star binaries or may be accelerated off the surface of pulsars. Relics from the cosmological quark-hadron phase transition are usually called quark nuggets, while nuclearites are nuggets

that hit the Earth and may leave detectable signatures as unusual meteor-events, earth-quakes, etched tracks in old mica, in meteorites and in cosmic-ray detectors [243].

Current searches for SQM states have excluded quark nuggets as dark matter candidates with  $3 \times 10^7 < A < 5 \times 10^{25}$ , but a lower flux of relics or strange star collision debris has not been ruled out. Several experiments have searched for strangelets in cosmic rays with some interesting events not claimed as discoveries but interpreted as flux limits reviewed here [244, 245]. More recently the Lunar Soil Strangelet Search (LSSS) has reported new strangelet limits [246] in a sample of 15 grams of lunar soil from Apollo 11. The Alpha Magnetic Spectrometer (AMS) is currently searching for strangelets from the International Space Station [247]. AMS is uniquely suited to discover extreme rigidity strangelets and should be able to probe a wide mass range. AMS recently released their first results [12] and have presented accurate measurements of cosmic ray electrons, positrons, protons, and nuclei at the International Cosmic Ray Conference 2013. No results from the strangelet searches has been announced to date.

#### 2.4.8 Quark anti-nuggets (Angela)

### 2.5 New Facilities

#### 2.5.1 UHECR Experiments

**Auger** The Pierre Auger collaboration is currently planning an upgrade of the existing  $3000\text{km}^2$  hybrid observatory located near Malargüe, Argentina. The current observatory is comprised of an array of 1600 12 ton water Cherenkov surface detectors, most of which are spaced on a 1.5 km hexagonal grid, together with air fluorescence detectors distributed at four sites overlooking the surface detector array. The objectives of the planned upgrade are to elucidate the origin of the flux suppression at the highest energies, measure the composition of UHECRs up to highest energies with sufficient resolution to detect a 10% proton component, provide composition-tagging to facilitate anisotropy studies, and study hadronic interactions at center-of-mass energies an order-of-magnitude greater than at the LHC.

To address these objectives, the Auger upgrade focuses on enhancing the ability of the detector to better separately determine the lateral distribution function of the muon and electromagnetic (EM) components of showers, and to extend these measurements to smaller core distances (and large shower particle fluxes) than is possible with the existing system. The upgrades also would improve measurement not only of the depth of shower maximum for the EM component of the shower (as is done at present using the fluorescence detectors in hybrid events) but also the depth at which muon production reaches its maximum, using the surface detector alone.

An upgrade of the electronics of the surface detectors is the first step in separating the muon and EM components of the showers on an event by event basis [3]. It includes faster timing of surface detector signals, improving significantly the ability to distinguish close-in-time muon pulses across the entire array. The updated electronics will also facilitate the addition of dedicated muon detectors over all or part of the surface detector array to further improve the muon/EM separation and reduce model-dependent systematic errors. This gives rise to a ‘boot-strap’ approach, where the model-independent, direct muon determination abilities of the upgraded detector are used to validate and refine the more indirect detection methods and analyses.

Distinct strategic options appear in how to use muon identification and/or separation of the muonic and EM components of the signal, to test and improve the hadronic physics modeling and to assign a composition-probability to each event. The most direct method is to simply separate the muonic and EM signals in each



tank, and use timing and geometry to infer the location of peak muon production point in the development of the air shower[4]. A second approach is to fit the total signal in every tank, including some elements of the FADC timing, to a superposition of templates of EM and muonic components. This gives a more accurate energy and angular reconstruction than the traditional method, and at the same time gives  $X_{max}$  with remarkable accuracy, about  $30 g cm^{-2}$ .

The additional muon identification technologies under study and prototyping include (1) segmentation of the interiors of surface detectors, to separate penetrating muons from the lower-energy electromagnetic component, and (2) placement of external particle detectors (such as RPCs or scintillators) with the existing Auger detectors.

In addition, it is planned to extend fluorescence light measurements into twilight by running with reduced gain, thereby increasing the duty cycle for the highest energy showers by up to a factor of two. This does not involve a hardware upgrade but rather is an operational change in the existing detector.

It is planned to operate the upgraded Pierre Auger Observatory from 2015 to 2023, which would approximately double the data set which will have been collected prior to implementation of the upgrade.

**Telescope Array** The Telescope Array (TA) collaboration has several upgrades in progress and planned for the near future. The TA Low Energy (TALE) extension will extend the observatory’s reach in energy spectrum and composition studies into the  $10^{16}$  eV decade, enabling TA to probe the “second knee” region and the galactic-to-extragalactic transition. An additional decade downward in energy will be achieved via the Non-Imaging Cherenkov (NICHE) array, bridging the gap between Telescope Array and experiments operating in the knee regime. At the highest energies, the TA $\times$ 4 (“TA times four”) detector will greatly enhance Northern Hemisphere statistics, of particular importance in arrival direction anisotropy and composition studies.

*TALE* While TA has been able to extend analysis down to about  $10^{18}$  eV, this is insufficient to fully observe the galactic-to-extragalactic transition. In addition, it is optimal to observe cosmic rays from LHC energies through the second knee and up to the GZK cutoff with one well cross-calibrated detector. TALE, the low energy extension to the Telescope Array, is designed to lower the energy threshold to about  $10^{16.5}$  eV. To do this, an additional ten fluorescence telescopes were installed, viewing up to 57 degrees in elevation angle. Installation of a new graded array of about 100 scintillator detectors is currently in progress. This extension will enable the Telescope Array to measure the energy and composition of cosmic rays to much lower energies while cross calibrated with the detectors of the main Telescope Array. By pushing the energy threshold down to  $10^{16.5}$  eV, the TA collaboration hopes to sort out the galactic and extragalactic contributions to the cosmic ray flux.

*NICHE* Co-sited with TA/TALE, the Non-Imaging Cherenkov Array (NICHE) will measure the flux and nuclear composition of cosmic rays from below  $10^{16}$  eV to  $10^{18}$  eV in its initial deployment. Furthermore, the low-energy threshold can be significantly decreased below the cosmic ray knee via counter redeployment or by including additional counters. NICHE uses easily deployable detectors — consisting of a single phototube and Winston cone — to measure the amplitude and time-spread of the air-shower Cherenkov signal to achieve an event-by-event measurement of  $X_{max}$  and energy, each with excellent resolution. NICHE will have sufficient area and angular acceptance to have significant overlap with the TA/TALE detectors to allow for energy cross-calibration. Simulated NICHE performance has shown that the array has the ability to distinguish between several different composition models as well as measure the end of Galactic cosmic ray spectrum.

**TA $\times$ 4** The Telescope Array (TA) collaboration is proposing to build TA $\times$ 4. This is a project to expand the TA surface detector by a factor of four, bringing the total instrumented area to 3000 km<sup>2</sup>. The plan is to build 500 more scintillation counters and deploy them in an array of 2.08 km spacing. This array, plus the existing TA SD would reach the design size. There is plenty of room at the TA site to expand on the northern, western, and southern sides of the TA SD. The new array would need a fluorescence detector overlooking it to set the energy scale, so the TA $\times$ 4 plan includes a fluorescence detector of 10 telescopes. These will be reconditioned HiRes telescopes.

The aim of the design is to collect data for anisotropy studies at the highest energies. An anisotropy signal due to the local large scale structure of the universe (the local 250 Mpc) really should be present at energies larger than about 57 EeV, where the extragalactic and galactic magnetic fields have an effect on cosmic rays trajectories smaller than the size of the local large scale structures. Telescope Array has already seen hints of such structure. If successful, the TA $\times$ 4 project will take 3 years to acquire the funds, build and deploy the detectors. Including the current 5 TA-years of data, 3 years of operation of TA $\times$ 4 would yield 20 TA-years of data. These data will be sufficient to determine unambiguously whether an LSS anisotropy exists. If the LSS signal really comes from the TA hot spot, 3 years of TA $\times$ 4 data will clarify this signal and yield a 5 $\sigma$  observation.

**JEM-EUSO** JEM-EUSO will be the first space observatory for the study of extreme energy cosmic rays with energies of  $\sim 10^{20}$  eV. The Extreme Universe Space Observatory (EUSO) to be accommodated on the Japanese Experiment Module (JEM) of the International Space Station (ISS) will look down towards the Earth and use the atmosphere as a giant detector [30, 31]. The 2.5 m ultraviolet (UV) telescope with a 60° field of view (FOV) will observe the fluorescence signal produced by the extensive air-showers (EAS) generated by extremely energetic cosmic rays (EECRs) that enter the Earths atmosphere.

The main objective of JEM-EUSO is to identify the sources of the highest energy cosmic rays and thus begin particle astronomy. JEM-EUSO will significantly increase the worldwide data collection of particles at extreme energies providing clear anisotropy signals for the identification of the first sources of extragalactic cosmic rays and the measurement of the energy spectrum beyond the Greisen-Zatsepin-Kuzmin (GZK) feature. Identifying the sources will solve a longstanding mystery and further the study of particle interactions with center of mass energies beyond 100 TeV.

JEM-EUSO is also sensitive to very low fluxes of extremely high-energy neutrinos that may be produced if cosmic accelerators reach higher energies than those observed thus far. The observation of extremely energetic neutrinos would make possible studies of neutrino interactions with center of mass above 100 TeV.

JEM-EUSO will also contribute to the investigation of phenomena intrinsic to the Earths atmosphere or induced by the flux of meteoroids and strangelets (or nucleorites) incoming from space.

A worldwide collaborating of 75 research groups from 13 countries is designing JEM-EUSO to operate for more than 3 years onboard the ISS which orbits around the Earth every 91 minutes at an altitude of about 400 km. JEM-EUSO will image light from the isotropic nitrogen fluorescence excited by the EAS, and the forward-beamed Cherenkov radiation reflected from the Earths surface or cloud tops. The highly-pixelized high-speed JEM-EUSO camera will capture the time development of an EAS to determine the energy and arrival direction of the EECR. The cameras focal plane is covered by MAPMTs with  $3 \times 10^5$  pixels, each less than 3 mm, giving a 0.07° resolution per pixel; a pixel covers about 0.5 km on the surface of the Earth. The characteristics of the EAS can be used to determine the original direction, energy, and nature of the EECR. JEM-EUSO will be able to discriminate between hadron, gamma ray, and neutrino initiated showers.

**Radio Detection of Cosmic Rays** Detection of cosmic ray air showers using radio techniques has undergone a resurgence of interest in recent years. Detectors have been operated in coincidence with air shower arrays at Auger [248, 249], Telescope Array [250], and Cascade-Grande [251, 252]. Cosmic ray radio emission has also been detected by the ANITA balloon-borne interferometer [57]. The dominant mechanisms include geosynchrotron emission and Cherenkov emission, and result in polarized emission beamed near the shower axis. The intensity and lateral distribution of the radio signal can be used to infer shower energy and depth of maximum [252]. In addition detectors being planned in conjunction with air shower arrays, there are prospects for radio detection using large interferometric array such as LOFAR [253, 254] and SKA, as well as from space [255].

**Radar Detection of Cosmic Ray Showers** Radar is another candidate remote sensing technique with a potential to achieve a 100% duty cycle. The Telescope Array Radar (TARA) project in Utah is designed to test the idea that ionization produced by extensive air showers should scatter RF radiation.

TARA employs two analog television transmitters, with a combined output power of 40 kW, broadcasting a 54.1 MHz (low-VHF) signal over the Telescope Array surface detector. The signal is enhanced by use of a high gain (over 20 dBi) phased array of Yagi antennas which boosts the equivalent isotropic radiated power to over 8 MW.

Due to the high velocity of the air shower ionization front, the RF scattered off of an extensive air shower will be characterized by a Doppler shift of several tens of Megahertz. To detect such signals, TARA employs a 250 MS/s receiver along with an onboard FPGA to allow smart triggering at a level well below that of galactic sky noise.

TARA commissioning is currently underway, with preliminary results anticipated in Fall of 2013.

## 2.5.2 Future Gamma-Ray Experiments

At energies above 100 GeV the flux of gamma rays from astrophysical objects is sufficiently small that detection using a space-based instrument becomes prohibitively expensive. Ground-based VHE gamma-ray instruments are of two types: Imaging Atmospheric Cherenkov Telescopes (IACTs), that use large mirrors to image the Cherenkov light generated in the atmosphere by extensive air showers and Extensive Air Shower (EAS) arrays, that directly detect particles that reach the ground - predominantly gamma rays, electrons and positrons. The characteristics of the two types of instruments complement each other and together they provide excellent coverage of a broad array of astrophysical objects. IACTs have significantly better instantaneous sensitivity, better energy resolution, and better angular resolution. However, they can only view a small portion of the sky at any one time and they can only operate on clear moonless nights (though progress has been made in extending operations into the lunar cycle). (Current instruments have a field-of-view of  $\sim 5$  milli-sr and the planned CTA will have a field-of-view of  $\sim 15$  milli-sr.) In contrast, EAS arrays can operate continuously and are sensitive to air showers from the entire overhead sky. Because the energy threshold of EAS arrays depends upon the atmospheric depth and therefore the zenith angle of the primary gamma ray, field-of-view is typically considered to be 2 sr. In IACTs the rejection of the cosmic-ray background is accomplished through a combination of image analysis and angular resolution. In EAS arrays background rejection is accomplished through a combination of muon detection and angular resolution.

Given the above characteristics IACTs are to:

- perform detailed morphological studies (spectrally resolved) of Galactic sources for multi wavelength studies - required to understand acceleration mechanisms

- extend ground-based measurements to relatively low energies (below 50 GeV) - required to probe the pulsar mechanism, provide overlap with space-based instruments, and for sensitivity to lower mass WIMPs
- observe the fastest transients from known sources - required to understand the acceleration mechanism and environment in active galaxies and provide the best limits on violation of Lorentz invariance
- detect faint sources and thereby provide the best indirect limits on dark matter annihilation
- resolve energy spectra of astrophysical sources - required for dark matter detection, understanding acceleration processes, and searching for evidence of axion-like particles

Similarly EAS arrays:

- monitor the sky and alert the more sensitive IACTs and other instruments operating at different wavelengths (and particle type) for followup observations of transient phenomena - critical to understanding complex astrophysical environments).
- detect prompt VHE emission from gamma-ray bursts
- perform unbiased sky surveys to discover new sources and phenomena (including undetected high M/L dark matter sources)
- study the highest energy gamma rays, where sensitivity is typically flux limited
- study large sources such as galaxy clusters (for dark matter annihilation) and Galactic and extragalactic diffuse emission

Given the complexity and diversity of sources of VHE gamma rays it is important to have both types of instruments available as well as instrument operating at lower wavelengths (100 MeV gamma rays, x-rays, radio, and optical) to glean the full benefit from any of the instruments. Single observations at a single wavelength are rarely (if ever) sufficient to properly understand astrophysical sources - a requirement if one is to extract fundamental physics from VHE gamma-ray observations. Therefore it is important to operate Fermi, VERITAS, and HAWC simultaneously for a period of several years. Results from such a period will inform us of the value of these observations and allow one to make physically motivated decisions about further operations.

**VERITAS** VERITAS (the Very Energetic Radiation Imaging Telescope Array System) is a ground-based gamma-ray instrument operating at the Fred Lawrence Whipple Observatory in southern Arizona, USA. It comprises an array of four 12m optical reflectors, which exploit the imaging atmospheric Cherenkov technique to measure emission from astrophysical sources in the  $\sim 100$  GeV to  $\sim 30$  TeV energy range. The array has been operating smoothly since 2007, recording around 1000 hours of data per year. The angular and energy resolution are energy dependent: at 1 TeV they are  $\sim 0.1^\circ$  (68% containment radius) and  $\sim 15\%$ , respectively. The sensitivity of the array is sufficient to detect a source with 1% of the steady Crab Nebula flux in less than 25 hours, while the Crab itself is detected in a matter of seconds. VERITAS has recently completed a series of upgrades, which included relocating the original prototype telescope, installing a new trigger system, and upgrading the telescope cameras with more sensitive photomultiplier tubes. These upgrades combined have halved the time required to detect a typical gamma-ray source.

VERITAS has now detected 46 sources - around one-third of the known TeV catalog - and over half of these detections were new discoveries. The catalog comprises active galaxies (blazars and radio galaxies),

a starburst galaxy, a pulsar, many pulsar wind nebulae, binary systems, supernova remnants, and sources whose nature remains unknown. Core science goals include the study of cosmic ray particle acceleration, both within our Galaxy (e.g. in supernova remnants) and externally (e.g. in AGN jets), searching for the gamma-ray signature of dark matter annihilation and primordial black hole evaporation, and constraining fundamental physical effects such as Lorentz invariance violation. The attenuation and cascading of TeV gamma-ray photons from distant sources can also be used to measure or constrain the extragalactic infra-red background light, and the extragalactic magnetic field strength. All of these studies are greatly enhanced by contemporaneous overlap with complementary gamma-ray instruments including the Fermi gamma-ray space telescope and HAWC.

**Cherenkov Telescope Array** The Cherenkov Telescope Array (CTA) is a concept for a ground-based observatory [28] for very high-energy (VHE, 30 GeV - 300 TeV)  $\gamma$  rays. It will use imaging atmospheric Cherenkov telescopes (IACTs) deployed over  $\geq 10 \text{ km}^2$  to detect flashes of Cherenkov light from air showers initiated by  $\gamma$  rays, a technique pioneered at Whipple Observatory in the US. Current IACTs have cameras consisting of  $\sim$  thousand fast photomultiplier tubes, and their effective collecting areas typically reach  $\sim 0.1 \text{ km}^2$ . The current generation, namely H.E.S.S., MAGIC, and VERITAS, have up to 5 IACTs with separations of  $\sim 100 \text{ m}$  to record multiple views of each shower. CTA will be an array of  $\sim$  one hundred IACTs to increase the collection area and the number of recorded images of each  $\gamma$ -ray shower.

The current concept for CTA consists of subarrays with telescopes of 3 different sizes. The CTA-US consortium is working towards contributing mid-sized telescopes (MSTs, 9 - 12 m) to CTA (e.g., 36 MSTs were recommended by Astro2010 [256] and PASAG [257]) to optimize the performance of CTA in the 80 GeV - 5 TeV regime. The U.S. groups are currently designing and building a prototype telescope to test the feasibility of an innovative, Schwarzschild-Couder telescope (SCT) design [258, 259, 260] that will allow much smaller, less expensive cameras, yet providing  $\sim 10^4$  pixels, better angular resolution and a much larger field of view than conventional Davies-Cotton designs. An important aspect of the prototype program is the design and testing of a new optical system, mirror technologies and camera electronics for the necessary advances in performance, reliability and lowered cost.

This work is a collaboration between national laboratories, universities and industry and consists of  $\sim 20$  research groups in the US. The US groups have received 5M\$ through an NSF-MRI program to construct a prototype telescope between 2012-2015 with the goal to get a realistic estimate of construction costs and performance.

Overall, CTA will (a) provide an order of magnitude better sensitivity for deep observations ( $\sim 10^{-3}$  Crab nebula flux); (b) have a much greater detection area ( $\sim 1 \text{ km}^2$ ), and hence detection rates, for transient phenomena; (c) improve the angular resolution ( $0.02^\circ$  at 1 TeV) to resolve cosmic accelerators; (d) provide uniform energy coverage from  $\sim 30 \text{ GeV}$  to beyond 100 TeV photon energy; and (e) enhance the sky survey capability, monitoring capability, and flexibility of operation relative to current IACTs. These improvements will provide a dramatic step in exploring non-thermal processes in our Universe.

Figure 10 shows simulation results of the flux sensitivity for several possible telescope configurations: the baseline array [261] (solid green line) using up to 25 mid-sized telescopes (MSTs) and the large-sized and small-sized telescopes to cover the low energies ( $E \leq 0.1 \text{ TeV}$ ) and high energies ( $E \geq 10 \text{ TeV}$ ). Furthermore we show the effect when adding the US contribution of mid-sized telescopes (recommended by Astro2010 and PASAG), amounting to either 61 DC-MSTs or 61 SC-MSTs.

The addition of the US telescopes would bring the sensitivity to the  $\sim 10^{-3}$  Crab level, and improve the sensitivity up to a factor of 3 in the 80 GeV - 5 TeV regime. This large improvement is due to increasing the

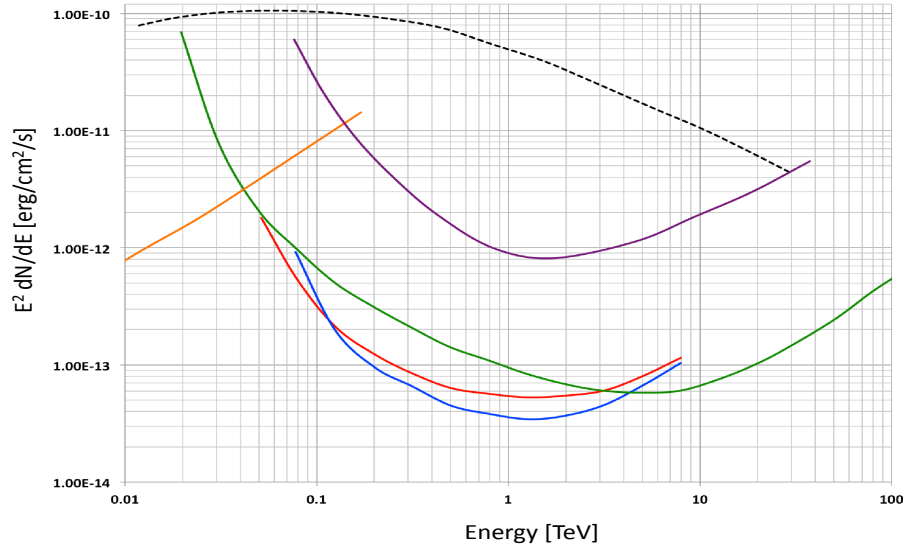


**Figure 10.** - The dashed line shows the differential energy spectrum of the Crab Nebula. The solid lines depict the sensitivity for a 50 hour exposure ( $\geq 5\sigma$  detection and  $\geq 10$  photons per energy bin) for various configurations of CTA and the current generation H.E.S.S. and VERITAS (solid purple) observatories. The CTA baseline array is shown in green using the best performance of any of the arrays considered in [261]. The redline shows the addition of the US contribution to a total of 61 mid-sized telescopes (e.g., 25 baseline and 36 CTA-US telescopes) based on the DC design, whereas the blue line show the addition of a US contribution with a total of 61 mid-sized telescopes based on the SC design. The sensitivity for Fermi is shown (solid orange) for an exposure time of 10 years.

MST array to its optimal size, where a much larger fraction of events fall within the array (contained events) for excellent event reconstruction, and the better resolution SC telescope compared to the DC design.

Figure 11 shows the results of a simulation of the angular resolution for several telescope configurations for CTA as a function of energy. The black dashed line shows the CTA requirement for angular resolution [262], the green line corresponds to the baseline array. The blue line and the red line show the angular resolution with and without the US contribution of more than doubling the number of mid-sized telescopes, the 61 SC-MSTs or 61 DC-MSTs, respectively. For comparison we also show the angular resolution of Fermi (orange line). It should be emphasized that the use of the SC design provides a substantial improvement in angular resolution, which not only translates into a better sensitivity for point sources, but also potentially provides new physics capabilities through high-resolution imaging in the TeV regime.

**The High Altitude Water Cherenkov Experiment** The High Altitude Water Cherenkov Experiment (HAWC) is a wide field-of-view ( $>2$  sr), high duty-cycle ( $> 95\%$ ) TeV gamma-ray experiment currently under construction at the vulcan Sierra Negra in Mexico. HAWC will be composed of 300 large water Cherenkov detectors (WCDs) (7m diameter by 4.3 meters high), instrumented with 4 photomultiplier tubes (PMTs). Three of the PMTs are 8" Hamamatsu R5912 (reused from the Milagro experiment) and the 4<sup>th</sup> central PMT is a high quantum efficiency 10" R7081-MOD Hamamatsu PMT. The WCDs will be placed in a close-packed array covering a total area of approximately 20,000 m<sup>2</sup>. The array will begin operations with 100 WCDs in August of 2013 and the full array should begin operations approximately one year later. HAWC builds

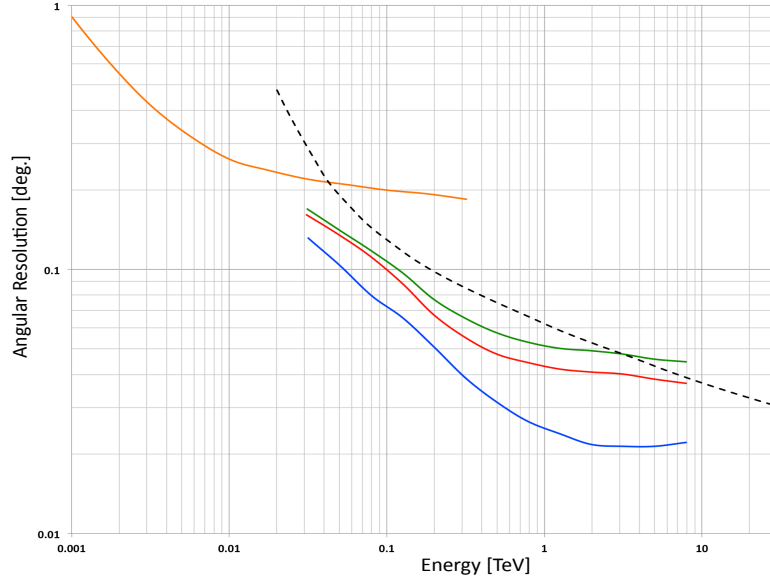


**Figure 11.** - The angular resolution is shown the CTA baseline array (solid green), the addition of the US contribution of mid-sized telescopes, for 61 DC-MSTs (solid red) and 61 SC-MSTs (solid blue). For comparison we also show the angular resolution of Fermi (solid orange).

upon the success of the Milagro experiment, which demonstrated the advantages of using water Cherenkov technology for wide-field ground-based gamma-ray instruments (dense sampling of the air shower particles on the ground and sensitivity to the gamma rays in an air shower) that lead to a dramatically lower energy threshold over previous generation of instruments based upon a sparse array of plastic scintillators. In five years of operation HAWC will survey 8 sr of the sky with a sensitivity roughly 15 times greater than that of Milagro and well matched to the sensitivity of current IACTs.

The sensitivity of HAWC to point sources of TeV gamma rays will be roughly 15 times that of Milagro, enabling HAWC to detect the Crab Nebula in a single transit (compared to 3-4 months for Milagro). As an all-sky instrument with a low energy threshold below 100 GeV, HAWC is well suited to detect transient phenomena in the VHE sky. Flares from active galaxies and gamma-ray bursts are prime scientific targets for HAWC [126]. Extrapolations from current detections of GRBs by the Fermi LAT indicate that HAWC should detect about 1.6 GRBs each year [263]. The detection of a GRB at  $>100$  GeV would enable HAWC to probe for violations of Lorentz Invariance with a sensitivity about a factor of two beyond current limits. Flares (or lack of flares) from distant AGN will directly test the UHECR origin of the highest energy gamma rays from these objects, which is critical to understanding the sources of UHECRs and the role of axion-like particles in the propagation of VHE gamma rays. The final state emission from a primordial black hole will have a signature that is similar too - but distinct from - a gamma-ray burst and HAWC will be sensitive to such emission over a volume roughly 2 orders of magnitude larger than has been probed to date. HAWC's sensitivity to the annihilation of dark matter particles peaks in the dark matter mass range above 10 TeV and the large field-of-view gives HAWC unique sensitivity to baryon-poor dwarf galaxies for high-mass dark matter.

**LHAASO** The LHAASO (Large High Altitude Air Shower Observatory) is an ambitious project based upon a combination of water Cherenkov technology, scintillation detectors, and air Cherenkov technology. LHAASO will consist of a  $\sim 90,000\text{m}^2$  water Cherenkov detector surrounded by 5100 scintillation detectors distributed over an area of  $\sim 1\text{km}^2$  with 43,000  $\text{m}^2$  of buried muon detectors. In addition 24 air fluorescence/Cherenkov telescopes will be located onsite. At an altitude of  $\sim 4300\text{m}$ , it is expected that LHAASO will have somewhat better sensitivity than HAWC at low energies ( $<10\text{ TeV}$ ), with significantly improved sensitivity at higher energies. This project recently received approval from the Chinese government and the completion of construction is expected in 2018.

**A Future Wide-Field High-Duty Cycle Gamma-Ray Experiment** HAWC was designed and built based on the results from the Milagro experiment. Similarly, the design of a future wide-field high duty-cycle experiment will be based upon the results from HAWC (or LHAASO). There are two distinct paths for a future instrument: significantly higher sensitivity to higher energy gamma rays, in excess of 100 TeV or significantly reducing the useful energy threshold. If the HAWC data shows that exciting physics is to be found at the highest energies (cosmic-ray origins, Galactic gamma-ray sources), then a plan to increase the collecting area at the highest energies would be recommended. Such an upgrade could be performed at the existing HAWC site or at a new location, perhaps in the Southern hemisphere to provide an alert system for the CTA South. On the other hand, if extragalactic phenomena, especially transient events such as flares from active galaxies to gamma-ray bursts, yield a rich source of information on particle acceleration, ultra-high-energy cosmic rays, and tests of fundamental physics, a detector with a significantly lower energy threshold would be recommended. Such an instrument would require the highest altitude site attainable, and thus would naturally be placed in the Southern hemisphere. Within the Chajnantor plateau in Chili it seems feasible to site such an instrument at  $\sim 6\text{km}$  above sea level.

### 2.5.3 Neutrino Experiments

**IceCube and KM3NeT** IceCube is a  $1\text{ km}^3$  neutrino observatory located at the South Pole [19]. Completed in December, 2010, it instruments  $1\text{ km}^3$  of Antarctica ice with 5,160 optical sensors, mounted at depths between 1450 and 2450 m, on 86 vertical strings which are emplaced in holes drilled in the icecap. These sensors observe the Cherenkov radiation from the charged particles which are produced when high-energy neutrinos interact in the Antarctic ice. 78 of the strings are arranged on a 125 m triangular grid; this array has an energy threshold of about 100 GeV. The remaining 8 strings form a denser subarray called “DeepCore” [18]; these strings have smaller spacings, with most of DOMs on the bottom 350 m of the strings. DeepCore has an energy threshold of about 10 GeV.

A surface array, called IceTop, completes the installation [264]. It comprises 162 ice filled tanks. The array is sensitive to cosmic-ray air showers with energy above about 100 TeV. One key feature of IceTop is its altitude; at 2735 m above sea level, so IceTop is relatively near shower maximum for the showers of greatest interest (above 1 PeV); this reduces its sensitivity to many systematic errors, such as hadronic interaction models.

IceCube observes about 200 neutrino interactions per day, mostly produced in cosmic-ray air showers. It has measured the  $\nu_\mu$  spectrum from energies of 100 GeV up to 1 PeV, the atmospheric  $\nu_e$  spectrum from energies of 80 GeV up to 6 TeV, and has set limits on  $\nu_\tau$  [265]. Using DeepCore, it has observed atmospheric neutrino oscillations, studying neutrinos with energies in the 10-60 GeV region [266].

IceCube has searched for astrophysical neutrinos in many channels, including searches for point sources [267], episodic sources, GRBs [268] and diffuse searches. The point source searches have not observed any excesses over atmospheric backgrounds, but the diffuse searches have seen a clear excess of expectations,



most notably "Bert" and "Ernie," two neutrino events with energies above 1 PeV [4]. A systematic study found 28 contained events, with energies above 60 TeV, over an expected background of about 12 events; this is roughly a  $4\sigma$  excess [269].

IceCube has also studied cosmic-ray air showers, including measurements of the energy spectrum, composition (combining IceTop air shower data with buried measurements of TeV muon fluxes) and anisotropy [270]. Surprisingly, the anisotropy persists up to energies of at least 400 TeV; this challenges our models of cosmic-ray production and propagation [271]. It also studies high transverse momentum muons produced in air showers, establishing the connection between cosmic-ray physics and perturbative quantum chromodynamics [272].

IceCube also searches for a variety of beyond-standard model phenomena: neutrinos from WIMP annihilation in the Sun, the Earth, the galactic halo or nearby dwarf galaxies, searches for magnetic monopoles and upward-going particle pairs; the latter is expected many variants of supersymmetry with a high mass scale.

A consortium of European institutions are proposing to build the KM3NeT detector [273]. This 5-6 km<sup>3</sup> detector would be located in the Mediterranean sea, where it would have a good (neutrino) view of the galactic center. Seawater has a somewhat longer optical scattering length than Antarctic ice, so KM3NeT should also have somewhat better angular resolution than IceCube.

**PINGU and other high-density detectors** PINGU (Precision IceCube Next Generation Upgrade) is a proposed high-density infill array within IceCube and DeepCore [274]. It will consist of 20 to 40 additional strings, with at least 60 optical modules per string, to observe neutrinos with energies down to a few GeV. The optical modules would be similar to those used in IceCube. Its main physics goal is to determine whether the neutrino mass hierarchy is 'normal' or 'inverted.' It is sensitive to the hierarchy because low energy electron neutrinos passing through dense matter (i.e. the Earth's core and mantle) can resonantly oscillate into other flavors; the energy dependence of this resonant oscillation depends on the hierarchy.

ORCA (Oscillation Research with Cosmics in the Abyss) [275] is a proposed high-density phototube array in the Mediterranean. It would study a similar set of physics topics as PINGU.

Looking further ahead, MICA (Multi-Megaton Ice Cherenkov Array) would be an array with an even denser array of photosensors [276]. It will instrument a large volume (several megatons) with enough photosensor area to be able to search for proton decay and observe supernova neutrinos from other galaxies. The supernova search will benefit from both the large volume and the high photon sensor density to allow nearly background-free searches for neutrinos from supernovas in moderately nearby galaxies; the goal is a detector big enough to will collect a statistically meaningful number of supernovae.

**Radio Cherenkov Experiments** Radio Cherenkov experiments exploit the Askaryan emission produced by the excess negative charge which develops in showers occurring in dense media. Active and proposed radio Cherenkov experiments can be classified as balloon-borne and *in situ*. Balloon experiments have a higher threshold, but can view an enormous volume of ice from their high altitudes. Radio arrays *in situ* expect to be able to reconstruct the neutrino locations and directions better than balloon experiments due to their close proximity to the interactions. Balloon experiments view the neutrino sky at low declinations while *in situ* arrays can view downward and Earth-grazing directions.

**ANITA** The ANITA (ANtarctic Impulsive Transient Antenna) is a balloon-borne radio Cherenkov experiment designed to search for radio impulsive signals induced by UHE neutrino interactions from  $\sim 37$  km altitude above the Antarctic ice. ANITA has flown twice (ANITA 1 in the 2006-2007 season and ANITA 2 in

2008-2009) under NASA's long-duration balloon program, and has a third flight approved and planned for the 2014-2015 season. ANITA flies broadband (200 MHz-1200 MHz), dually polarized antennas that view the typically 1.5 million km<sup>2</sup> of ice in view of the payload. The signature for a UHE neutrino interaction in ANITA would be a set of impulsive signals that are not consistent with being from any known base or other human activity, or any other event. From the non-observation of a neutrino signal in its first two flights, ANITA places the world's best constraints on the UHE neutrino flux above 10<sup>19</sup> eV. ANITA 3 will fly 48 antennas (compared to 40 for ANITA 2) with improved response at the crucial low end of the band, and will for the first time perform cursory interferometric analysis at the trigger level, allowing for a  $\sim 20 - 30\%$  reduction of the threshold.

*ARA* The Askaryan Radio Array (ARA) is an *in situ* array being deployed near the South Pole. The ARA collaboration aims to detect of order 10 UHE neutrinos per year by instrumenting the 100's of km<sup>3</sup> detection volume of ice with a 200 m deep array arranged in stations of 16 antennas, horizontally and vertically polarized and bandwidths approximately 150 MHz-800 MHz. A prototype testbed station and the first three ARA stations were deployed between the 2010-2011 and 2012-2013. In the last season the ARA drill team successfully reached the 200 m design depth below the snow-ice transition layer called the firn. The ARA collaboration is proposing to deploy another seven stations in the 2013-2014 and 2014-2015 seasons, bring the detector to 10 stations (ARA10) on the path towards a ARA37 spanning 100 km<sup>2</sup> of ice area. ARA10 will have discovery potential for many data-driven neutrino flux models while ARA37 will either begin to collect a sample of neutrinos from those models, or reach even the more pessimistic models where the cosmic ray composition at the highest energies is mixed.

*ARIANNA* ARIANNA (Antarctic Ross Ice-Shelf Antenna Neutrino Array) is a surface array being deployed on the Ross Ice Shelf with a similar aim to reach the detector volume necessary to measure a sample of order 100 UHE neutrinos. ARIANNA aims to detect the impulsive radio Cherenkov signals from neutrino interactions both directly, and after reflections from the highly reflective ice-sea water boundary below the shelf. Together the direct and reflected signals complete the coverage of the upper sky. Initial results using a broadband pulser have verified the integrity of signals post-reflection. ARIANNA is on-track to complete a 7-station hexagonal detector unit in the 2013-2014 season and proposes to deploy a 960 station array. Although ARIANNA requires a large number of stations for the same detection volume compared to a deep array like ARA, a surface array is in principle simpler to deploy.

*EVA* The ExaVolt Antenna (EVA) is a next-generation balloon experiment that would turn the stadium-sized balloon itself into an enormous antenna, which would make EVA the world's largest airborne telescope. An impulsive signal from the ice below would be incident on  $\sim 10$  m high reflector region that would be affixed along the bulge of the balloon, and focused onto the receiver array suspended on the inside of the balloon. EVA takes advantage of the Super Pressure Balloon technology that is being developed by NASA, where the internal pressure of the balloon is higher than the outside pressure and the balloon holds its shape to  $\sim 1\%$  along any dimension. EVA expects to use a 18.5 Mft<sup>3</sup> balloon for the full flight. Microwave scale models of EVA reflector sections built and tested at the University of Hawaii have demonstrated a 23 dBi antenna gain and a focus region that would scale to one to a few meters for the full balloon. The EVA collaboration was awarded a 3 year engineering grant and will carry out a hang test of a 1/20 scale, 5 m diameter EVA prototype in the Fall of 2013 or Spring of 2014 before proposing a flight of the full EVA. EVA would boast the best sensitivity to the neutrino spectrum at the highest energies.

### 3 CF6-B: The Matter Of the Cosmological Asymmetry

The Cosmological Asymmetry between matter and anti-matter provides firm evidence for non-dark physics beyond the standard model. The current net density of baryons implies an asymmetry during the hot early universe between quarks and anti quarks, with about  $10^8 + 1$  quarks for every  $10^8$  anti-quarks. This asymmetry must have arisen after the end of inflation, due to some unknown mechanism called *baryogenesis*. In 1967 Andrei Sakharov proposed that baryogenesis could arise from out of equilibrium new physics which violates baryon number conservation, and the C and CP symmetries between matter and antimatter[277]. At nonzero temperature baryon number violation in the standard model proceeds via the baryon number violating electroweak field configurations are known as *sphalerons*[278]. In 1985 Kuzmin, Rubakov and Shaposhnikov pointed out that sphaleron processes are sufficiently rapid at the high temperatures of the early universe to play a role in baryogenesis [279]. They also proposed that a strongly first order electroweak phase transition could provide the necessary departure from thermal equilibrium. However it is now known that the minimal standard model with a 125 GeV Higgs does not undergo a phase transition[280, 281, 282], and also does not have sufficient CP violation to produce an asymmetry of order  $10^{-8}$  [87]. However many extensions of the standard model do provide the necessary conditions for baryogenesis, as well as exciting opportunities for a wide variety of experiments. For recent reviews, see ref. [283, 284]. Here we summarize the most well motivated possibilities.

#### 3.1 Leptogenesis

The recent advent of the evidence of non-zero neutrino masses opens up the possibility of *leptogenesis* [88], generation of a net lepton number. As sphaleron processes conserve  $B - L$ , the difference between baryon number and lepton number, they tend to convert part of the primordial lepton number asymmetry into a baryon number asymmetry. The successful implementation of leptogenesis requires the existence of new CP violating phases in the lepton sector. In this scenario, the baryon asymmetry is related to the properties of the neutrinos. This subject is an example of the synergy between physics at the Cosmic and the Intensity Frontiers [285].

##### 3.1.1 Standard Leptogenesis

Standard leptogenesis [88] is implemented within the seesaw mechanism for small neutrino masses in the presence of right-handed neutrinos. The full seesaw Lagrangian contains the Yukawa interactions for the neutrinos that in turn gives the Dirac mass terms for the neutrinos, as well as the lepton number violating Majorana mass terms,  $M_R$ , for the right-handed neutrinos. At temperature  $T < M_R$ , right-handed neutrinos,  $N$ , can generate a primordial lepton number asymmetry via out-of-equilibrium decays,  $N \rightarrow \ell H$  and  $N \rightarrow \bar{\ell} \bar{H}$ , where  $H$  is the SU(2) Higgs doublet and  $\ell$  is the lepton doublet. The quantum interference between the tree-level and one-loop contributions to the decay can lead to a lepton number asymmetry.

The predictions for the baryon number asymmetry through standard leptogenesis depends on the coupling constants in the seesaw Lagrangian. Thus, by demanding that sufficient baryon number asymmetry to be generated, constraints [89] on neutrino parameters can be obtained. Specifically, the mass of the lightest right-handed neutrino is constrained to be  $M_1 > 3 \times 10^9$  GeV. One also obtains an upper bound on the light effective neutrino mass,  $m_1 < 0.12$  eV, which is incompatible with the quasi-degenerate spectrum.

If the right-handed neutrinos are produced thermally, the lower bound on the lightest right-handed neutrino mass is then translated into a lower bound on the reheating temperature,  $M_{\text{RH}} > M_1 > O(10^9)$  GeV. Such a high reheating temperature is problematic for many extensions of the Standard Model. For instance in many variants of supersymmetry, constraints from WMAP (for stable gravitino) and BBN (for unstable gravitino) typically require the reheating temperature to be several orders of magnitude lower than  $10^9$  GeV, incompatible with the condition for successful standard leptogenesis in supersymmetric models.

### 3.1.2 Alternative Realizations

To evade the gravitino over production problem, several scenarios have been proposed in which the conflicts between leptogenesis and gravitino over-production problem are overcome in different ways:

- resonant enhancement in the self-energy diagrams due to near degenerate right-handed neutrino masses: in resonant leptogenesis [90], it has been shown that sufficient asymmetry can be generated even with TeV scale right-handed neutrino masses, leading to the possibility of testing this scenario at the collider experiments.
- relaxing the relation between the lepton number asymmetry and the right-handed neutrino mass: one example is the soft leptogenesis [286], where the asymmetry arises in mixing, instead of decay. In this case, the source of CP violation is the complex phases in the soft SUSY parameters.
- relaxing the relation between the reheating temperature and the right-handed neutrino mass: one realization of non-thermal leptogenesis is the production of the right-handed neutrinos by inflaton decay [287].

### 3.1.3 Dirac Leptogenesis

It was pointed out [288] that leptogenesis can be implemented even in the case when neutrinos are Dirac fermions which acquire small masses through highly suppressed Yukawa couplings without violating lepton number. The realization of this depends critically on the following three characteristics of the sphaleron effects: (i) only the left-handed particles couple to the sphalerons; (ii) the sphalerons change (B+L) but not (B-L); (iii) the sphaleron effects are in equilibrium for  $T > T_{EW}$ . For the neutrinos, given that the neutrino Dirac mass is very tiny ( $m_D < 10$  keV), the left-right equilibration can occur at a much longer time scale compared to the electroweak epoch when the sphaleron washout is in effect. Suppose that some processes initially produce a negative lepton number ( $\Delta L_L$ ), which is stored in the left-handed neutrinos, and a positive lepton number ( $\Delta L_R$ ), which is stored in the right-handed neutrinos. Because sphalerons only couple to the left-handed particles, part of the negative lepton number stored in left-handed neutrinos get converted into a positive baryon number by the electroweak anomaly. This negative lepton number  $\Delta L_L$  with reduced magnitude eventually equilibrates with the positive lepton number,  $\Delta L_R$  when the temperature of the Universe drops to  $T \ll T_{EW}$ . Because the equilibrating processes conserve both the baryon number  $B$  and the lepton number  $L$  separately, they result in a Universe with a total positive baryon number and a total positive lepton number. And hence a net baryon number can be generated even with  $B = L = 0$  initially.

### 3.1.4 Possible connections to CP violation in neutrino oscillation.

In the seesaw Lagrangian at high scale in the presence of three right-handed neutrinos, there are in total 6 mixing angles and 6 physical CP phases. On the other hand, the effective Lagrangian at low energy after integrating out the right-handed neutrinos, only three mixing angles and three physical CP phases remain. Given the presence of extra mixing angles and phases at high energy, it is generally impossible to connect leptogenesis (within the standard leptogenesis framework) and low energy CP violation processes in a model independent way. Nevertheless, this statement is weakened when the flavor effects, which are relevant if leptogenesis takes place at  $T < 10^{12}$  GeV, are taken into account. On the other hand, within certain predictive models for neutrino masses, strong connections can be established even in the absence of flavor effects.

Generally, two classes of models have been shown to exhibit possible connection between leptogenesis and CP violation in neutrino oscillation. These include:

- models with rank-2 mass matrix: It has been shown that in a model with only two right-handed neutrinos with a rank-2 neutrino mass matrix, the sign of the baryon number asymmetry is related to the sign of CP violation in neutrino oscillation [289].
- models where CP violation comes from a single source: These include models with spontaneous CP violation, for example in minimal left-right symmetry model, there is only one physical CP phase in the lepton sector [290]. All leptonic CP violating processes (leptogenesis, neutrino oscillation, etc) are determined solely by this phase. Another example is a model with finite group family symmetry  $T'$  with complex Clebsch-Gordan coefficients. CP violation in this model is due entirely to the complex CG coefficients. As the only non-vanishing leptonic phases are the low energy ones due to the symmetry of the model, there exists a strong connection between leptogenesis and low energy CP violating processes in this model [291].

### 3.1.5 Affleck-Dine Baryogenesis

In supersymmetric extensions of the Standard Model, there exist field configurations—condensates— of squark and slepton fields with very large expectation values and relatively low energy density compared with the thermal energy. In supersymmetric theories, at the exit from inflation, the observable universe would typically be in one of these configurations. Affleck and Dine showed that  $CP$  and baryon number violation at high energy would lead to net baryon production from the coherent evolution and subsequent decay of the condensates [91]. The Affleck-Dine scenario is consistent with a low reheat scale, and in some variants, can provide an explanation for dark matter as well. Decay of the condensates into baryons and WIMPS can provide an explanation for the similar cosmological densities of dark matter and baryons [292, 293]. Another interesting possibility is that the condensates will fragments into stable lumps of matter with macroscopic amounts of baryon number and lower energy/baryon number than ordinary matter. For some parameters, these lumps, called Q-balls, are a viable dark matter candidate with unusual phenomenology [92, 93, 94].

### 3.1.6 Electroweak Baryogenesis

A strongly first order electroweak phase transition can occur in some extensions of the standard model, and provide the departure from thermal equilibrium necessary for baryogenesis. Such a phase transition proceeds via nucleation of bubbles of broken phase which expand to fill the entire universe. Inside the bubbles the Higgs expectation value is large, sphaleron transitions are suppressed, and baryon number is conserved,

while the symmetric phase with no Higgs expectation value and unsuppressed sphalerons exists outside the bubbles. CP violating scattering of particles with the expanding bubble walls can lead to an CP asymmetric particle content in the symmetric phase, which will bias the sphalerons towards producing a net baryon number. This baryon number will then pass into the bubbles and, provided the sphalerons inside the bubble are suppressed by a large enough Higgs expectation value, survive until the present. For strongly first order phase transition, the effective potential at the critical temperature for the Higgs field must possess degenerate minima with a barrier between them. This barrier requires new bosons which are coupled to the Higgs field. Some well explored contenders for electroweak baryogenesis models are the MSSM [95], and generic two Higgs doublet models[96]. The MSSM is still a viable baryogenesis model provided the scalar partner of the right handed top quark is lighter than the top quark[294], and nonminimal supersymmetric theories are much less constrained[295]. In general two Higgs doublet models have a large parameter space[296, 297], a significant portion of which remains viable for baryogenesis after the recent 126 GeV Higgs boson discovery[298]. Both the MSSM and two Higgs doublet models possess potential additional sources of CP violation and new contributions to Electric Dipole Moments (EDMs), which constrain the magnitude of the new CP violating phases. The theory connecting the new sources of CP violation with the total baryon number produced is very complicated and still possesses considerable sources of uncertainty, and is still being actively developed. See ref. [299] for a recent review. Eventually reliable theoretical computations of the baryon asymmetry will allow for predictions for EDMs and for new particle properties in electroweak baryogenesis models, but we are not quite there yet.

### 3.1.7 Other Baryogenesis mechanisms

Sakharov’s original model, and subsequent baryogenesis models based on Grand Unified Theories, relied on the out of equilibrium decays of very heavy particles of mass of order  $10^{15}$  GeV. Such theories are mostly now inconsistent within the modern theory of inflation, as it is difficult to obtain a high enough reheat temperature to produce such particles.

A variety of other mechanisms for baryogenesis have been suggested, at energy scales ranging from just above the nucleosynthesis temperature of an MeV [300] to very high temperatures or high scale out of equilibrium processes occurring at the end of inflation. Some theories do not require baryon number violation at all, as the dark matter can carry an equal and opposite baryon number [301].

## 3.2 Experimental Signatures of Baryogenesis

The origin of the matter—anti-matter asymmetry in the universe is one of the most profound scientific questions of our time. A wide variety of experiments at all three frontiers can provide illumination.

### 3.2.1 Cosmic Frontier Experiments and Baryogenesis:

- Constraining the scale of inflation from the impact of tensor fluctuations on the CMB is important.
- Gravity wave experiments could provide evidence for a first order phase transition.
- Certain dark matter models are connected with baryogenesis and can provide unusual signatures.

### 3.2.2 Intensity Frontier experiments and Baryogenesis:

- CP violation in the neutrino sector would provide support for the leptogenesis scenario, and some models make for specific predictions.
- Evidence for or against neutrino Majorana masses would also impact leptogenesis theory.
- Electroweak baryogenesis scenarios provide strong motivation to search for EDMs, exotic CPV in meson physics, and rare decays.
- Proton decay provides an important constraint on Grand Unified Model Building and on new sources of Baryon number violation.

### 3.2.3 Energy Frontier experiments and Baryogenesis:

- Collider tests of extended Higgs sectors and searches for new light scalars are important.
- Electroweak baryogenesis models typically have sizeable modifications of the triple Higgs self coupling [302, 303]

## 4 CF6-C: Exploring the Basic Nature of Space and Time

### 4.1 Quantum Geometry and The Holographic Universe

New quantum degrees of freedom of space-time, originating at the Planck scale, could create a coherent indeterminacy and noise in the transverse position of massive bodies on macroscopic scales.

Quantum effects of space-time are predicted to originate at the Planck scale,  $ct_P \equiv \sqrt{\hbar G/c^3} = 1.616 \times 10^{-35} \text{m}$ . In standard quantum field theory, their effects are strongly suppressed at experimentally accessible energies, so space-time is predicted to behave almost classically, for practical purposes, in particle experiments. However, new quantum effects of geometry originating at the Planck scale— from geometrical degrees of freedom not included in standard field theory— may have effects on macroscopic scales that could be measured by laser interferometers.

The possibility of new quantum-geometrical degrees of freedom is suggested from several theoretical directions. Quantum physics is experimentally proven to violate the principle of locality on which classical space-time is based. Gravitational theory suggests that quantum states of space-time systems do not respect locality of the kind assumed by quantum field theory, and suggests that space-time and gravity are approximate statistical behaviors of a quantum system with a holographic information content, far less than that predicted by quantum field theory.[97, 98]

Quantum geometry could arise in Planck scale physics, but still produce a detectable displacement in a macroscopic experiment.[99] A typical uncertainty in wave mechanics, if information about transverse position is transmitted nonlocally with a bandwidth limit, is the scale familiar from diffraction-limited imaging: the geometric mean of inverse bandwidth and apparatus size. For separations on a laboratory scale, a Planck scale frequency limit leads to a transverse uncertainty in position on the order of attometers. Displacements of massive bodies of this order are detectable using laser interferometry.

No fundamental theory of quantum geometry exists, but a consistent effective theory, based on general properties of quantum mechanics and covariance, can be used to precisely predict a phenomenology on macroscopic scales. In particular, the theory precisely relates the number of geometrical position eigenstates to the amplitude of indeterminacy in transverse position at separation  $L$ , so it can be related to the holographic density of states predicted from gravitational theory. This hypothesis leads to an exact prediction for the variance in transverse position with no free parameters,[304]

$$\langle x_{\perp}^2 \rangle = Lct_P / \sqrt{4\pi}. \quad (7)$$

Planckian indeterminacy leads to a new form of noise in position with this displacement, on a timescale  $L/c$ . This form of indeterminacy would have escaped detection to date, and indeed is overwhelmed by standard quantum indeterminacy on the mass scale of elementary particles. However, it is detectable as a new source of quantum-geometrical noise in an interferometer that coherently measures the positions of massive bodies in two directions over a macroscopic volume.[305, 99]

## 4.2 The Fermilab Holometer

An experiment is under development at Fermilab designed to detect or rule out a transverse position noise with Planck spectral density, using correlated signals from an adjacent pair of Michelson interferometers. A detection would open an experimental window on quantum space-time.

The Fermilab Holometer is an experiment (E-990) designed to detect or rule out quantum-geometrical noise with these properties.[306] Much of the technology has been developed by LIGO and other projects to measure displacements due to gravitational radiation. The quantum-geometrical measurement however calls for application of the technology in a new experimental design. Measurements can be made at relatively high (MHz) frequencies, where environmental and gravitational noise sources are smaller, both shrinking and simplifying the layout. The experiment is designed to measure the specific and peculiarly quantum-mechanical signatures of the effect, such as nonlocal coherence and transverse nature of the indeterminacy, the frequency cross spectrum, and time-domain cross correlation function. It is anticipated that the experiment will be complete, and either detect or rule out this form of Planckian noise, within about two years.

If the noise is found not to exist, only a modest followup effort may be motivated to pursue the limits somewhat past the Planck scale for a conclusive result. If it is found, a significantly expanded experimental program can be pursued to obtain high precision results and map out the spatiotemporal properties of quantum geometry.

## 4.3 Torsion Balance Experiments

Another example of table top experiments with sensitivity to quantum gravitational effects are torsion balance experiments [307], which are sensitive to preferred frame effects, noncommutative geometry, new dimensions at short distances, and equivalence principle violation.



## 5 Tough Questions

*CF34. What are the roles of cosmic-ray, gamma-ray, and neutrino experiments for particle physics? What future experiments are needed in these areas and why? Are there areas in which these can have a unique impact?*

In this document we have discussed a broad range of fundamental physics that can be gleaned from cosmic rays, gamma rays, and neutrinos (dark matter, axions, primordial black holes, Q-balls, Lorentz invariance violation, intergalactic magnetic fields, particle interactions at high energies, neutrino mass hierarchy, etc.) that can not be reached through other methods.

**CTA** will usher in the era of precision VHE astrophysics and in conjunction with current instruments (Fermi and HAWC) will provide a view of the high-energy universe that will lead to an understanding of the astrophysical processes at work in these extreme objects and enable us to probe the laws of physics at energies, couplings, and mass scales that are beyond the reach of traditional high-energy physics experiments. Most importantly perhaps is the indirect detection of dark matter (see CF-2), where gamma-ray experiments have sensitivity to regions of parameter space not accessible to other techniques (accelerator and direct search techniques). The discovery of a primordial black hole or a Q-ball would provide a wealth of data on the early universe and particle physics at energies not attainable in accelerators. Measurement of a vacuum dispersion relation for light would provide unique insight into the merging of quantum mechanics and general relativity. A measurement of the intergalactic magnetic fields would give insight into primordial magnetogenesis and the early universe processes, phase transitions or inflation dynamics that may have given rise to such a field.

**PINGU** will use the atmospheric neutrinos to measure the neutrino mass hierarchy. By using the atmospheric neutrinos generated by cosmic-ray interactions in the atmosphere a large range of  $L/E$  is available, enabling sensitive searches for matter effects on neutrino oscillations. At a relatively low cost, this can be used to make a definitive measurement of the neutrino mass hierarchy.

**JEM-EUSO and a large aperture ground array** Cosmic-ray experiments provide a window into particle interactions at the highest energies. While only large cross-section physics is accessible, given the low flux, well measured data with well-understood systematics, may offer channels to new physics. With much improved control over systematics and detector resolution and by combining various detectors (hybrid approach) current data has yielded interesting hints that we don't fully understand how to predict hadronic interactions at these energies. The measurement of total cross-section by HiRes and Auger at energies well beyond the LHC, while still crude, can be refined and be an important constraint on hadronic interaction models. A future large area surface detector will extend this measurement to higher energies, over an order of magnitude greater than achievable at the LHC.

From an astrophysics point of view, the next big question is the anisotropy of UHECR, i.e. the search for astrophysical sources. This is beginning to show interesting hints of association with nearby Large Scale Structure, but to really pin this down will require another order of magnitude or more of collecting area. JEM-EUSO, can achieve the required exposure. We know that UHECR originate within  $\sim 100$  Mpc of us. But until we can clearly state that the highest energy cosmic-ray flux anisotropy is understood from the point of view of astrophysical sources, the potential for new physics remains as strong as ever.

*CF35. What will it take to identify the mechanism for baryogenesis or leptogenesis? Are there scenarios that could conceivably be considered to be established by experimental data in the next 20 years?*

There are 3 well motivated scenarios for baryogenesis. Of these, electroweak baryogenesis is the one which is most likely to be definitively established or excluded within 20 years. In this scenario the baryon asymmetry of

the universe can be related to the properties of new particles which couple to the Higgs boson, to properties of the Higgs boson, and to electric dipole moments (EDMs) of the neutron, the electron, and atoms. In particular difficult but doable theoretical calculations can relate the size and sign of a new CP violating phase to the baryon asymmetry and to EDMs.

It will be more difficult to establish the leptogenesis scenario, especially in the versions where it proceeds via the decay of very heavy ( $> 10^9$  GeV) neutrinos. Some generic indications of this scenario are Majorana neutrinos, a light neutrino below 0.1 eV, and CP violation in neutrino oscillations, but verification of these features does not prove the theory is right, and the theory does not make a specific prediction for the phase which is observable in oscillations. However the heavy neutrino version requires a high inflation scale and high reheat temperature after inflation, which could be inconsistent with some kinds of new physics such as neutron-anti-neutron oscillations or supersymmetry with a gravitino in the mass range between a keV and  $10^4$  GeV, and so, depending on what other new physics is discovered, it could be excluded. Other leptogenesis scenarios involve new neutral leptons at or below the weak scale, or Dirac neutrinos, and have a restricted enough parameter space to be excluded or confirmed.

Affleck-Dine baryogenesis requires supersymmetry but does not necessarily require a specific SUSY spectrum, so definitively establishing or excluding this scenario is difficult. It is possible that this scenario can lead to the formation of stable Q-balls, an interesting dark matter candidate whose discovery would be strong evidence for the Affleck Dine scenario. Evidence of a high inflation scale from CMB B-modes would likely exclude this scenario, as fluctuations in the condensate would lead to isocurvature perturbations with an amplitude that has been ruled out by CMB measurements.

*CF36. What are the leading prospects for detecting GZK neutrinos? What experimental program is required to do this in the next 5 years, 10 years, 20 years, and how important is this?*

The prospects for detecting GZK neutrinos in the next decade are quite good. We know that there is a bottom to the flux of these neutrinos. Current efforts have ruled out the more optimistic scenarios and are now reaching into realistic parameter space. The next generation of instruments can improve upon current sensitivity by an order of magnitude giving sensitivity that is close to the lowest possible fluxes (an all iron composition). At the same time, the fraction of iron in the highest energy cosmic rays is lower than previously thought, significantly increasing the likelihood that the next generation of experiments will detect the GZK neutrinos.

How important is this? The GZK neutrinos provide a method to measure the neutrino cross section at a center-of-mass energy of 100 TeV! Observation of these interactions can provide information on beyond standard model physics that is many orders of magnitude beyond what is achievable in accelerator-based neutrino experiments. These observations will also enable us to understand cosmic accelerators.

## References

- [1] M. Ackermann *et al.* *Science* **339** (2013) .
- [2] **AGILE Collaboration** Collaboration, A. Giuliani *et al.*, “Neutral pion emission from accelerated protons in the supernova remnant W44,” *Astrophys.J.* **742** (2011) L30, [arXiv:1111.4868](#) [[astro-ph.HE](#)].
- [3] V. A. Acciarri *et al.* *Astrophys. J. Lett.* **730** (2011) .
- [4] **IceCube Collaboration** Collaboration, M. Aartsen *et al.*, “First observation of PeV-energy neutrinos with IceCube,” *Phys.Rev.Lett.* **111** (2013) 021103, [arXiv:1304.5356](#) [[astro-ph.HE](#)].
- [5] K. Greisen, “‘End to the cosmic ray spectrum’,” *Phys. Rev. Lett.* **16** (1966) 748.
- [6] G. Zatsepin and V. Kuzmin, “‘Upper limit of the spectrum of cosmic rays’,” *JETP Lett.* **4** (1966) 78.
- [7] R. Abbasi *et al.*, “‘First observation of the Greisen-Zatsepin-Kuzmin suppression’,” *Phys. Rev. Lett.* **100** (2008) 101101. [astro-ph/0703099](#).
- [8] J. Abraham *et al.*, “‘Observation of the suppression of the flux of cosmic rays above  $4 \times 10^{19}$  eV’,” *Phys. Rev. Lett.* **101** (2008) 061101. [arXiv:0806.4302](#).
- [9] T. Abu-Zayyed *et al.*, “‘The Cosmic Ray Energy Spectrum Observed with the Surface Detector of the Telescope Array Experiment’,” *Astrophys. J. Lett.* **768** (2013) L1. [arXiv:1205.5067](#) [[astro-ph.HE](#)].
- [10] J. Abraham *et al.*, “‘Measurement of the energy spectrum of cosmic rays above  $10^{18}$  eV using the Pierre Auger Observatory’,” *Phys. Lett. B* **685** (2010) 239. [arXiv:1002.1975](#).
- [11] O. Adriani *et al.* *Nature* **458** (2009) .
- [12] **AMS Collaboration** Collaboration, M. Aguilar *et al.*, “First Result from the Alpha Magnetic Spectrometer on the International Space Station: Precision Measurement of the Positron Fraction in Primary Cosmic Rays of 0.5350 GeV,” *Phys.Rev.Lett.* **110** no. 14, (2013) 141102.
- [13] H. Yuksel, M. D. Kistler, and T. Stanev *Phys. Rev. Lett.* **103** (2009) .
- [14] F. Aharonian, J. Buckley, T. Kifune, and G. Sinnis, “High energy astrophysics with ground-based gamma ray detectors,” *Rept.Prog.Phys.* **71** (2008) 096901.
- [15] S. Funk [arXiv:1204.4529](#) [[astro-ph.HE](#)].
- [16] F. Rieger, E. de One-Wilhelmi, and F. Aharonian *to appear in Frontiers of Physics* (2013) , [arXiv:1302.5603](#) [[astro-ph.HE](#)].
- [17] S. Wakely and D. Horan, 2013. <http://tevcat.uchicago.edu/>.
- [18] **IceCube Collaboration** Collaboration, R. Abbasi *et al.*, “The Design and Performance of IceCube DeepCore,” *Astropart.Phys.* **35** (2012) 615–624, [arXiv:1109.6096](#) [[astro-ph.IM](#)].
- [19] F. Halzen and S. R. Klein, “IceCube: An Instrument for Neutrino Astronomy,” *Rev.Sci.Instrum.* **81** (2010) 081101, [arXiv:1007.1247](#) [[astro-ph.HE](#)].
- [20] W. Atwood *et al.* *Astrophys. J.* **697** (2009) .
- [21] W. Menn *et al.* *Adv. Space Res.* **51** (2013) .

- [22] A. Kounine *et al.*
- [23] J. Boyer *et al.* *Nucl. Instr. Meth.* **A482** (2002) .
- [24] F. Aharonian *et al.* *Science* **307** (2005) .
- [25] T. Weekes *et al.* *Astropart. Phys.* **17** (2002) .
- [26] J. Aleksic *et al.* *Astrophys. J.* **742** (2011) .
- [27] R. A. Atkins *et al.* *Astrophys. J.* **595** (2003) .
- [28] **The CTA Collaboration** Collaboration, M. Actis *et al.* *Experimental Astronomy* **32** (2011) .
- [29] M. G. Aartsen *et al.* [arXiv:1306.5846](#) [astro-ph.IM].
- [30] **JEM-EUSO Collaboration** Collaboration, J. Adams *et al.*, “An evaluation of the exposure in nadir observation of the JEM-EUSO mission,” *Astropart. Phys.* **44** (2013) 76–90, [arXiv:1305.2478](#) [astro-ph.HE].
- [31] **The JEM-EUSO Collaboration** Collaboration, “The JEM-EUSO Mission: Contributions to the ICRC 2013,” [arXiv:1307.7071](#) [astro-ph.IM].
- [32] V. Berezhinsky, A. Z. Gazizov, and S. I. Grigorieva *Phys. Rev. D* **74** (2006) .
- [33] S. Klein and A. Connolly, 2013. [arXiv:1304.4891](#).
- [34] D. Hooper *Phys. Rev. D.* **65** (2002) 097303. [hep-ph/0203239](#).
- [35] E. Borriello *et al.* *Phys. Rev. D* **77** (2008) 045019. [arXiv:0711.0152](#) [astro-ph].
- [36] A. Connolly *et al.* *Phys. Rev. D* **83** (2011) 113009.
- [37] I. Romero and O. Sampayo *JHEP* **0905** (2009) 111. [arXiv:0906.5245](#) [hep-ph].
- [38] R. Ellsworth, T. Gaisser, T. Stanev, and G. Yodh *Phys. Rev. D* **26** (1982) .
- [39] R. M. Baltrusaitis, G. L. Cassiday, J. W. Elbert, P. R. Gerhardy, S. Ko, E. C. Loh, Y. Mizumoto, P. Sokolsky, , and D. Steck *Phys. Rev. Lett.* **52** (1984) .
- [40] P. Abreu *et al.*, “Measurement of the proton-air cross-section at  $\sqrt{s} = 57$  TeV with the Pierre Auger Observatory’,” *Phys. Rev. Lett.* **109** (2012) 062002. [arXiv:1208.1520](#) [hep-ex].
- [41] D. Bird *et al.* *Phys. Rev. Lett.* **71** (1993) 3401.
- [42] T. Gaisser *et al.* *Phys. Rev. D* **47** (1993) .
- [43] D. Bird *et al.* *Astrophys. J.* **424** (1994) .
- [44] P. Abreu *et al.*, “Interpretation of the Depths of Maximum of Extensive Air Showers Measured by the Pierre Auger Observatory’,” *JCAP* **1302** (2013) 026. [arXiv:1301.6637](#) [astro-ph.HE].
- [45] G. Farrar *Proceedings of the 33rd International Cosmic Ray Conference* (2013) .
- [46] G. Farrar and J. Allen, “A new physical phenomenon in ultra-high energy collisions’,” *EPJ Web of Conferences* **53** (2013) 07007. [arXiv:1307.2322](#) [hep-ph].
- [47] J. Abraham *et al.*, “Correlation of the highest energy cosmic rays with nearby extragalactic objects,” *Science* **318** (2007) 938. [arXiv:0711.2256](#) [astro-ph].

- [48] J. A. anod others, “Correlation of the highest-energy cosmic rays with the positions of nearby active galactic nuclei’,” *Astropart. Phys.* **29** (2008) 188. Erratum-ibid. **30**, 45 (2008); arXiv:0712.2843 [astro-ph].
- [49] P. Abreu *et al.*, “Update on the correlation of the highest energy cosmic rays with nearby extragalactic matter’,” *Astropart. Phys.* **34** (2010) 314. arXiv:1009.1855 [astro-ph.HE].
- [50] K. Kampert *et al.* arXiv:1207.4823.
- [51] T. AbuZayyad *et al.*, “Search for Anisotropy of Ultra-High Energy Cosmic Rays with the Telescope Array Experiment’,” *Astrophys. J.* **757** (2012) 26. arXiv:1205.5984 [astro-ph.HE].
- [52] P. Tinyakov *et al.* *Proceedings of the 33rd International Cosmic Ray Conference* (2013) .
- [53] **IceCube** Collaboration, R. Abbasi *et al.* *Phys. Rev. D* **83** (2011) .
- [54] **IceCube** Collaboration, A. Ishihara *et al.* *Nucl. Phys. B Proc. Suppl.* **235-236** (2012) .
- [55] P. Abreu *et al.*, “A Search for Ultra-High Energy Neutrinos in Highly Inclined Events at the Pierre Auger Observatory’,” *Phys. Rev. D* **84** (2011) 122005. arXiv:1202.1493 [astro-ph.HE].
- [56] I. Kravchenko, S. Hussain, D. Seckel, D. Besson, E. Fensholt, *et al.*, “Updated Results from the RICE Experiment and Future Prospects for Ultra-High Energy Neutrino Detection at the South Pole,” *Phys.Rev.* **D85** (2012) 062004, arXiv:1106.1164 [astro-ph.HE].
- [57] **ANITA Collaboration** Collaboration, S. Hoover *et al.*, “Observation of Ultra-high-energy Cosmic Rays with the ANITA Balloon-borne Radio Interferometer,” *Phys.Rev.Lett.* **105** (2010) 151101, arXiv:1005.0035 [astro-ph.HE].
- [58] S. Barwick *et al.* *Phs. Rev. Lett.* **96** (2006) .
- [59] **LBNE Collaboration** Collaboration, C. Adams *et al.*, “Scientific Opportunities with the Long-Baseline Neutrino Experiment,” arXiv:1307.7335 [hep-ex].
- [60] H. Duan, G. Fuller, J. Carlson, and Y.-Z. Qian *Phys. Rev. D* **74** (2006) .
- [61] H. Duan, G. Fuller, J. Carlson, and Y.-Z. Qian *Phys. Rev. Lett* **99** (2007) .
- [62] H. Duan, G. Fuller, and Y. Qian *Ann. Rev. Nucl. Part. Sci.* **60** (2010) .
- [63] B. Dasgupta, A. Dighe, G. Raffelt, and A. Smirnov *Phys. Rev. Lett.* **103** (2009) .
- [64] M. Boettcher *Astrophys. Sp. Sci.* **309** (2007) .
- [65] A. Bykov, N. Gehrels, H. Krawczynski, M. Lemoine, G. Pelletier, *et al.*, “Particle acceleration in relativistic outflows,” *Space Sci.Rev.* **173** (2012) 309–339, arXiv:1205.2208 [astro-ph.HE].
- [66] D. Hooper, P. Blasi, and P. D. Serpico, “Pulsars as the Sources of High Energy Cosmic Ray Positrons,” *JCAP* **0901** (2009) 025, arXiv:0810.1527 [astro-ph].
- [67] T. Linden and S. Profumo, “Probing the Pulsar Origin of the Anomalous Positron Fraction with AMS-02 and Atmospheric Cherenkov Telescopes,” *Astrophys.J.* **772** (2013) 18, arXiv:1304.1791 [astro-ph.HE].
- [68] V. Zirakashvili and V. Ptuskin, “Numerical simulations of diffusive shock acceleration in SNRs,” *Astropart.Phys.* **39-40** (2012) 12–21, arXiv:1109.4482 [astro-ph.HE].

- [69] R. Cowsik and B. Burch, “Positron fraction in cosmic rays and models of cosmic-ray propagation,” *Phys. Rev. D* **82** (Jul, 2010) 023009. <http://link.aps.org/doi/10.1103/PhysRevD.82.023009>.
- [70] M. S. Turner and F. Wilczek *Phys. Rev. D* **42** (1990) .
- [71] A. Abdo *et al.* *Astrophys. J. Lett.* **700** (2009) .
- [72] F. W. Stecker, M. A. Malkan, and S. T. Scully, “A Determination of the Intergalactic Redshift Dependent UV-Optical-NIR Photon Density Using Deep Galaxy Survey Data and the Gamma-ray Opacity of the Universe,” *Astrophys.J.* **761** (2012) 128, [arXiv:1205.5168 \[astro-ph.HE\]](#).
- [73] A. Dominguez *et al.* *Mon. Not. R. Astron. Soc.* **410** (2011) .
- [74] E. Dwek and F. Krennrich *Astropart. Phys.* **43** (2013) .
- [75] R. J. Gould and G. P. Schreder, “Opacity of the Universe to High-Energy Photons,” *Phys.Rev.* **155** (1967) 1408–1411.
- [76] F. Aharonian, P. Coppi, and H. Volk, “Very high-energy gamma-rays from AGN: Cascading on the cosmic background radiation fields and the formation of pair halos,” *Astrophys.J.* **423** (1994) L5–L8, [arXiv:astro-ph/9312045 \[astro-ph\]](#).
- [77] A. Kandus, K. E. Kunze, and C. G. Tsagas, “Primordial magnetogenesis,” *Phys.Rept.* **505** (2011) 1–58, [arXiv:1007.3891 \[astro-ph.CO\]](#).
- [78] R. Plaga, “Intergalactic magnetic fields and time delays in pulses of gamma radiation,” *Nature* (1994) .
- [79] S. Ando and A. Kusenko, “Evidence for Gamma-Ray Halos Around Active Galactic Nuclei and the First Measurement of Intergalactic Magnetic Fields,” *Astrophys.J.* **722** (2010) L39, [arXiv:1005.1924 \[astro-ph.HE\]](#).
- [80] W. Essey and A. Kusenko, “On weak redshift dependence of gamma-ray spectra of distant blazars,” *Astrophys.J.* **751** (2012) L11, [arXiv:1111.0815 \[astro-ph.HE\]](#).
- [81] W. M. Saslow *Eur. Jour. Phys.* **19** (1998) 313.
- [82] C. Rovelli *Liv. Rev. Rel.* **11** (2008) 15.
- [83] S. N. Solodukhin *Liv. Rev. Rel.* **14** (2011) 8.
- [84] A. Abdo *et al.* *Nature* **462** (2009) 331.
- [85] A. Abromowski *et al.* *Astropart. Phys.* **34** (2011) 738.
- [86] **CTA** Collaboration, B. Acharya *et al.* *Astropart. Phys.* **43** (2013) .
- [87] M. Gavela, P. Hernandez, J. Orloff, O. Pene, and C. Quimbay, “Standard model CP violation and baryon asymmetry. Part 2: Finite temperature,” *Nucl.Phys.* **B430** (1994) 382–426, [arXiv:hep-ph/9406289 \[hep-ph\]](#).
- [88] M. Fukugita and T. Yanagida, “Baryogenesis Without Grand Unification,” *Phys.Lett.* **B174** (1986) 45.
- [89] P. Di Bari, “An introduction to leptogenesis and neutrino properties,” *Contemp.Phys.* **53** (2012) ISSUE4, [arXiv:1206.3168 \[hep-ph\]](#).

- [90] A. Pilaftsis and T. E. Underwood, “Resonant leptogenesis,” *Nucl.Phys.* **B692** (2004) 303–345, [arXiv:hep-ph/0309342](#) [hep-ph].
- [91] I. Affleck and M. Dine, “A New Mechanism for Baryogenesis,” *Nucl.Phys.* **B249** (1985) 361.
- [92] A. Kusenko and M. E. Shaposhnikov, “Supersymmetric Q balls as dark matter,” *Phys.Lett.* **B418** (1998) 46–54, [arXiv:hep-ph/9709492](#) [hep-ph].
- [93] A. Kusenko, V. Kuzmin, M. E. Shaposhnikov, and P. Tinyakov, “Experimental signatures of supersymmetric dark matter Q balls,” *Phys.Rev.Lett.* **80** (1998) 3185–3188, [arXiv:hep-ph/9712212](#) [hep-ph].
- [94] A. Kusenko, L. C. Loveridge, and M. Shaposhnikov, “Astrophysical bounds on supersymmetric dark-matter Q-balls,” *JCAP* **0508** (2005) 011, [arXiv:astro-ph/0507225](#) [astro-ph].
- [95] A. G. Cohen and A. Nelson, “Supersymmetric baryogenesis,” *Phys.Lett.* **B297** (1992) 111–117, [arXiv:hep-ph/9209245](#) [hep-ph].
- [96] N. Turok and J. Zadrozny, “Electroweak baryogenesis in the two doublet model,” *Nucl.Phys.* **B358** (1991) 471–493.
- [97] T. Jacobson, “Thermodynamics of space-time: The Einstein equation of state,” *Phys. Rev. Lett.* **75** (1995) 1260. [arXiv:gr-qc/9504004](#).
- [98] E. P. Verlinde, “On the Origin of Gravity and the Laws of Newton,” *JHEP* **1104** (2011) 029. [arXiv:1001.0785](#) [hep-th].
- [99] C. Hogan, “Quantum Geometry and Interferometry,” 2012. [arXiv:1208.3703](#) [quant-ph].
- [100] G. Amelino-Camelia *et al.*, “Tests of quantum gravity from observations of gamma-ray bursts,” *Nature* **395** (1998) 525.
- [101] M. Ackermann *et al.* *Science* **339** (2013) 807.
- [102] M. Aartsen *et al.* *Phys. Rev. Lett.* **111** (2013) 021103.
- [103] M. Aguilar *et al.* *Phys. Rev. Lett.* **110** (2013) 14102.
- [104] J. Linsley, “Evidence for a primary cosmic-ray particle with energy  $10^{20}$  eV,” *Phys. Rev. Lett.* **10** (1963) 146.
- [105] Abu-Zayyad *et al.* *Astrophys. J.* **556** (2001) 686.
- [106] Prosin *et al.* *Proceedings of the 32nd International Cosmic Ray Conference (ICRC2011)* (2011) .
- [107] S. Knurenko and A. Sabourov *Nucl. Phys. B (Proc. Suppl.)* **212-213** (2011) 241.
- [108] D. Allard, “Extragalactic propagation of ultrahigh energy cosmic-rays,” *Astropart. Phys.* **39-40** (2012) 33. [arXiv:1111.3290](#) [astro-ph.HE].
- [109] J. Abraham *et al.*, “Measurement of the Depth of Maximum of Extensive Air Showers above  $10^{18}$  eV,” *Phys. Rev. Lett.* **104** (2010) 091101. [arXiv:1002.0699](#) [astro-ph.HE].
- [110] R. Aloisio, V. Berezhinsky, and A. Gazizov, “Ultra High Energy Cosmic Rays: The disappointing model,” *Astropart. Phys.* **34** (2011) 620. [arXiv:0907.5194](#) [astro-ph.HE].
- [111] J. Allen and G. Farrar *Proceedings of the 33rd. International Cosmic Ray Conference* (2013) .

- [112] R. Abbasi *et al.*, “Indications of Proton-Dominated Cosmic Ray Composition above 1.6 EeV,” *Phys. Rev. Lett.* **104** (2010) 161101. arXiv:0910.4184 [astro-ph.HE].
- [113] Y. Tsunesada *et al.*, “Highlights from Telescope Array’,” arXiv:1111.2507 [astro-ph.HE].
- [114] W. Hanlon *et al.* *Proceedings of the 33rd International Cosmic Ray Conference* (2013) . ICRC 2013 (id 964).
- [115] P. Abreu *et al.*, “Constraints on the origin of cosmic rays above  $10^{18}$  eV from large scale anisotropy searches in data of the Pierre Auger Observatory’,” *Astrophys. J. Lett.* **762** (2012) L13. arXiv:1212.3083 [astro-ph.HE].
- [116] P. Abreu *et al.*, “Large scale distribution of arrival directions of cosmic rays detected above  $10^{18}$  eV at the Pierre Auger Observatory,” *Astrophys. J. Suppl.* **203** (2012) 34. arXiv:1210.3736 [astro-ph.HE].
- [117] O. Deligny *et al.* *Proceedings of the 33rd International Cosmic Ray Conference* (2013) . id 679.
- [118] R. Abbasi *et al.*, “Search for Correlations between HiRes Stereo Events and Active Galactic Nuclei’,” *Astropart. Phys.* **30** (2008) 175. arXiv:0804.0382 [astro-ph].
- [119] O. D. for the TA and Auger Collaborations *Proc. 33<sup>rd</sup> Int. Cosmic Ray Conf.* (2013) . id 679.
- [120] R. J. G.R. Farrar and J. Roberts, “Deflections of UHECRs in the Galactic Magnetic Field’,” in preparation.
- [121] R. Jansson and G. Farrar *Ap. J. Lett.* **761** (2012) L11.
- [122] V. Hess *Physik. Zeitschr.* **XIII** (1912) .
- [123] M. Aguilar *et al.* *Phys. Rev. Lett.* **110** (2013) .
- [124] V. A. Acciarri *et al.* *Nature* **462** (2009) .
- [125] S. Zhu *et al.*, “GRB 130427A Fermi-LAT detection of a burst,”. GCN Circular 14471.
- [126] A. U. Abeysekara *et al.* *Astropart. Phys.* **35** (2012) .
- [127] F. An *et al.* *Phys. Rev. Lett.* **108** (2012) .
- [128] **IceCube Collaboration** Collaboration, R. Abbasi *et al.*, “IceCube Sensitivity for Low-Energy Neutrinos from Nearby Supernovae,” *Astron.Astrophys.* **535** (2011) A109, arXiv:1108.0171 [astro-ph.HE].
- [129] D. Mattingly *Liv. Rev. Rel.* **8** (2005) 5.
- [130] D. Colladay and V. A. Kostelecky *Phys. Rev. D* **55** (1997) 6760.
- [131] D. Colladay and V. A. Kostelecky *Phys. Rev. D* **58** (1998) 116002.
- [132] V. A. Kostelecky and M. Mewes *Phys. Rev. D* **80** (2009) 015020.
- [133] J. Albert *et al.* *Phys. Lett. B* **668** (2008) 253.
- [134] J. Bolmont and A. Jacholkowska *Adv. Space. Res.* **47** (2011) 380.
- [135] S. D. Biller *et al.* *Phys. Rev. Lett.* **83** (1999) 2108.
- [136] **HAWC Collaboration**, L. Nellen *et al.* *Proc. 33<sup>rd</sup> Int. Cosmic Ray Conf.* (2013) .



- [137] M. Doro *et al.* *ArXiv:1208.5356* (2012) .
- [138] **PAMELA** Collaboration, O. Adriani *et al.*, “Observation of an anomalous positron abundance in the cosmic radiation,” *Nature* **458** (2009) 607. doi:10.1038/nature07942.
- [139] **Fermi LAT Collaboration** Collaboration, M. Ackermann and others., “Measurement of Separate Cosmic-Ray Electron and Positron Spectra with the Fermi Large Area Telescope,” *Phys. Rev. Lett.* **108** (Jan, 2012) 011103. <http://link.aps.org/doi/10.1103/PhysRevLett.108.011103>.
- [140] **AMS Collaboration** Collaboration, M. Aguilar *et al.*, “First Result from the Alpha Magnetic Spectrometer on the International Space Station: Precision Measurement of the Positron Fraction in Primary Cosmic Rays of 0.5–350 GeV,” *Phys. Rev. Lett.* **110** (Apr, 2013) 141102. <http://link.aps.org/doi/10.1103/PhysRevLett.110.141102>.
- [141] A. De Simone, A. Riotto, and W. Xue, “Interpretation of AMS-02 results: correlations among dark matter signals,” *J. Cosmol. Astropart. P.* **5** (May, 2013) 3, arXiv:1304.1336 [hep-ph].
- [142] J. Kopp, “Constraints on dark matter annihilation from AMS-02 results,” *arXiv:1304.1184* (Apr., 2013) , arXiv:1304.1184 [hep-ph].
- [143] Q. Yuan, X.-J. Bi, G.-M. Chen, Y.-Q. Guo, S.-J. Lin, and X. Zhang, “Implications of the AMS-02 positron fraction in cosmic rays,” *arXiv:1304.1482* (Apr., 2013) , arXiv:1304.1482 [astro-ph.HE].
- [144] M. Ibe, S. Iwamoto, S. Matsumoto, T. Moroi, and N. Yokozaki, “Recent Result of the AMS-02 Experiment and Decaying Gravitino Dark Matter in Gauge Mediation,” *arXiv:1304.1483* (Apr., 2013) , arXiv:1304.1483 [hep-ph].
- [145] Y. Kajiyama, H. Okada, and T. Toma, “New Interpretation of the Recent Result of AMS-02 and Multi-component Decaying Dark Matters with non-Abelian Discrete Flavor Symmetry,” *arXiv:1304.2680* (Apr., 2013) , arXiv:1304.2680 [hep-ph].
- [146] T. Linden and S. Profumo, “Probing the Pulsar Origin of the Anomalous Positron Fraction with AMS-02 and Atmospheric Cherenkov Telescopes,” *Astrophys. J.* **772** (July, 2013) 18, arXiv:1304.1791 [astro-ph.HE].
- [147] L. Feng, R.-Z. Yang, H.-N. He, T.-K. Dong, Y.-Z. Fan, and J. Chang, “AMS-02 positron excess: new bounds on dark matter models and hint for primary electron spectrum hardening,” *arXiv:1303.0530* (Mar., 2013) , arXiv:1303.0530 [astro-ph.HE].
- [148] Y. Asaoka *et al.*, “Measurements of Cosmic-Ray Low-Energy Antiproton and Proton Spectra in a Transient Period of Solar Field Reversal,” *Phys. Rev. Lett.* **88** (Jan, 2002) 051101. <http://link.aps.org/doi/10.1103/PhysRevLett.88.051101>.
- [149] K. Abe *et al.*, “Measurement of the cosmic-ray low-energy antiproton spectrum with the first BESS-Polar Antarctic flight,” *Phys. Lett. B* **670** (Dec., 2008) 103–108, arXiv:0805.1754.
- [150] **PAMELA** Collaboration, O. Adriani *et al.*, “PAMELA Results on the Cosmic-Ray Antiproton Flux from 60 MeV to 180 GeV in Kinetic Energy,” *Phys. Rev. Lett.* **105** no. 12, (Sept., 2010) 121101, arXiv:1007.0821 [astro-ph.HE].
- [151] M. Cirelli and G. Giesen, “Antiprotons from Dark Matter: current constraints and future sensitivities,” *J. Cosmol. Astropart. P.* **4** (Apr., 2013) 15, arXiv:1301.7079 [hep-ph].
- [152] H. Baer and S. Profumo, “Low energy antideuteron: shedding light on dark matter,” *J. Cosmol. Astropart. P.* **12** (Dec., 2005) 8, arXiv:astro-ph/0510722.

- [153] A. Ibarra and S. Wild, “Prospects of antideuteron detection from dark matter annihilations or decays at AMS-02 and GAPS,” *J. Cosmol. Astropart. P.* **2** (Feb., 2013) 21, [arXiv:1209.5539 \[hep-ph\]](#).
- [154] A. Ibarra and S. Wild, “Determination of the cosmic antideuteron flux in a Monte Carlo approach,” *Phys. Rev. D* **88** no. 2, (July, 2013) 023014, [arXiv:1301.3820 \[astro-ph.HE\]](#).
- [155] **B.E.S.S.** Collaboration, H. Fuke *et al.*, “Search for Cosmic-Ray Antideuterons,” *Phys. Rev. Lett.* **95** (Aug, 2005) 081101. <http://link.aps.org/doi/10.1103/PhysRevLett.95.081101>.
- [156] V. Choutko and F. Giovacchini *Proc. 30th Int. Cosmic ray Conf.* **4** (2007) 765.
- [157] P. von Doetinchem *Proc. 10th Symposium on Sources and Detection of Dark Matter and Dark Energy in the Universe (UCLA Dark Matter 2012)* (2012) .
- [158] T. Aramaki *to be published* (2013) .
- [159] S. A. I. Mognet, T. Aramaki, N. Bando, S. E. Boggs, P. von Doetinchem, H. Fuke, F. H. Gahbauer, C. J. Hailey, J. E. Koglin, N. Madden, K. Mori, S. Okazaki, R. A. Ong, K. M. Perez, G. Tajiri, T. Yoshida, and J. Zweerink, “The Prototype GAPS (pGAPS) Experiment,” *arXiv:1303.1615* (Mar., 2013) , [arXiv:1303.1615 \[astro-ph.IM\]](#).
- [160] P. von Doetinchem, T. Aramaki, N. Bando, S. E. Boggs, H. Fuke, F. H. Gahbauer, C. J. Hailey, J. E. Koglin, S. A. I. Mognet, N. Madden, S. Okazaki, R. A. Ong, K. M. Perez, T. Yoshida, and J. Zweerink, “The flight of the GAPS prototype experiment,” *arXiv:1307.3538* (July, 2013) , [arXiv:1307.3538 \[astro-ph.IM\]](#).
- [161] Y. B. Zeldovich and I. D. Novikov *Soviet Astronomy A. J.* **10** (1967) 602.
- [162] S. W. Hawking *Nature* **248** (1974) 30.
- [163] H. I. Kim, C. Lee, and J. H. MacGibbon *Phys. Rev. D* **59** (1999) 063004.
- [164] B. J. Carr, K. Kohri, Y. Sendoud, and J. Yokoyama *Phys. Rev. D* **81** (2010) 104019.
- [165] K. Jedamzik *Phys. Rev. D.* **55** (1997) 5871.
- [166] B. C. Lacki and J. F. Beacom *Astrophys. J. Lett.* **720** (2010) L67.
- [167] M. R. S. Hawkins *Mon. Not. R. Astron. Soc.* **415** (2011) 2744.
- [168] F. Halzen *et al. Nature* **353** (1991) 807.
- [169] B. J. Carr and J. H. MacGibbon *Physics Reports* **307** (1998) 141.
- [170] E. L. Wright *Astrophys. J.* **459** (1996) 487.
- [171] K. Maki, T. Mitsui, and S. Orito *Phys. Rev. Lett.* **76** (1996) 3474.
- [172] K. Abe *et al. Phys. Rev. Lett.* **108** (2012) 051102.
- [173] S. Barrau *et al. Astron. Astrophys.* **398** (2003) 403.
- [174] **HAWC** Collaboration, T. Ukwatta *et al. Proc. 33<sup>rd</sup> Int. Cosmic Ray Conf.* (2013) .
- [175] E. Linton, R. Atkins, H. Badran, G. Blaylock, P. Boyle, *et al.*, “A new search for primordial black hole evaporations using the Whipple gamma-ray telescope,” *JCAP* **0601** (2006) 013.
- [176] **VERITAS** Collaboration, G. Tesic *et al. J. Phys. Conf. Series* **375** (2012) .

- [177] D. Alexandreas, G. Allen, D. Berley, S. Biller, R. Burman, *et al.*, “New limit on the rate density of evaporating black holes,” *Phys.Rev.Lett.* **71** (1993) 2524–2527.
- [178] M. Amenomori *et al.* *Proc. 24<sup>th</sup> Int. Cosmic Ray Conf.* **2** (1995) .
- [179] **H.E.S.S.** Collaboration, J.-F. Glicenstein *et al.* [arXiv:1307.4898](#) [[astro-ph.HE](#)].
- [180] F. Krennrich and M. Orr *arXiv:1304.8057* (2013) .
- [181] R. D. Peccei and H. R. Quinn *Phys. Rev. Lett.* **38** (1997) .
- [182] D. Horns and M. Meyer *JCAP* **2** (2012) .
- [183] E. Ferrer-Ribas *et al.* *arXiv:1209.6347* (2012) .
- [184] D. Wouters, P. Brun, *et al.* *arXiv:1304.0700* (2013) .
- [185] W. Essey and A. Kusenko, “A new interpretation of the gamma-ray observations of active galactic nuclei,” *Astropart.Phys.* **33** (2010) 81–85, [arXiv:0905.1162](#) [[astro-ph.HE](#)].
- [186] W. Essey, O. E. Kalashev, A. Kusenko, and J. F. Beacom, “Secondary photons and neutrinos from cosmic rays produced by distant blazars,” *Phys.Rev.Lett.* **104** (2010) 141102, [arXiv:0912.3976](#) [[astro-ph.HE](#)].
- [187] W. Essey, O. Kalashev, A. Kusenko, and J. F. Beacom, “Role of line-of-sight cosmic ray interactions in forming the spectra of distant blazars in TeV gamma rays and high-energy neutrinos,” *Astrophys.J.* **731** (2011) 51, [arXiv:1011.6340](#) [[astro-ph.HE](#)].
- [188] W. Essey, S. Ando, and A. Kusenko, “Determination of intergalactic magnetic fields from gamma ray data,” *Astropart.Phys.* **35** (2011) 135–139, [arXiv:1012.5313](#) [[astro-ph.HE](#)].
- [189] K. Murase, C. D. Dermer, H. Takami, and G. Migliori, “Blazars as Ultra-High-Energy Cosmic-Ray Sources: Implications for TeV Gamma-Ray Observations,” *Astrophys.J.* **749** (2012) 63, [arXiv:1107.5576](#) [[astro-ph.HE](#)].
- [190] S. Razzaque, C. D. Dermer, and J. D. Finke, “Lower limits on ultrahigh-energy cosmic ray and jet powers of TeV blazars,” *Astrophys.J.* **745** (2012) 196, [arXiv:1110.0853](#) [[astro-ph.HE](#)].
- [191] A. Prosekin, W. Essey, A. Kusenko, and F. Aharonian, “Time structure of gamma-ray signals generated in line-of-sight interactions of cosmic rays from distant blazars,” *Astrophys.J.* **757** (2012) 183, [arXiv:1203.3787](#) [[astro-ph.HE](#)].
- [192] F. Aharonian, W. Essey, A. Kusenko, and A. Prosekin, “TeV gamma rays from blazars beyond  $z=1$ ,” *Phys.Rev.* **D87** (2013) 063002, [arXiv:1206.6715](#) [[astro-ph.HE](#)].
- [193] Y. Zheng and T. Kang, “Evidence for secondary emission as the origin of hard spectra in TeV blazars,” *Astrophys.J.* **764** (2013) 113.
- [194] O. E. Kalashev, A. Kusenko, and W. Essey, “PeV neutrinos from intergalactic interactions of cosmic rays emitted by active galactic nuclei,” *Phys.Rev.Lett.* **111** (2013) 041103, [arXiv:1303.0300](#) [[astro-ph.HE](#)].
- [195] Y. Inoue, O. E. Kalashev, and A. Kusenko, “Prospects for future very high-energy gamma-ray sky survey: impact of secondary gamma rays,” [arXiv:1308.5710](#) [[astro-ph.HE](#)].
- [196] M. A. Sanchez-Conde, S. Funk, F. Krennrich, and A. Weinstein *arXiv:1305.05252* (2013) .

- [197] M. Kuster, G. Raffelt, and B. Beltran, “Axions: Theory, cosmology, and experimental searches. Proceedings, 1st Joint ILIAS-CERN-CAST axion training, Geneva, Switzerland, November 30-December 2, 2005,” *Lect.Notes Phys.* **741** (2008) 1–258.
- [198] P. P. Kronberg, “Extragalactic magnetic fields,” *Rept.Prog.Phys.* **57** (1994) 325–382.
- [199] R. Durrer and A. Neronov, “Cosmological Magnetic Fields: Their Generation, Evolution and Observation,” [arXiv:1303.7121 \[astro-ph.CO\]](#).
- [200] J. D. Barrow, P. G. Ferreira, and J. Silk, “Constraints on a primordial magnetic field,” *Phys.Rev.Lett.* **78** (1997) 3610–3613, [arXiv:astro-ph/9701063 \[astro-ph\]](#).
- [201] A.-C. Davis, M. Lilley, and O. Tornkvist, “Relaxing the bounds on primordial magnetic seed fields,” *Phys.Rev.* **D60** (1999) 021301, [arXiv:astro-ph/9904022 \[astro-ph\]](#).
- [202] A. Neronov, D. Semikoz, and M. Banafsheh, “Magnetic Fields in the Large Scale Structure from Faraday Rotation measurements,” [arXiv:1305.1450 \[astro-ph.CO\]](#).
- [203] S. Maeda, K. Takahashi, and K. Ichiki, “Primordial magnetic fields generated by the non-adiabatic fluctuations at pre-recombination era,” *JCAP* **1111** (2011) 045, [arXiv:1109.0691 \[astro-ph.CO\]](#).
- [204] V. Demozzi and C. Ringeval, “Reheating constraints in inflationary magnetogenesis,” *JCAP* **1205** (2012) 009, [arXiv:1202.3022 \[astro-ph.CO\]](#).
- [205] J. Barrow, C. Tsagas, and K. Yamamoto, “Origin of cosmic magnetic fields: Superadiabatically amplified modes in open Friedmann universes,” *Phys.Rev.* **D86** (2012) 023533, [arXiv:1205.6662 \[gr-qc\]](#).
- [206] T. Fujita and S. Mukohyama, “Universal upper limit on inflation energy scale from cosmic magnetic field,” *JCAP* **1210** (2012) 034, [arXiv:1205.5031 \[astro-ph.CO\]](#).
- [207] A. M. Beck, M. Hanasz, H. Lesch, R.-S. Remus, and F. A. Stasyszyn, “On the magnetic fields in voids,” [arXiv:1210.8360 \[astro-ph.CO\]](#).
- [208] T. Kahniashvili, A. Brandenburg, L. Campanelli, B. Ratra, and A. G. Tevzadze, “Evolution of inflation-generated magnetic field through phase transitions,” *Phys.Rev.* **D86** (2012) 103005, [arXiv:1206.2428 \[astro-ph.CO\]](#).
- [209] J. D. Barrow, C. G. Tsagas, and K. Yamamoto, “Do Intergalactic Magnetic Fields Imply An Open Universe?,” *Phys.Rev.* **D86** (2012) 107302, [arXiv:1210.1183 \[gr-qc\]](#).
- [210] C. Ringeval, T. Suyama, and J. Yokoyama, “Magneto-reheating constraints from curvature perturbations,” [arXiv:1302.6013 \[astro-ph.CO\]](#).
- [211] H. Tashiro and T. Vachaspati, “Cosmological magnetic field correlators from blazar induced cascade,” [arXiv:1305.0181 \[astro-ph.CO\]](#).
- [212] T. Vachaspati, “Magnetic fields from cosmological phase transitions,” *Phys.Lett.* **B265** (1991) 258–261.
- [213] M. Joyce and M. E. Shaposhnikov, “Primordial magnetic fields, right-handed electrons, and the Abelian anomaly,” *Phys.Rev.Lett.* **79** (1997) 1193–1196, [arXiv:astro-ph/9703005 \[astro-ph\]](#).
- [214] J. M. Cornwall, “Speculations on primordial magnetic helicity,” *Phys.Rev.* **D56** (1997) 6146–6154, [arXiv:hep-th/9704022 \[hep-th\]](#).

- [215] T. Vachaspati, “Estimate of the primordial magnetic field helicity,” *Phys.Rev.Lett.* **87** (2001) 251302, [arXiv:astro-ph/0101261](#) [[astro-ph](#)].
- [216] H. Tashiro, T. Vachaspati, and A. Vilenkin, “Chiral Effects and Cosmic Magnetic Fields,” *Phys.Rev.* **D86** (2012) 105033, [arXiv:1206.5549](#) [[astro-ph.CO](#)].
- [217] P. Dirac *Proc. Roy. Soc.* **A133** (1931) 60.
- [218] T. Kibble, “Topology of Cosmic Domains and Strings,” *J.Phys.* **A9** (1976) 1387–1398.
- [219] M. S. Turner, E. N. Parker, and T. Bogdan, “Magnetic Monopoles and the Survival of Galactic Magnetic Fields,” *Phys.Rev.* **D26** (1982) 1296.
- [220] **MACRO Collaboration** Collaboration, M. Ambrosio *et al.*, “Final results of magnetic monopole searches with the MACRO experiment,” *Eur.Phys.J.* **C25** (2002) 511–522, [arXiv:hep-ex/0207020](#) [[hep-ex](#)].
- [221] T. I. Collaboration *Proc. 33<sup>rd</sup> Int. Cosmic Ray Conf.* (2013) . id 572.
- [222] **IceCube Collaboration** Collaboration, R. Abbasi *et al.*, “Search for Relativistic Magnetic Monopoles with IceCube,” *Phys.Rev.* **D87** (2013) 022001, [arXiv:1208.4861](#) [[astro-ph.HE](#)].
- [223] **ANITA-II Collaboration** Collaboration, M. Detrixhe *et al.*, “Ultra-Relativistic Magnetic Monopole Search with the ANITA-II Balloon-borne Radio Interferometer,” *Phys.Rev.* **D83** (2011) 023513, [arXiv:1008.1282](#) [[astro-ph.HE](#)].
- [224] G. E. Pavallas, “Search for magnetic monopoles and nuclearites with the ANTARES experiment,” *Nucl.Instrum.Meth.* **A725** (2013) 94–97.
- [225] **BAIKAL Collaboration** Collaboration, K. Antipin *et al.*, “Search for relativistic magnetic monopoles with the Baikal Neutrino Telescope,” *Astropart.Phys.* **29** (2008) 366–372.
- [226] I. Affleck and M. Dine *Nucl. Phys. B* **249** (1985) 361.
- [227] S. Coleman *Nucl. Phys. B* **262** (1985) 263.
- [228] I. Dine and A. Kusenko *Rev. Mod. Phys.* **76** (2004) 1.
- [229] J. Arafune, T. Yoshida, S. Nakamura, and K. Ogure *Phys. Rev. D* **62** (2000) 105013.
- [230] Y. Takenaga *et al. Phys. Lett. B* **647** (2007) 18.
- [231] M. Ambrosio *et al. Eur. Phys. J. C* **26** (2002) 163.
- [232] **HAWC Collaboration**, P. Karn *et al. Proc. 33<sup>rd</sup> Int. Cosmic Ray Conf.* (2013) .
- [233] T. DeYoung *private communication* (2103) .
- [234] A. Bodmer, “Collapsed nuclei,” *Phys.Rev.* **D4** (1971) 1601–1606.
- [235] E. Witten, “Cosmic Separation of Phases,” *Phys.Rev.* **D30** (1984) 272–285.
- [236] C. Alcock and A. Olinto, “Exotic Phases of Hadronic Matter and their Astrophysical Application,” *Ann.Rev.Nucl.Part.Sci.* **38** (1988) 161–184.
- [237] J. Madsen, “Physics and astrophysics of strange quark matter,” *Lect.Notes Phys.* **516** (1999) 162–203, [arXiv:astro-ph/9809032](#) [[astro-ph](#)].

- [238] F. Weber, “Strange quark matter and compact stars,” *Prog.Part.Nucl.Phys.* **54** (2005) 193–288, [arXiv:astro-ph/0407155](#) [astro-ph].
- [239] J. Madsen, “Strangelets, Nuclearites, Q-balls: A Brief Overview,” [arXiv:astro-ph/0612740](#) [astro-ph].
- [240] C. Alcock, E. Farhi, and A. Olinto, “Strange stars,” *Astrophys.J.* **310** (1986) 261–272.
- [241] P. Haensel, J. Zdunik, and R. Schaeffer, “Strange quark stars,” *Astron.Astrophys.* **160** (1986) 121–128.
- [242] E. Farhi and R. Jaffe, “Strange Matter,” *Phys.Rev.* **D30** (1984) 2379.
- [243] A. De Rujula and S. Glashow, “Nuclearites: A Novel Form of Cosmic Radiation,” *Nature* **312** (1984) 734–737.
- [244] J. Sandweiss, “Overview of strangelet searches and Alpha Magnetic Spectrometer: When will we stop searching?,” *J.Phys.* **G30** (2004) S51–S59.
- [245] E. Finch, “Strangelets: Who is looking, and how?,” *J.Phys.* **G32** (2006) S251–S258, [arXiv:nuc1-ex/0605010](#) [nuc1-ex].
- [246] K. Han, J. Ashenfelter, A. Chikanian, W. Emmet, L. E. Finch, *et al.*, “Search for stable Strange Quark Matter in lunar soil,” *Phys.Rev.Lett.* **103** (2009) 092302, [arXiv:0903.5055](#) [nuc1-ex].
- [247] **AMS Collaboration** Collaboration, A. Kounine, “AMS experiment on the international space station,” *AIP Conf.Proc.* **1441** (2012) 63–70.
- [248] **Pierre Auger Collaboration** Collaboration, C. Berat, “Radio detection of extensive air showers at the Pierre Auger Observatory,” *Nucl.Instrum.Meth.* **A718** (2013) 471–474.
- [249] **Pierre Auger Collaboration** Collaboration, M. Kleifges, “Measurement of cosmic ray air showers using MHz radio-detection techniques at the Pierre Auger Observatory,” *Nucl.Instrum.Meth.* **A718** (2013) 499–501.
- [250] S. Ogio, T. Yamamoto, K. Kuramoto, T. Iijima, H. Akimune, *et al.*, “Search for molecular bremsstrahlung radiation signals in Ku band with coincidental operations of radio telescopes with air shower detectors,” *EPJ Web Conf.* **53** (2013) 08007.
- [251] R. Smida, F. Werner, R. Engel, J. Arteaga-Velazquez, K. Bekk, *et al.*, “Observation of Polarised Microwave Emission from Cosmic Ray Air Showers,” [arXiv:1306.6738](#) [astro-ph.IM].
- [252] W. Apel, J. Arteaga, L. Bhren, K. Bekk, M. Bertaina, *et al.*, “Reconstructing energy and Xmax of cosmic ray air showers using the radio lateral distribution measured with LOPES,” *AIP Conf. Proc.* **1535**, **89** (2013) , [arXiv:1308.0053](#) [astro-ph.IM].
- [253] M. van Haarlem, M. Wise, A. Gunst, G. Heald, J. McKean, *et al.*, “LOFAR: The LOw-Frequency ARray,” [arXiv:1305.3550](#) [astro-ph.IM].
- [254] **The LOFAR Collaboration** Collaboration, A. Nelles *et al.*, “Detecting Radio Emission from Air Showers with LOFAR,” [arXiv:1304.0976](#) [astro-ph.HE].
- [255] A. Romero-Wolf, P. Gorham, K. Liewer, J. Booth, and R. Duren, “Concept and Analysis of a Satellite for Space-based Radio Detection of Ultra-high Energy Cosmic Rays,” [arXiv:1302.1263](#) [astro-ph.IM].
- [256] R. Blandford *et al.*, “New Worlds New Horizons,”

- [257] S. Ritz *et al.*, “Report of the HEPAP Particle Astrophysics Scientific Assessment Group (PASAG),”.
- [258] K. Schwarzschild, “Untersuchungen zur geometrischen Optik II.,” *Astronomische Mitteilungen der Universitaets-Sternwarte zu Goettingen* **10** (1905) .
- [259] V. Vassiliev, S. Fegan, and P. Brousseau *Astropart. Phys.* **28** (2007) .
- [260] V. Vassiliev and S. Fegan *Proc. Int. Cosmic Ray Conf.* **3** (2008) .
- [261] K. Bernloehr *et al.* *Astropart. Phys.* **43** (2013) .
- [262] *Internal CTA Document* **MAN-PO/121004** .
- [263] I. Taboada and R. Gilmore *arXiv:1306.1127* (2013) .
- [264] **IceCube Collaboration** Collaboration, R. Abbasi *et al.*, “IceTop: The surface component of IceCube,” *Nucl.Instrum.Meth.* **A700** (2013) 188–220, [arXiv:1207.6326](#) [[astro-ph.IM](#)].
- [265] **IceCube Collaboration** Collaboration, R. Abbasi *et al.*, “A Search for UHE Tau Neutrinos with IceCube,” *Phys.Rev.* **D86** (2012) 022005, [arXiv:1202.4564](#) [[astro-ph.HE](#)].
- [266] **IceCube Collaboration** Collaboration, M. Aartsen *et al.*, “Measurement of Atmospheric Neutrino Oscillations with IceCube,” [arXiv:1305.3909](#) [[hep-ex](#)].
- [267] **IceCube Collaboration** Collaboration, M. Aartsen *et al.*, “Search for time-independent neutrino emission from astrophysical sources with 3 years of IceCube data,” [arXiv:1307.6669](#) [[astro-ph.HE](#)].
- [268] **IceCube Collaboration** Collaboration, R. Abbasi *et al.*, “An absence of neutrinos associated with cosmic-ray acceleration in  $\gamma$ -ray bursts,” *Nature* **484** (2012) 351–353, [arXiv:1204.4219](#) [[astro-ph.HE](#)].
- [269] Presentations by Claudio Kopper, Spencer Klein and Francis Halzen at the 2013 Intl. Cosmic Ray Conf., July 2-9, 2013, Rio de Janeiro, Brazil.
- [270] Presentations by Bakhtiyar Ruzybayev, Katherine Rawlins and Marcos Santander at the 2013 Intl. Cosmic Ray Conf., July 2-9, 2013, Rio de Janeiro, Brazil.
- [271] **IceCube Collaboration** Collaboration, R. Abbasi *et al.*, “Observation of an Anisotropy in the Galactic Cosmic Ray arrival direction at 400 TeV with IceCube,” *Astrophys.J.* **746** (2012) 33, [arXiv:1109.1017](#) [[hep-ex](#)].
- [272] **IceCube Collaboration** Collaboration, R. Abbasi *et al.*, “Lateral Distribution of Muons in IceCube Cosmic Ray Events,” *Phys.Rev.* **D87** (2013) 012005, [arXiv:1208.2979](#) [[astro-ph.HE](#)].
- [273] P. Kooijman, “KM3NeT status and plans,” *Nucl.Instrum.Meth.* **A725** (2013) 13–17.
- [274] **PINGU collaboration** Collaboration, T. IceCube, “PINGU Sensitivity to the Neutrino Mass Hierarchy,” [arXiv:1306.5846](#) [[astro-ph.IM](#)].
- [275] <http://antares.in2p3.fr/users/pradier/orca.html>.
- [276] T. Deyoung, “Toward precision neutrino physics with DeepCore and beyond,” *Nucl.Instrum.Meth.* **A725** (2013) 18–22.
- [277] A. Sakharov, “Violation of CP Invariance, c Asymmetry, and Baryon Asymmetry of the Universe,” *Pisma Zh.Eksp.Teor.Fiz.* **5** (1967) 32–35.

- [278] F. R. Klinkhamer and N. Manton, “A Saddle Point Solution in the Weinberg-Salam Theory,” *Phys.Rev.* **D30** (1984) 2212.
- [279] V. Kuzmin, V. Rubakov, and M. Shaposhnikov, “On the Anomalous Electroweak Baryon Number Nonconservation in the Early Universe,” *Phys.Lett.* **B155** (1985) 36.
- [280] K. Kajantie, K. Rummukainen, and M. E. Shaposhnikov, “A Lattice Monte Carlo study of the hot electroweak phase transition,” *Nucl.Phys.* **B407** (1993) 356–372, [arXiv:hep-ph/9305345](#) [hep-ph].
- [281] K. Jansen, “Status of the finite temperature electroweak phase transition on the lattice,” *Nucl.Phys.Proc.Suppl.* **47** (1996) 196–211, [arXiv:hep-lat/9509018](#) [hep-lat].
- [282] K. Kajantie, M. Laine, K. Rummukainen, and M. E. Shaposhnikov, “Is there a hot electroweak phase transition at  $m(H)$  larger or equal to  $m(W)$ ?,” *Phys.Rev.Lett.* **77** (1996) 2887–2890, [arXiv:hep-ph/9605288](#) [hep-ph].
- [283] A. Dolgov, “NonGUT baryogenesis,” *Phys.Rept.* **222** (1992) 309–386.
- [284] M. Dine and A. Kusenko, “The Origin of the matter - antimatter asymmetry,” *Rev.Mod.Phys.* **76** (2003) 1, [arXiv:hep-ph/0303065](#) [hep-ph].
- [285] M.-C. Chen, “TASI 2006 Lectures on Leptogenesis,” [arXiv:hep-ph/0703087](#) [HEP-PH].
- [286] Y. Grossman, T. Kashti, Y. Nir, and E. Roulet, “Leptogenesis from supersymmetry breaking,” *Phys.Rev.Lett.* **91** (2003) 251801, [arXiv:hep-ph/0307081](#) [hep-ph].
- [287] T. Asaka, K. Hamaguchi, M. Kawasaki, and T. Yanagida, “Leptogenesis in inflaton decay,” *Phys.Lett.* **B464** (1999) 12–18, [arXiv:hep-ph/9906366](#) [hep-ph].
- [288] K. Dick, M. Lindner, M. Ratz, and D. Wright, “Leptogenesis with Dirac neutrinos,” *Phys.Rev.Lett.* **84** (2000) 4039–4042, [arXiv:hep-ph/9907562](#) [hep-ph].
- [289] P. Frampton, S. Glashow, and T. Yanagida, “Cosmological sign of neutrino CP violation,” *Phys.Lett.* **B548** (2002) 119–121, [arXiv:hep-ph/0208157](#) [hep-ph].
- [290] M.-C. Chen and K. Mahanthappa, “Relating leptogenesis to low energy flavor violating observables in models with spontaneous CP violation,” *Phys.Rev.* **D71** (2005) 035001, [arXiv:hep-ph/0411158](#) [hep-ph].
- [291] M.-C. Chen and K. Mahanthappa, “Leptogenesis in a SUSY SU(5) x T’ Model with Geometrical CP Violation,” [arXiv:1107.3856](#) [hep-ph].
- [292] S. D. Thomas, “Baryons and dark matter from the late decay of a supersymmetric condensate,” *Phys.Lett.* **B356** (1995) 256–263, [arXiv:hep-ph/9506274](#) [hep-ph].
- [293] K. Enqvist and J. McDonald, “B - ball baryogenesis and the baryon to dark matter ratio,” *Nucl.Phys.* **B538** (1999) 321–350, [arXiv:hep-ph/9803380](#) [hep-ph].
- [294] M. S. Carena, M. Quiros, and C. Wagner, “Opening the window for electroweak baryogenesis,” *Phys.Lett.* **B380** (1996) 81–91, [arXiv:hep-ph/9603420](#) [hep-ph].
- [295] M. Pietroni, “The Electroweak phase transition in a nonminimal supersymmetric model,” *Nucl.Phys.* **B402** (1993) 27–45, [arXiv:hep-ph/9207227](#) [hep-ph].
- [296] J. M. Cline and P.-A. Lemieux, “Electroweak phase transition in two Higgs doublet models,” *Phys.Rev.* **D55** (1997) 3873–3881, [arXiv:hep-ph/9609240](#) [hep-ph].



- 
- [297] L. Fromme, S. J. Huber, and M. Seniuch, “Baryogenesis in the two-Higgs doublet model,” *JHEP* **0611** (2006) 038, [arXiv:hep-ph/0605242](#) [[hep-ph](#)].
- [298] G. Dorsch, S. Huber, and J. No, “A strong electroweak phase transition in the 2HDM after LHC8,” [arXiv:1305.6610](#) [[hep-ph](#)].
- [299] D. E. Morrissey and M. J. Ramsey-Musolf, “Electroweak baryogenesis,” *New J.Phys.* **14** (2012) 125003, [arXiv:1206.2942](#) [[hep-ph](#)].
- [300] S. Dimopoulos and L. J. Hall, “BARYOGENESIS AT THE MeV ERA,” *Phys.Lett.* **B196** (1987) 135.
- [301] S. Dodelson and L. M. Widrow, “BARYOGENESIS IN A BARYON SYMMETRIC UNIVERSE,” *Phys.Rev.* **D42** (1990) 326–342.
- [302] S. Kanemura, Y. Okada, and E. Senaha, “Electroweak baryogenesis and quantum corrections to the triple Higgs boson coupling,” *Phys.Lett.* **B606** (2005) 361–366, [arXiv:hep-ph/0411354](#) [[hep-ph](#)].
- [303] A. Noble and M. Perelstein, “Higgs self-coupling as a probe of electroweak phase transition,” *Phys.Rev.* **D78** (2008) 063518, [arXiv:0711.3018](#) [[hep-ph](#)].
- [304] C. J. Hogan, “Covariant Macroscopic Quantum Geometry,” 2012. [arXiv:1204.5948](#) [[gr-qc](#)].
- [305] C. J. Hogan, “Interferometers as Probes of Planckian Quantum Geometry,” *Phys. Rev. D* **85** (2010) 064007. [arXiv:1002.4880](#) [[gr-qc](#)].
- [306] <http://holometer.fnal.gov>.
- [307] E. Adelberger, “Torsion-balance probes of fundamental physics,” [arXiv:1308.3213](#) [[hep-ex](#)].